CHAPTER VII

RESULTS OF COMPUTATIONS AND DISCUSSION

7.1 COMPARISON OF NUMERICAL AND EXPERIMENTAL RESULTS

The main purpose of this section is to make the comparison between the computed data from doing the simulation and the measured data from the both parts of an experimental investigation. The conditions of the both procedures must be exactly identical , otherwise , some undesired error may occur. Such comparisons illustrate the mean velocity profiles of the developing flow at some distance and also the centerline mean velocity distribution over the length of the duct for both procedures simultaneously.

Figures 7.1(a) - (g) illustrate the comparison under the initial condition of the air flow in a square duct without any obstacle inside. The agreement between experiments and predictions is reasonably close over the length of the duct especially the regions beyond L / D = 28.

Figures 7.1(h) - (n) illustrate the comparison under the initial condition of the air flow in a square duct with the obstacle inside. it is appropriately specified to be 1-blade damper with inclination of 30 degree angle. The fair agreement between experiments and predictions is obtained. Some of the discrepancies of the both procedures are found in some regions. However , they still be acceptable for overall regions.

Figures 7.2 illustrate the comparisons of various initial conditions are in general satisfactory for downstream flow. Although some discrepancies are

found around the damper due to influence of swirl reduced the accuracy of a Pitot-static tube , which should be neglected for this region.

Consequently , the validity of the simulation has been verified and ready to confidently predict the flows with initial conditions under the range of the study that the experiments of this present study can not be done for some details as the separation zone behind the damper or even the exactly distance of the fully developed flow.

To determine the development length in a system , some criterion must be defined for the decision. In the present study , the change of norms is adopted for reference. Due to the calculation domain is three dimensions , hence the collected numerical data are aligned in the matrix along the diagonals of a square for each x-y plane as shown in figure 7.3.

The form of expression of the norm is

$$\text{norm} \quad [\, m / s \,] \qquad = \qquad \sqrt{\sum_{i=1}^{9} \left(V_i - \tilde{V}_i \right)^2} \qquad (7.1)$$

where V_i and $\tilde{V}_i$ are the mean velocity along the flow direction (or z-direction) at the same position of the adjacent cross-section (or x-y plane).

The definition of the criterion is that the fully developed flow region is promptly determined when the norm is lower than 0.03 for all of the present initial conditions. This value is obtained from doing the comparison among the theoretical background (in section 3.3) , the experimental results (in the

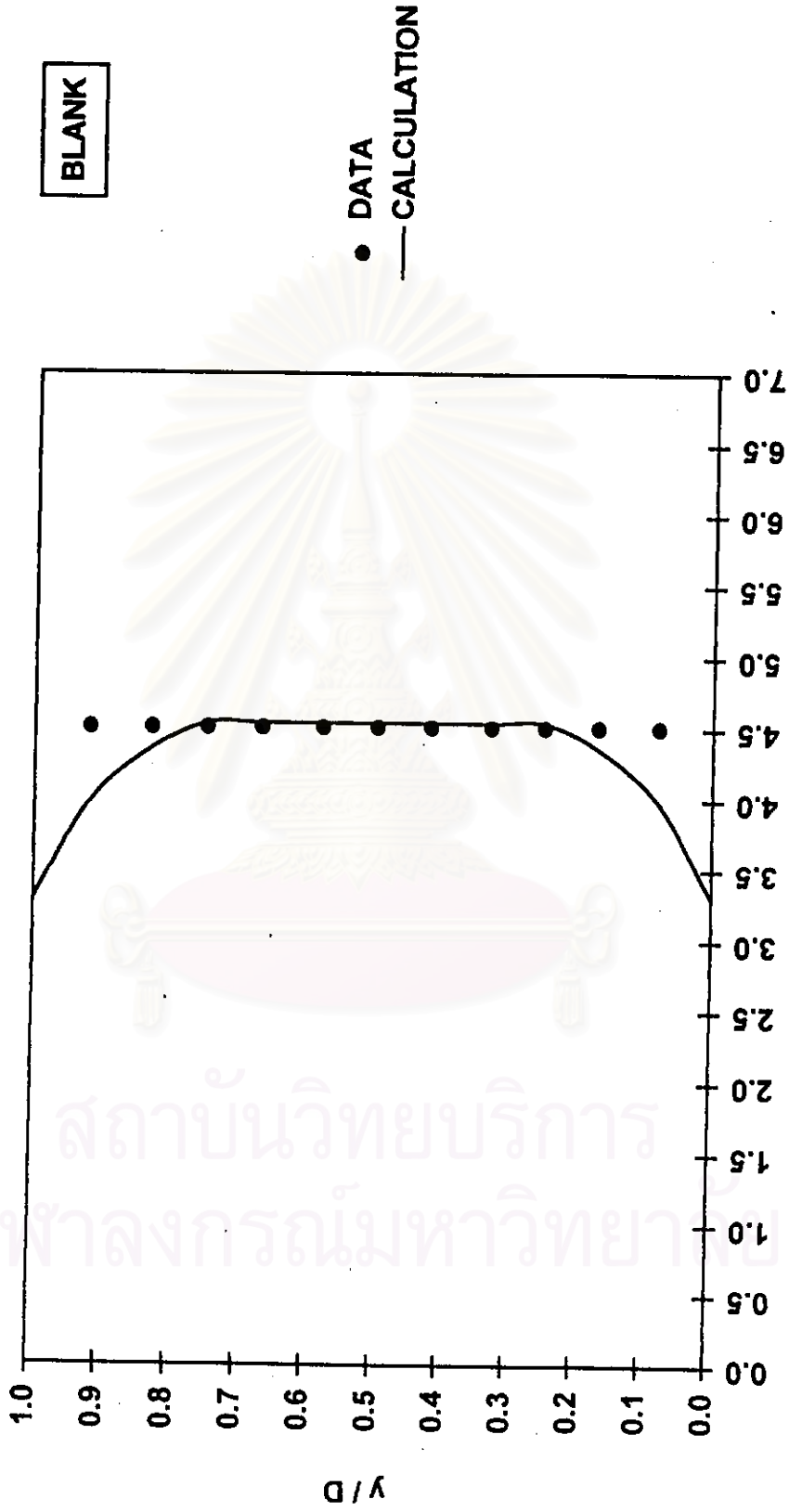

Figure 7.1(a) Measured and calculated mean-longitudinal-velocity profiles at L / D = 4.

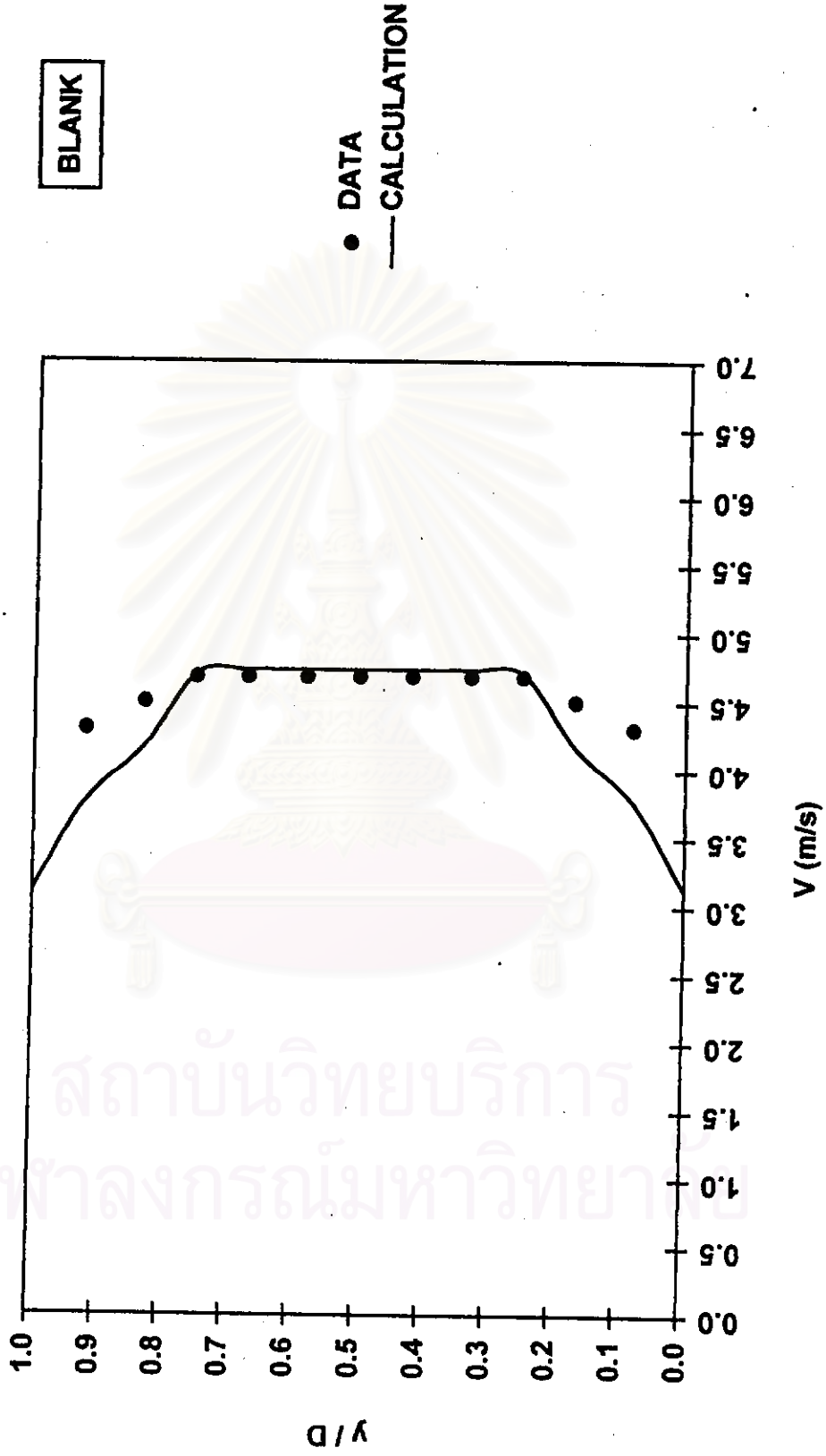

Figure 7.1(b) Measured and calculated mean-longitudinal-velocity profiles at L / D = 8.

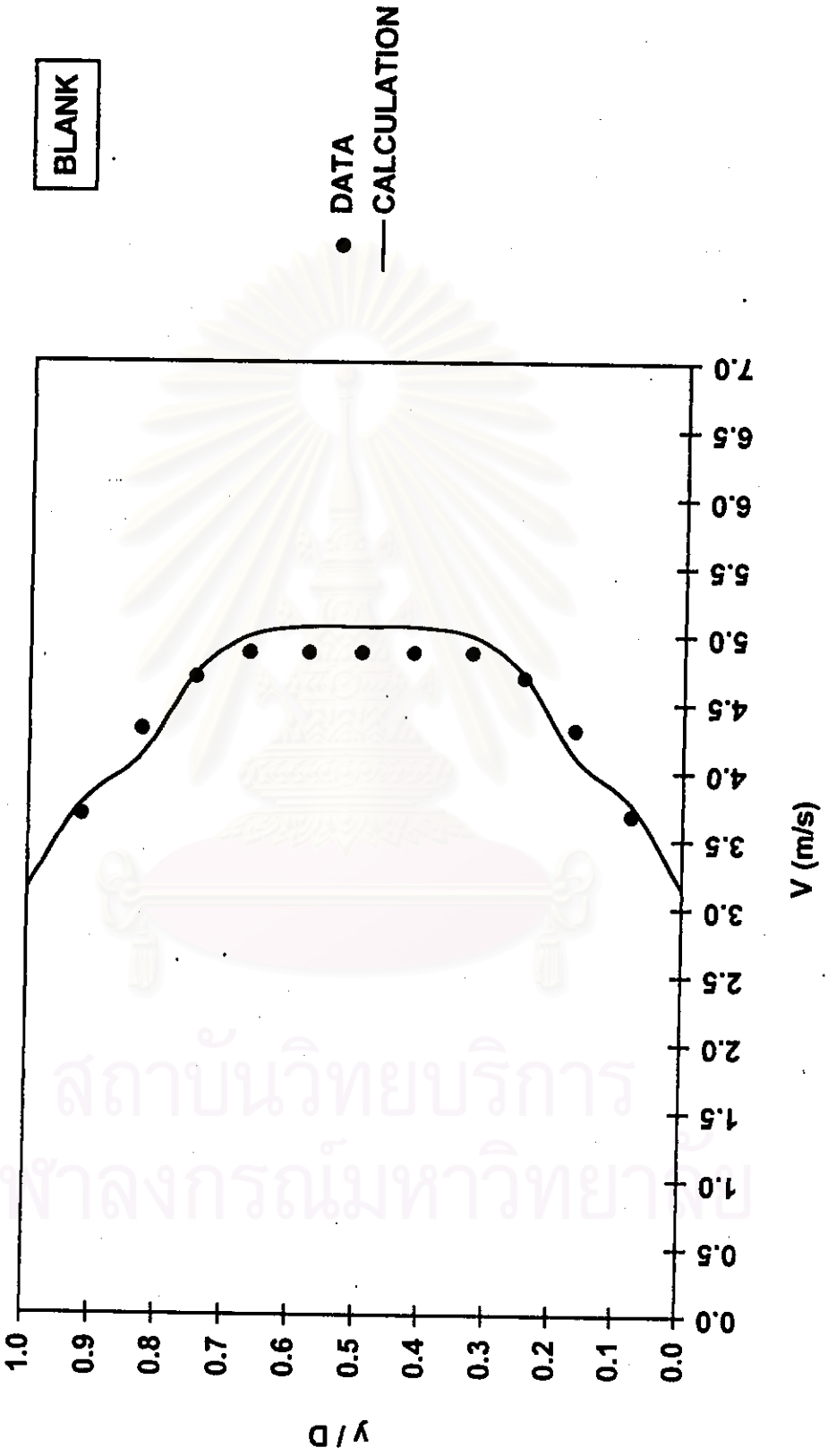

Figure 7.1(c) Measured and calculated mean-longitudinal-velocity profiles at L / D = 16.

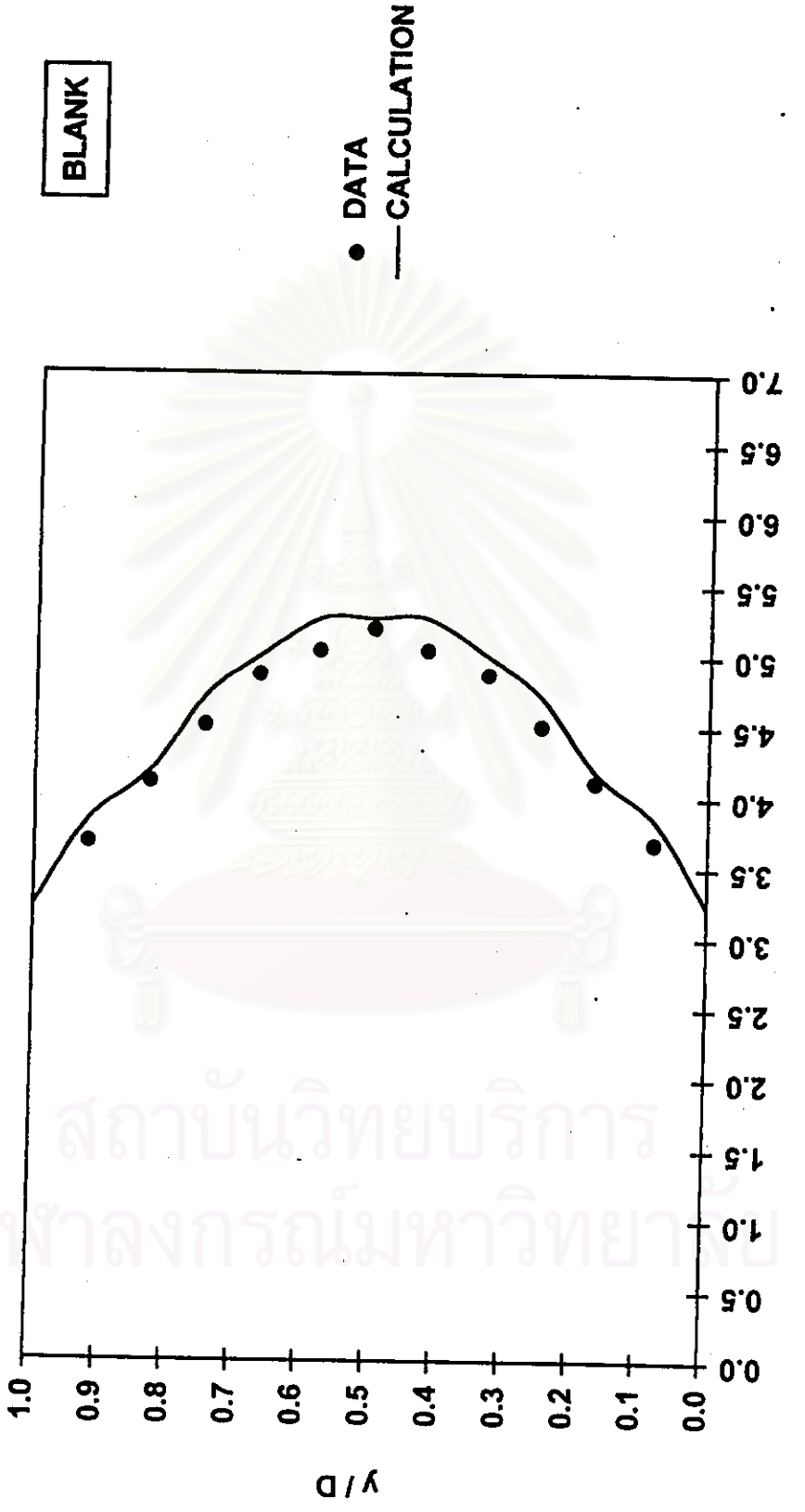

Figure 7.1(d) Measured and calculated mean-longitudinal-velocity profiles at L / D = 28.

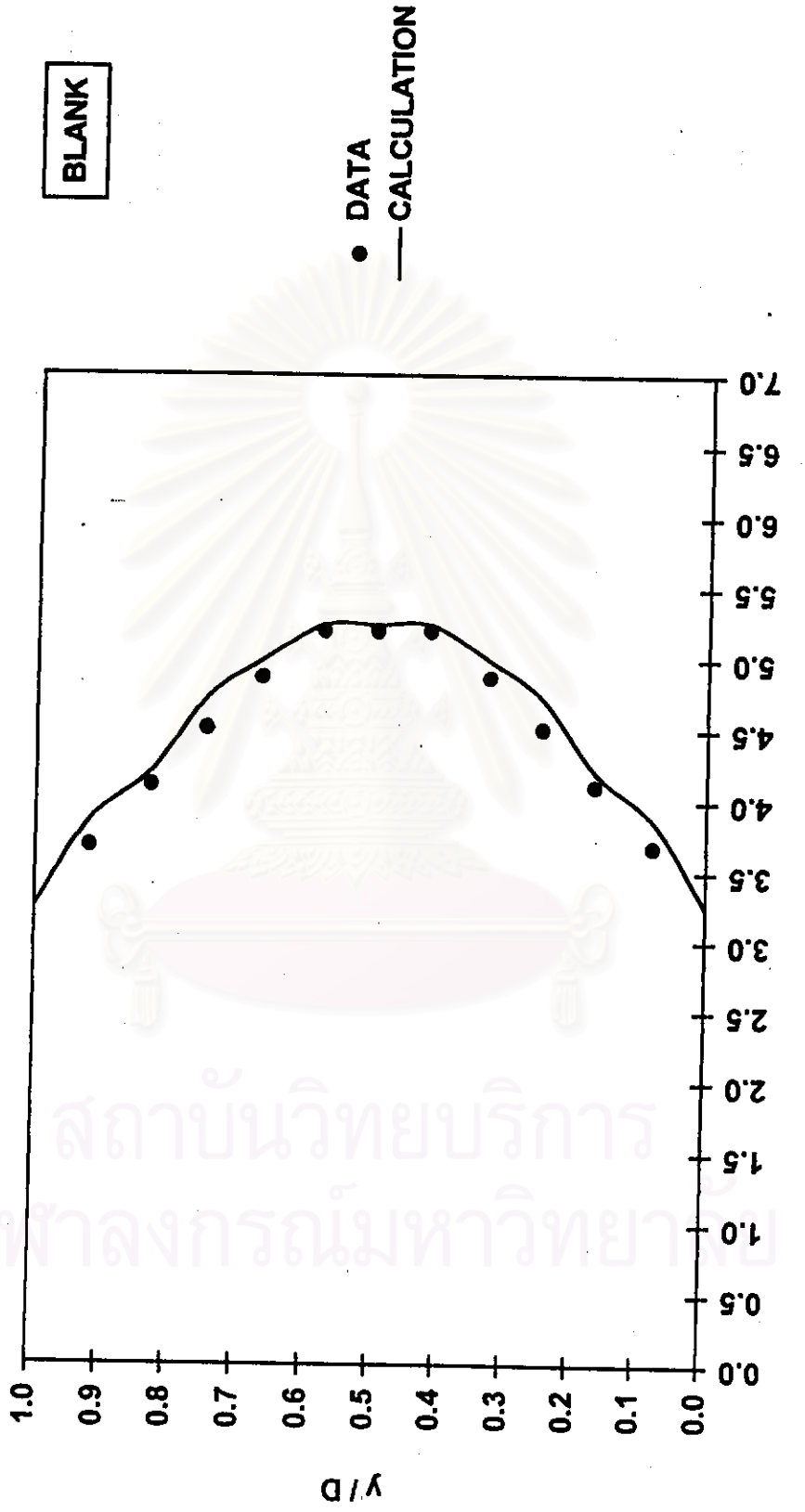

Figure 7.1(e) Measured and calculated mean-longitudinal-velocity profiles at L / D = 32.

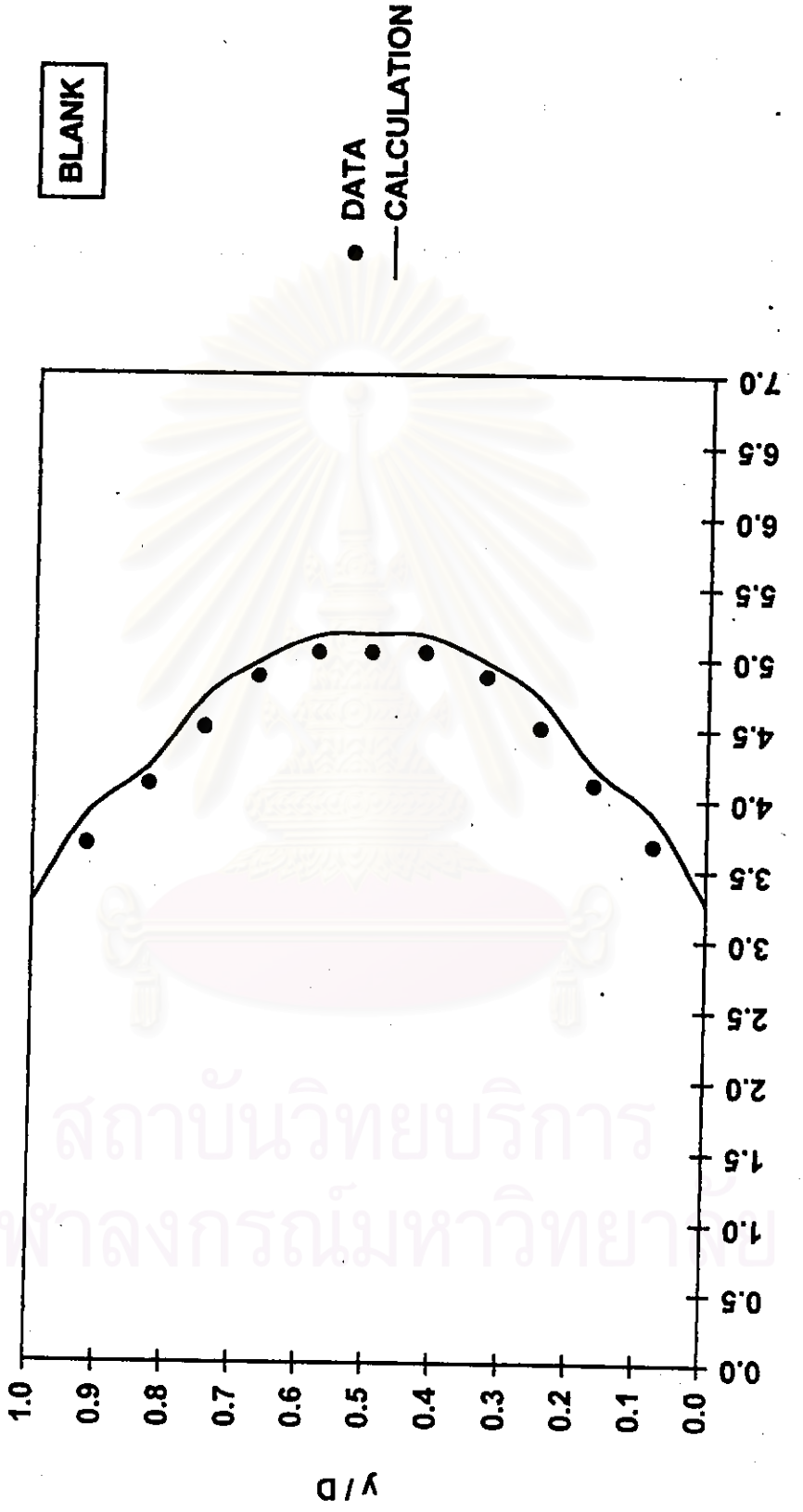

Figure 7.1(f) Measured and calculated mean-longitudinal-velocity profiles at L / D = 40.

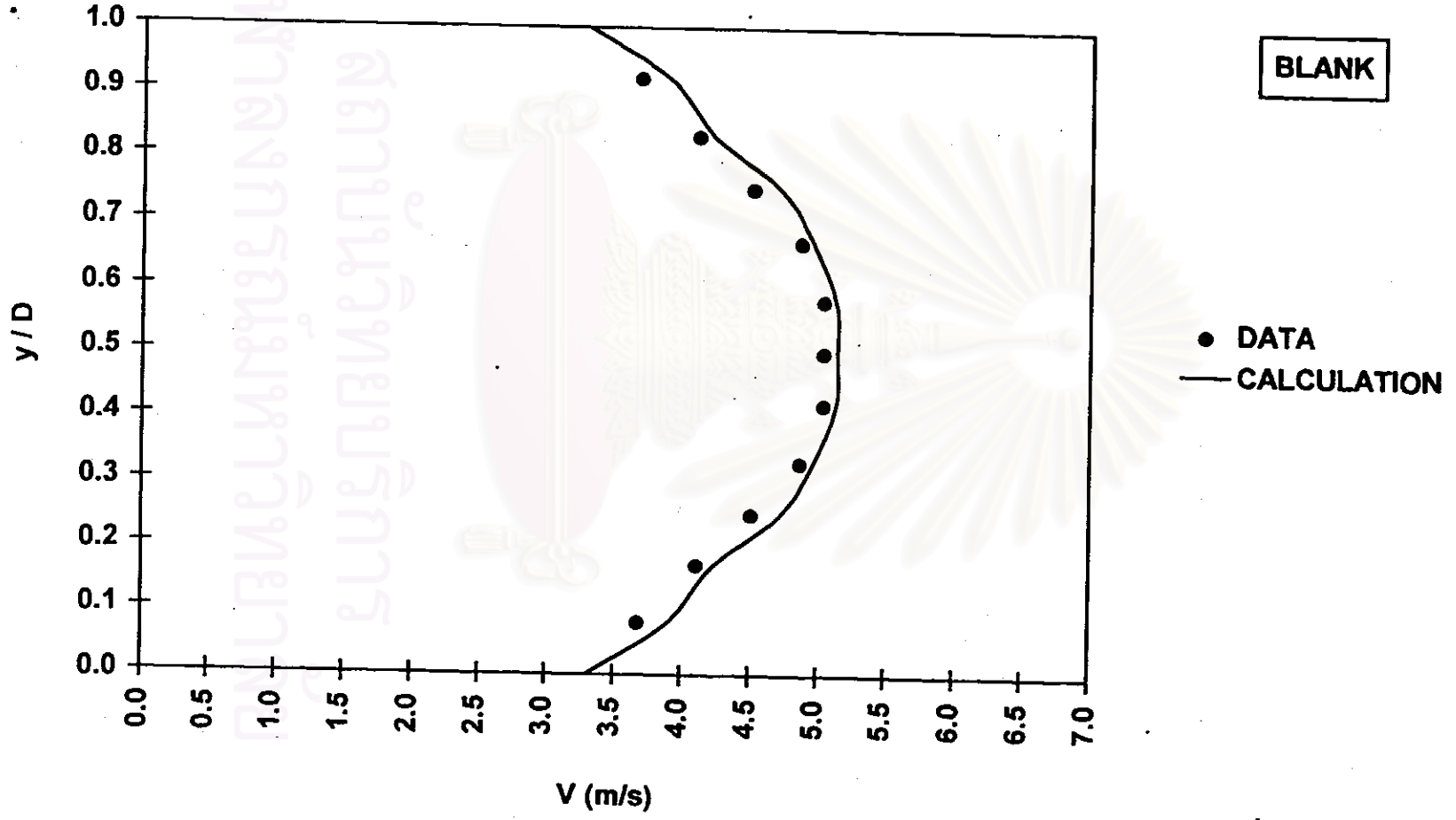

Figure 7.1(g) Measured and calculated mean-longitudinal-velocity profiles at L / D = 44.

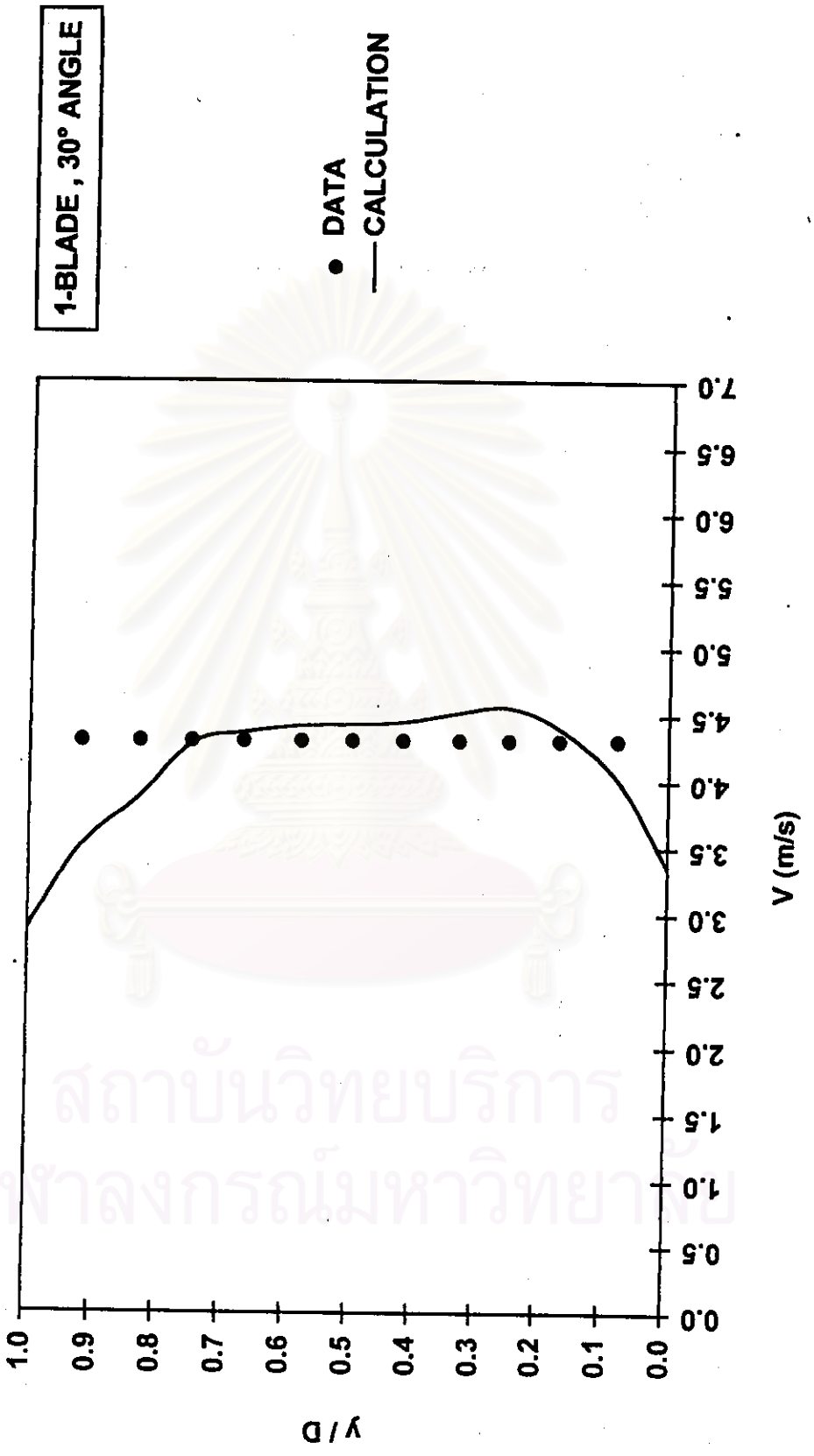

Figure 7.1(h) Measured and calculated mean-longitudinal-velocity profiles at L / D = 4.

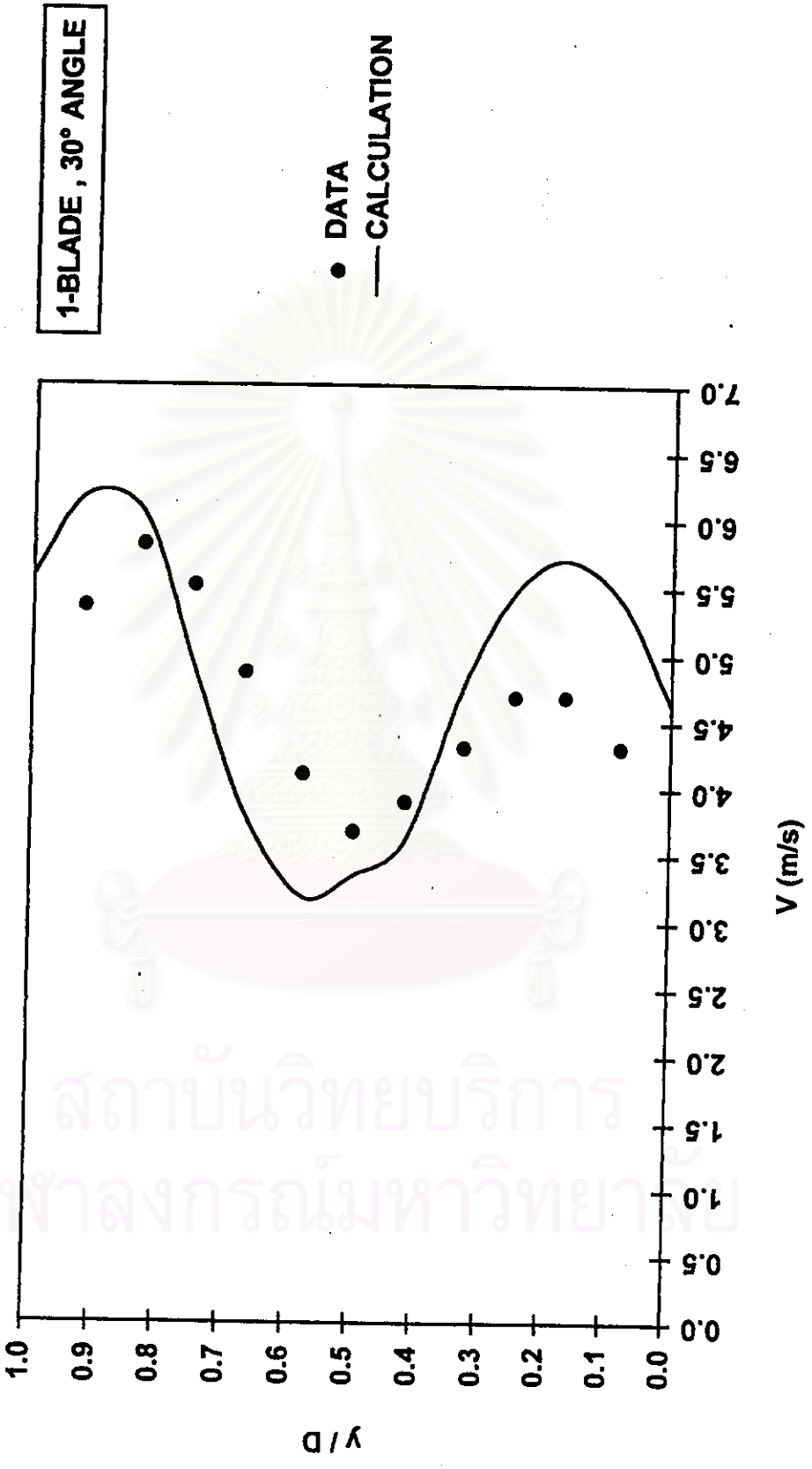

Figure 7.1(i) Measured and calculated mean-longitudinal-velocity profiles at L / D = 13.

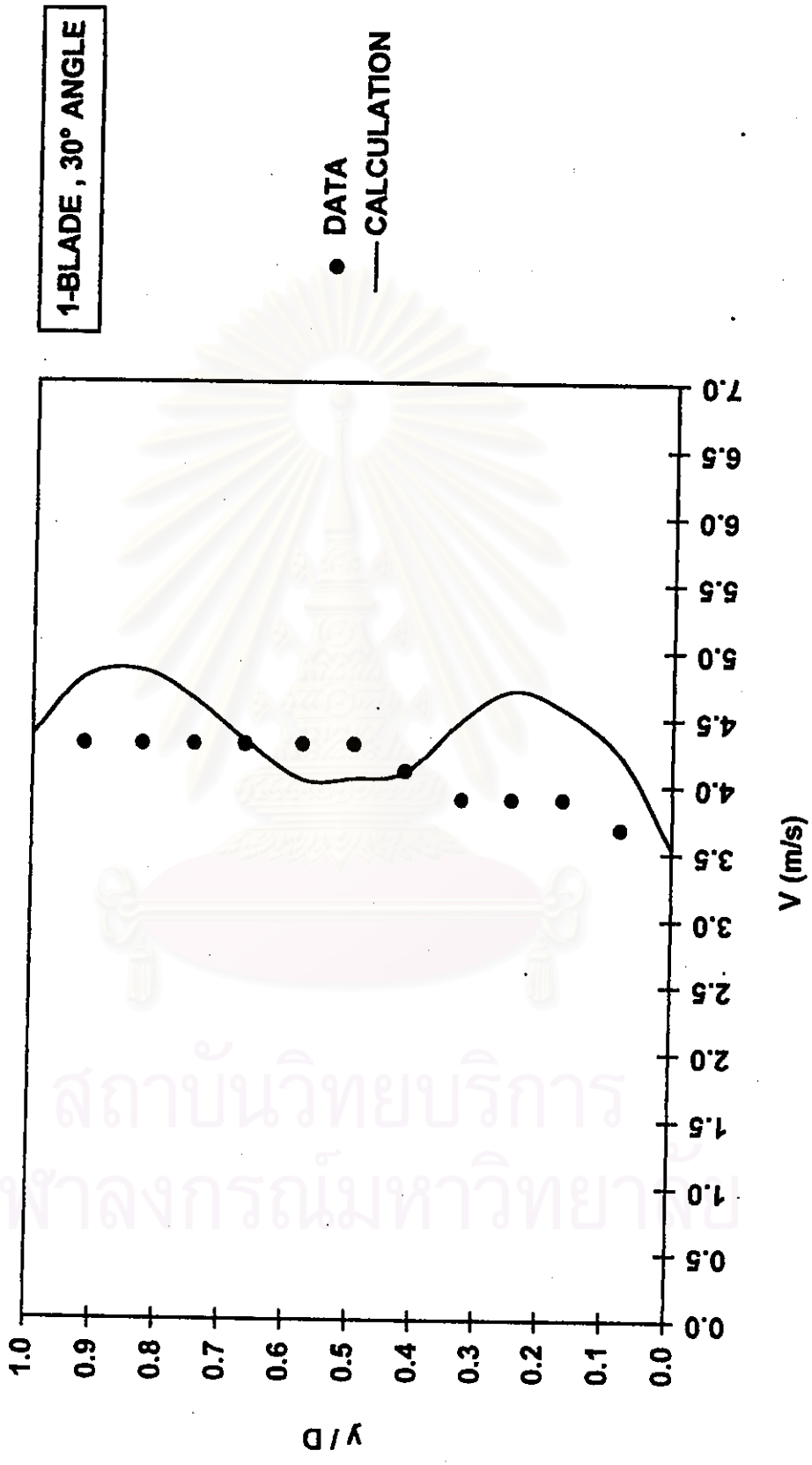

Figure 7.1(j) Measured and calculated mean-longitudinal-velocity profiles at L / D = 17.

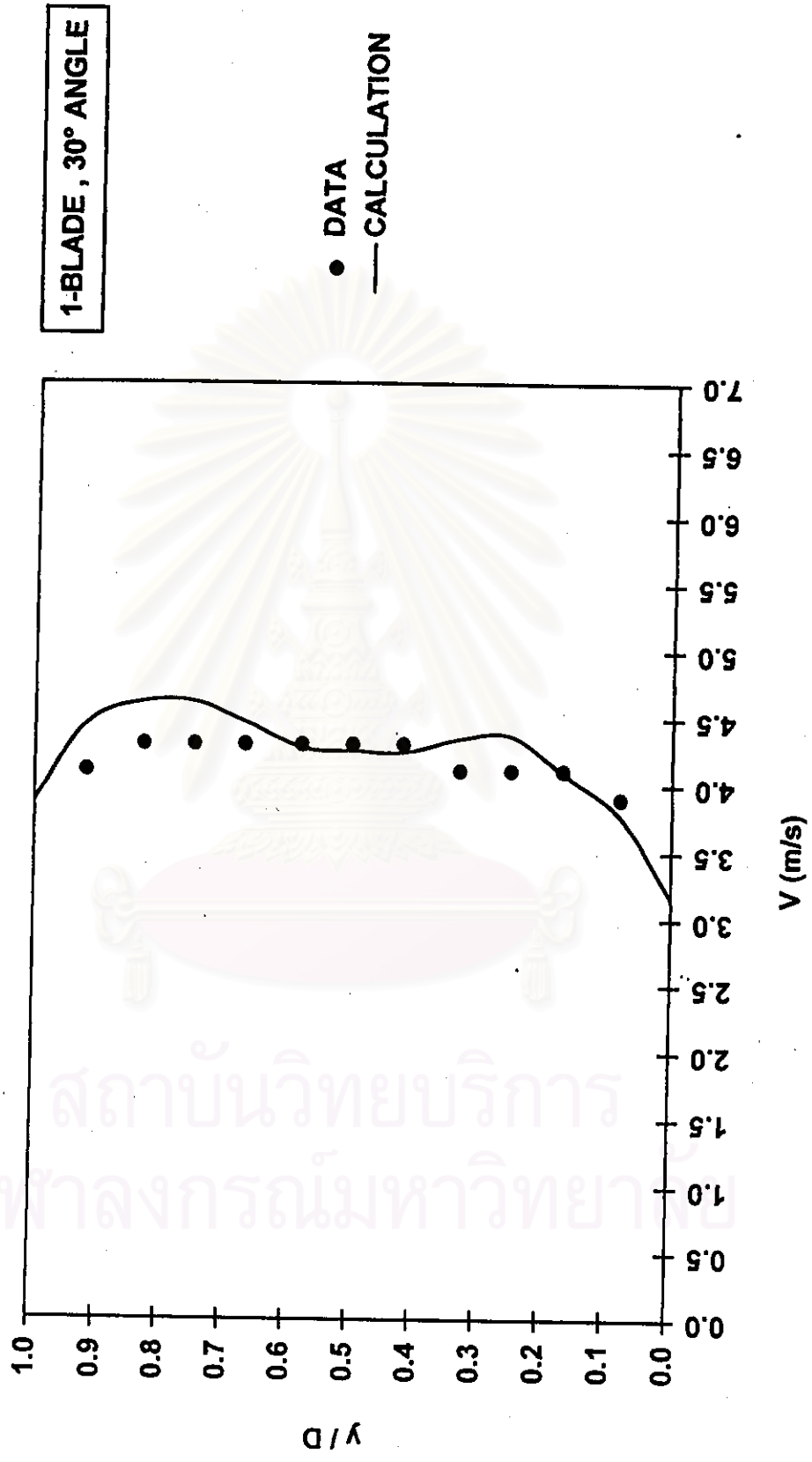

Figure 7.1(k) Measured and calculated mean-longitudinal-velocity profiles at L / D = 19.

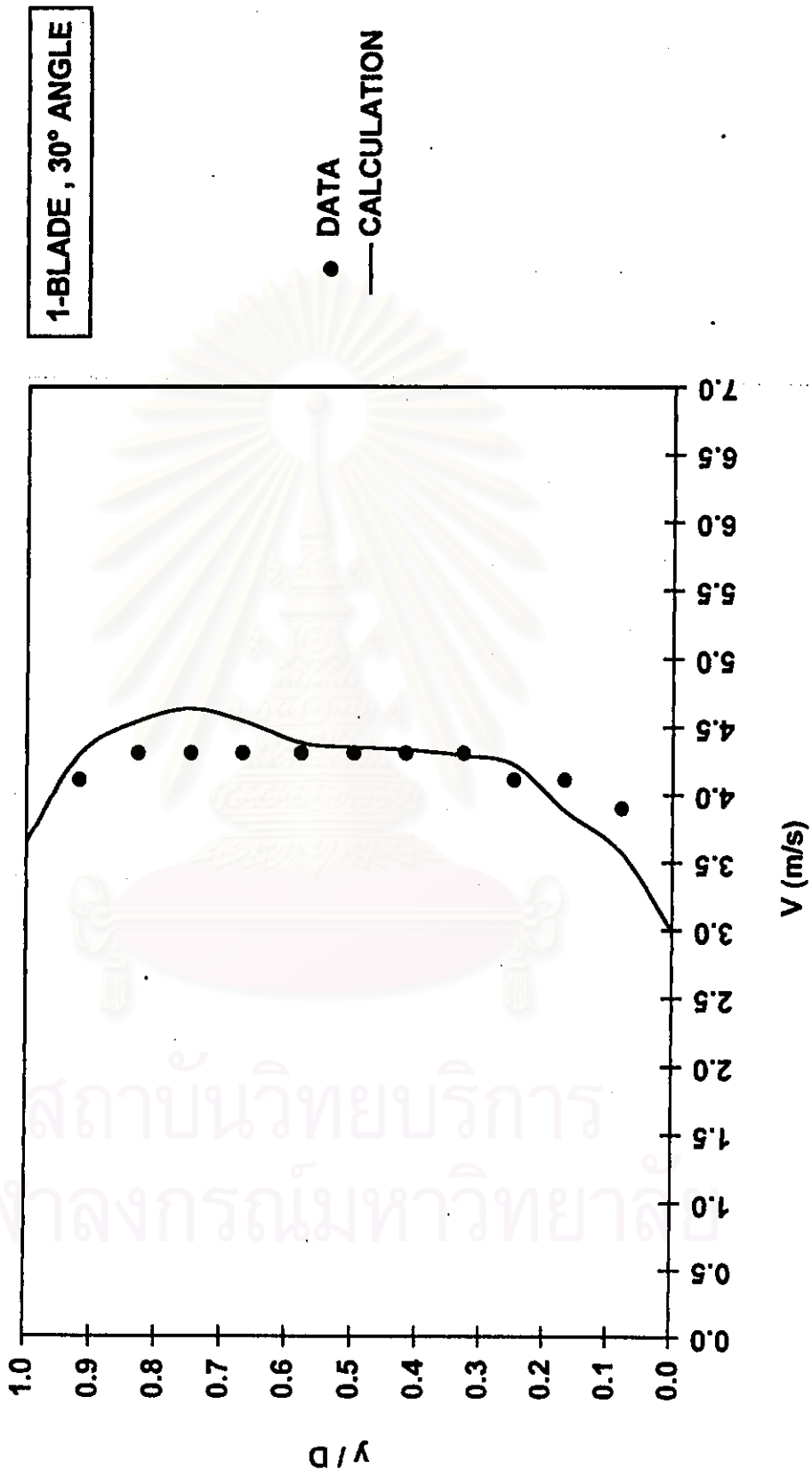

Figure 7.1(l) Measured and calculated mean-longitudinal-velocity profiles at L / D = 21.

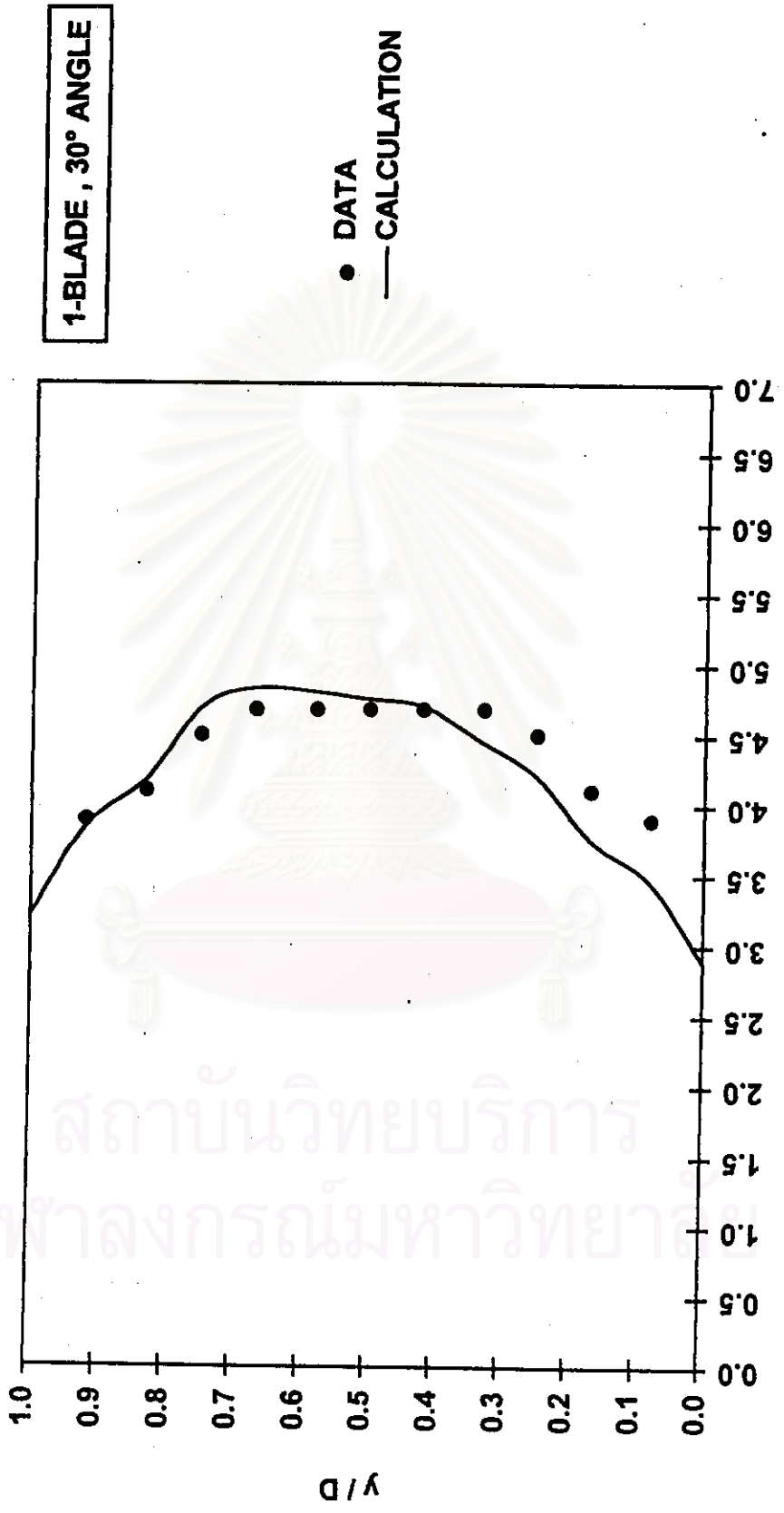

Figure 7.1(m) Measured and calculated mean-longitudinal-velocity profiles at L / D = 38.

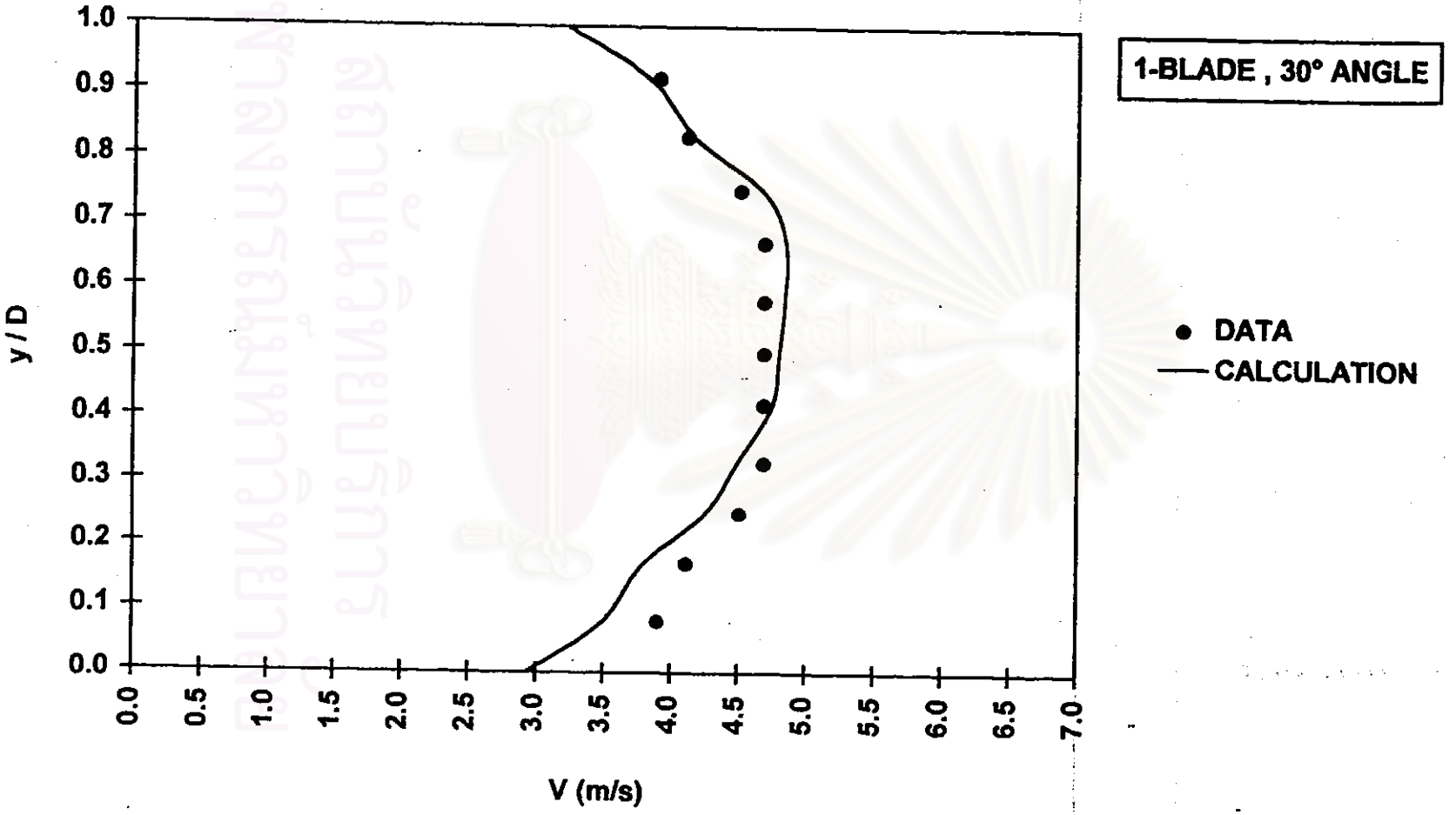

Figure 7.1(n) Measured and calculated mean-longitudinal-velocity profiles at L / D = 42.

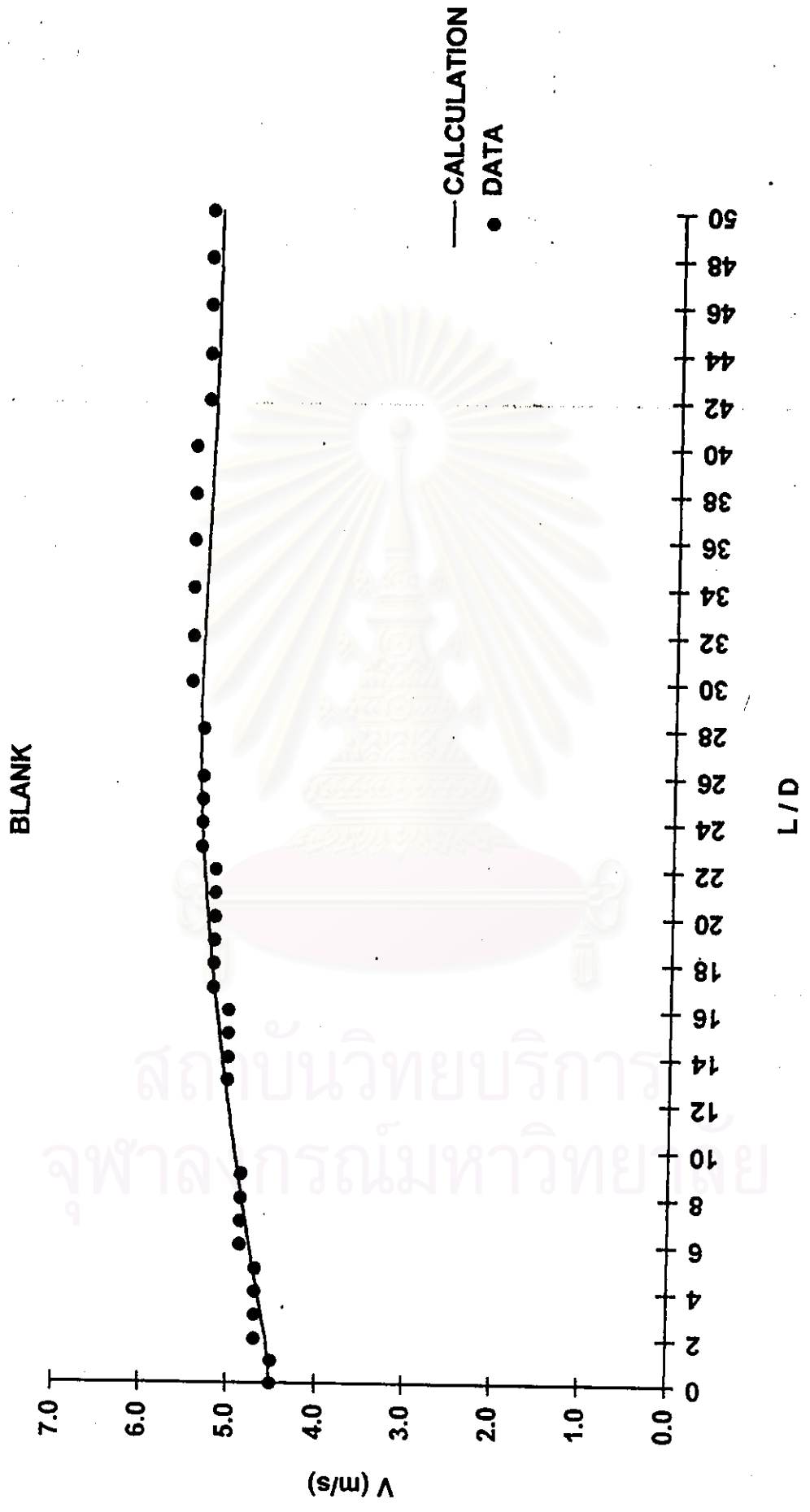

Figure 7.2(a) Measured and calculated mean-longitudinal-velocity distribution in a blank duct.

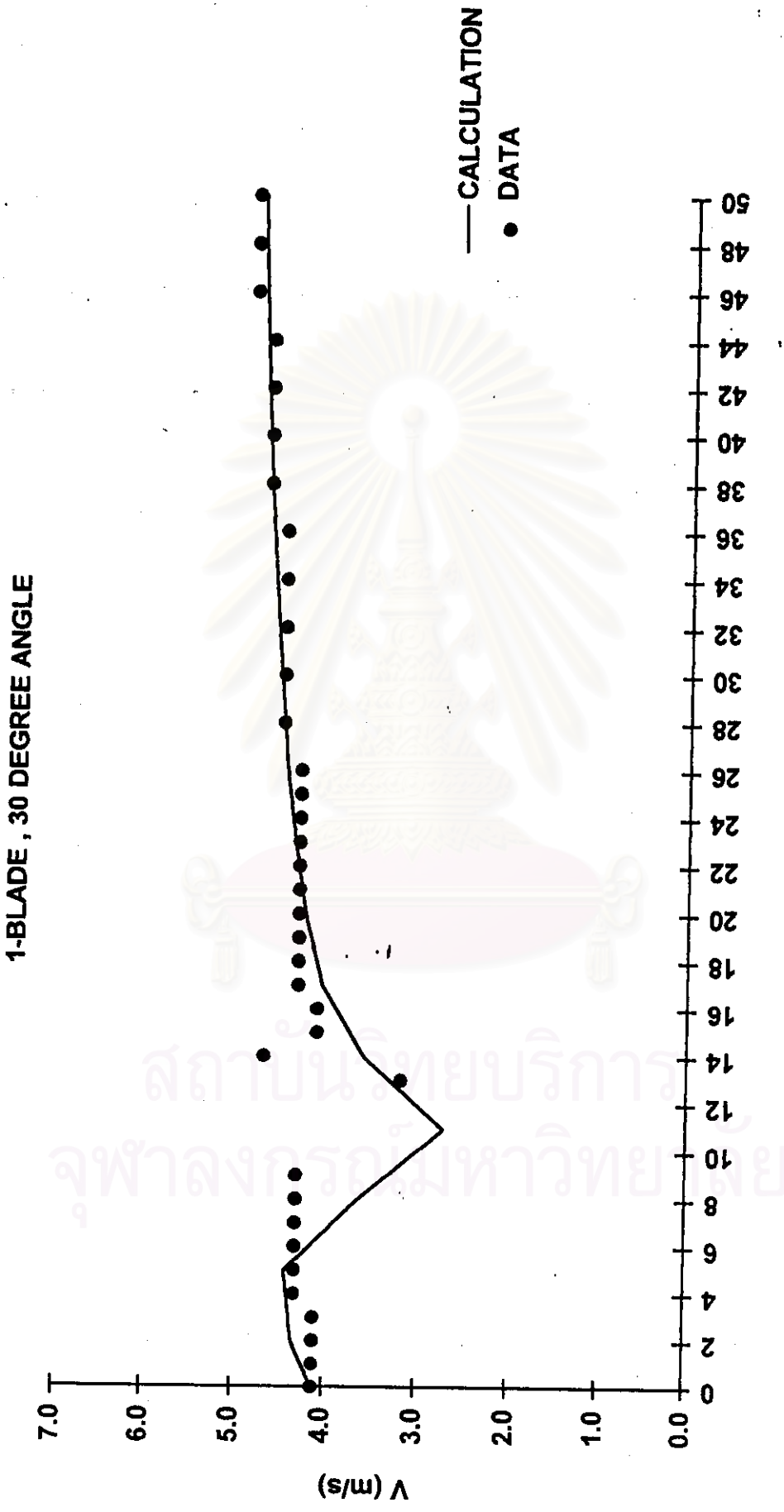

Figure 7.2(b) Measured and calculated mean-longitudinal-velocity distribution of 1-blade damper with 30 degree angle.

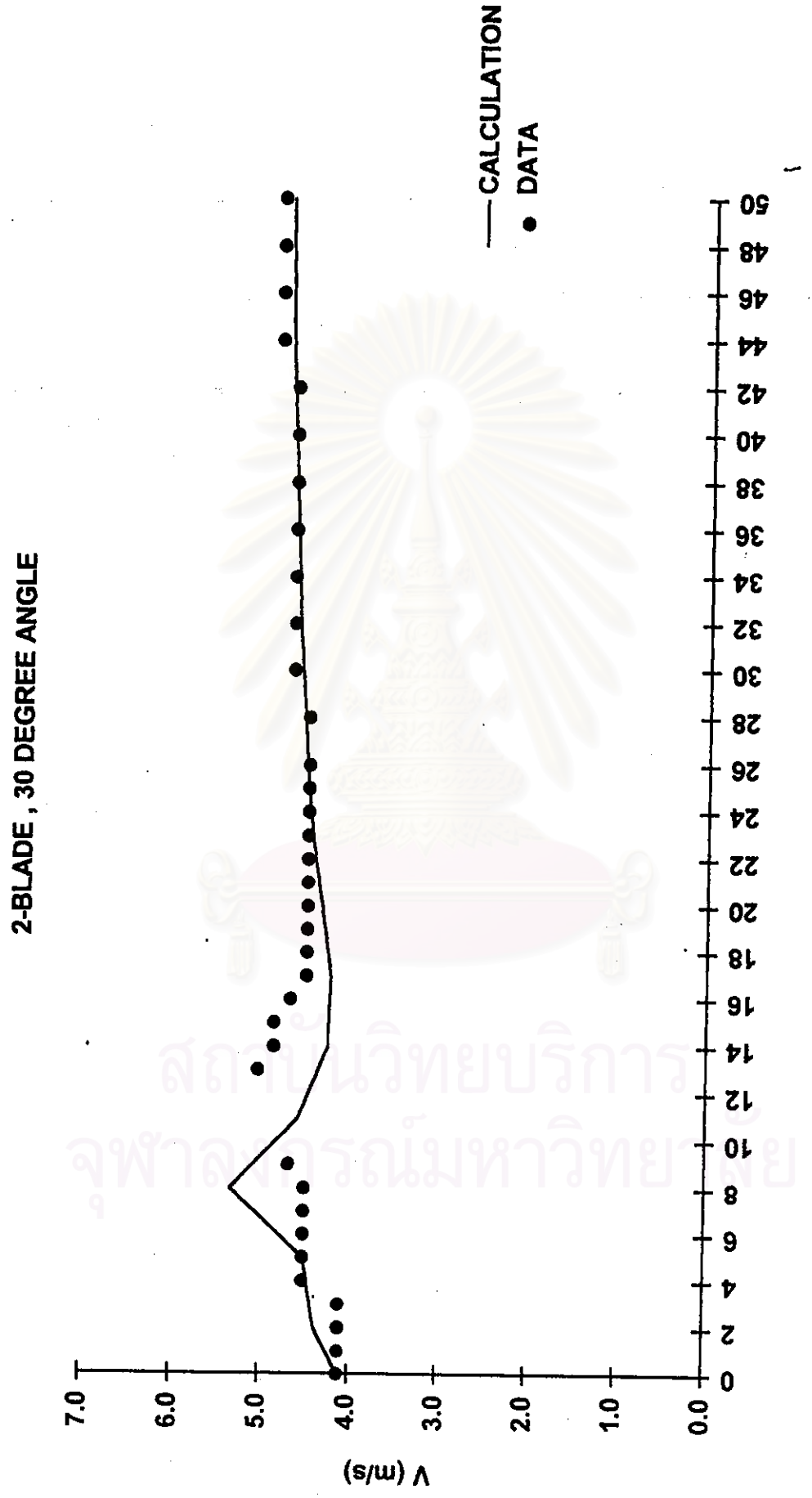

Figure 7.2(c) Measured and calculated mean-longitudinal-velocity distribution of 2-blade damper with 30 degree angle.

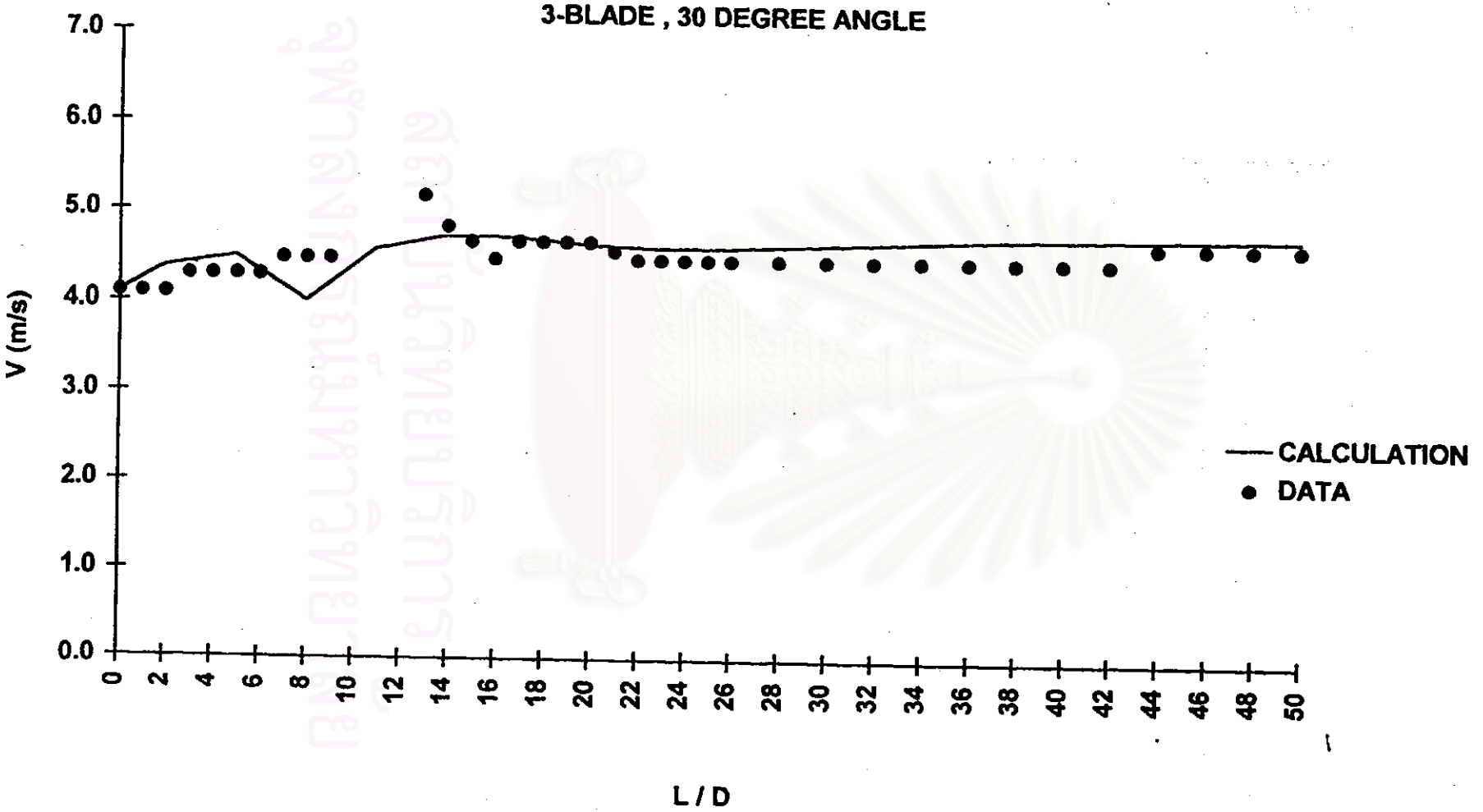

Figure 7.2(d) Measured and calculated mean-longitudinal-velocity distribution of 3-blade damper with 30 degree angle.

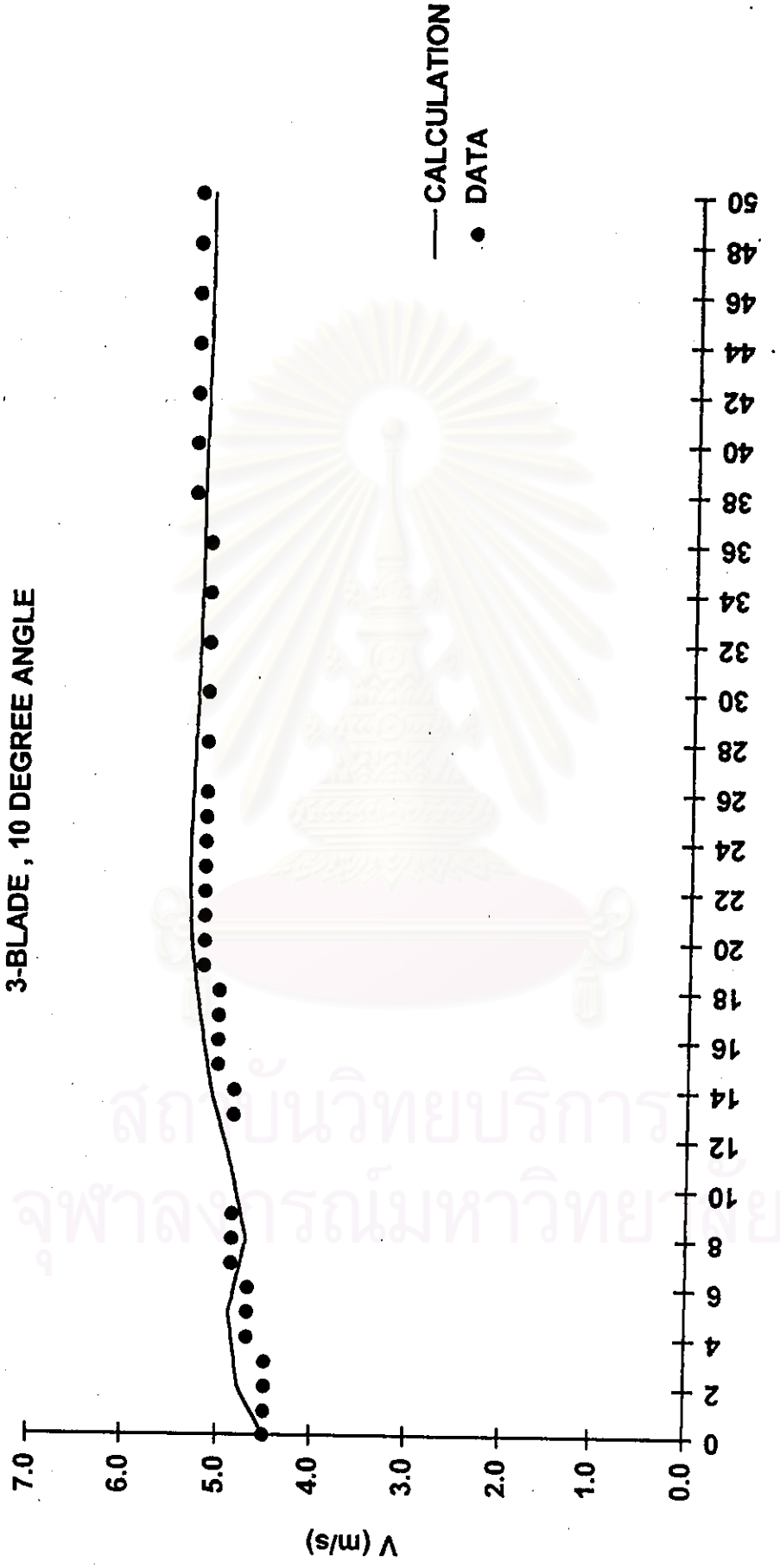

Figure 7.2(e) Measured and calculated mean-longitudinal-velocity distribution of 3-blade damper with 10 degree angle.

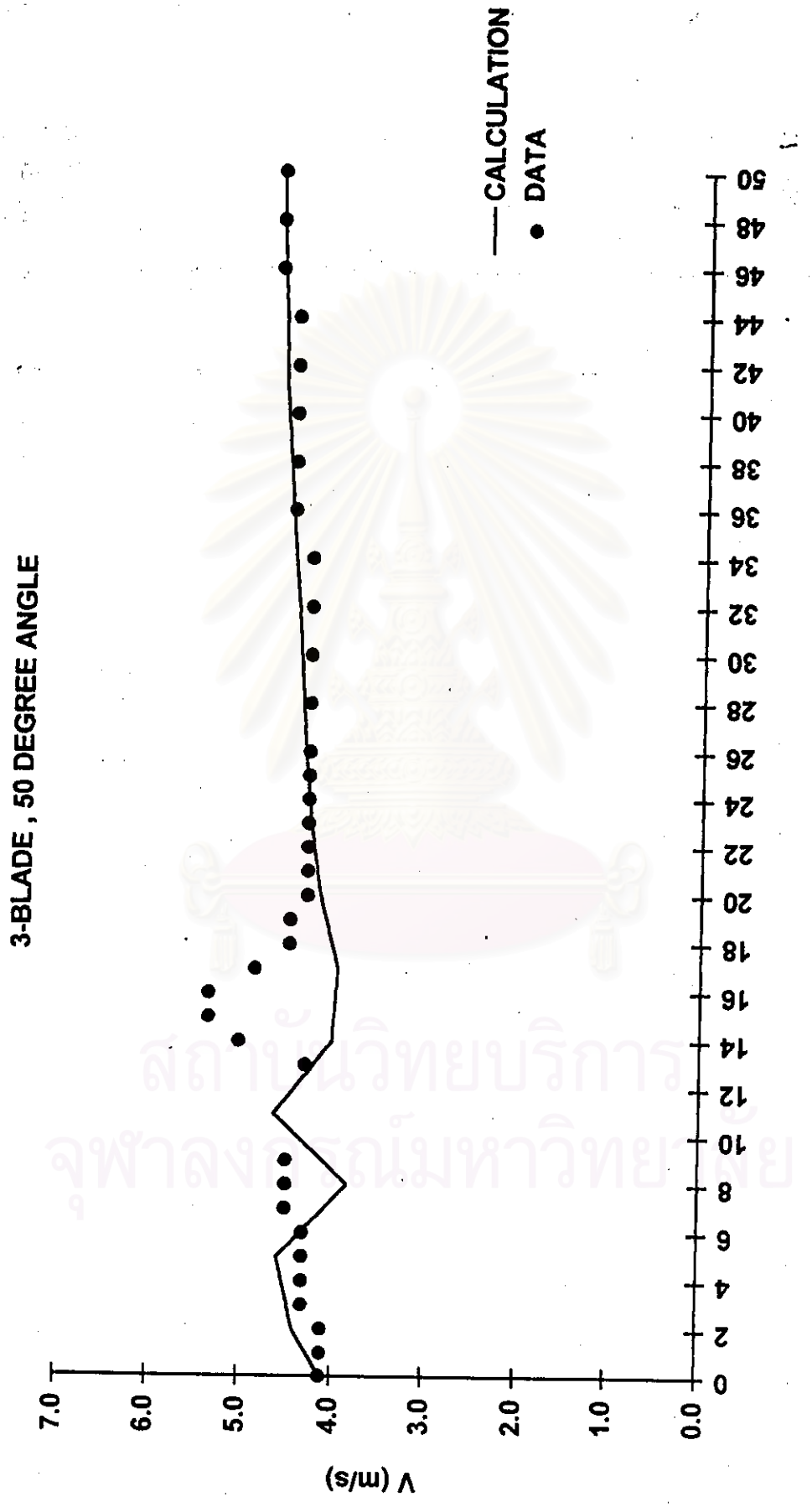

Figure 7.2(f) Measured and calculated mean-longitudinal-velocity distribution of 3-blade damper with 50 degree angle.

second part) and the numerical results (in this section) then find the corresponding value under the initial condition of the air flow in a blank duct. Therefore , at this criterion (norm < 0.03) , the simulations in the present study predict the phenomena of the flows which can be represented the actuality with reasonableness.

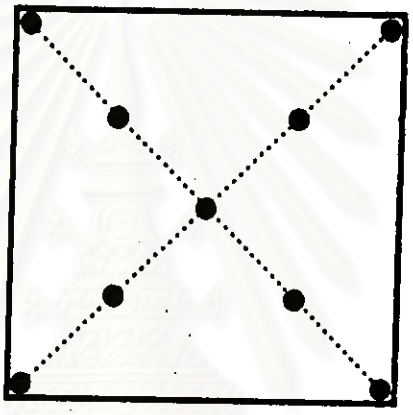

Figure 7.3 Positions of the collected numerical data for x-y plane.

The following predictions are performed up to Reynolds number of 3.9×10^4 that be common range of the engineering duct flow and maintained to be constant for all initial conditions in this section while the number and inclination of the flat plate in a square duct are varied.

By analogous with the experimental results , the computed mean velocity along flow direction at the centerline of the duct are demonstrated versus the dimensionless term of L / D , as shown in figures 7.4 to 7.9.

These results does not illustrate some expected information in the unmeasurable regions for the present experiments because of fitting the scale and ratio of the axis. However , such information as well as some interesting details of any initial condition is separately demonstrated by the graphic of the mean velocity profiles instead , as shown in figures 7.10 to 7.30.

First of all , a simplest fundamental case is considered that is the air flow in a square duct without any obstacle. Figure 7.10 shows the region around the inlet of a blank duct to confirm the inlet mean velocity is uniform then begins to develop the flow patterns along the increasing of the distance. When the flow becomes fully developed , according to the numerical results , the entrance length (L_e) is approximately 22 diameters of the duct as shown in figures 7.11 and 7.12 for the fully developed flow region in y-z plane (at the centerplane) and x-y plane respectively.

7.1.1 EFFECT OF THE NUMBER OF FLAT PLATES

Figure 7.4 illustrates the predictions of the centerline mean velocity distribution along flow direction of various dampers with 10 degree angle. At this small inclination , there are not so much different in the characteristic lines particularly 2-blade , 3-blade and a blank case. Moreover , figures 7.13 , 7.14 and 7.15 show the flow patterns at the test-section and nearby for 1- , 2- and 3-blade with 10 degree angle respectively.It is found that the velocity profiles of 3-blade case behind the flat plates are distorted from the undisturbed flow (as figure 7.10) less than the other cases. The numerical results also predict

the length behind the damper for fully developed flow as 18 diameters for 1-blade , 13 diameters for 2-blade and 11 diameters for 3-blade. Figures 7.22 , 7.23 and 7.24 present the corresponding informations by the developing mean velocity profiles about L / D = 20 (from the inlet) of 1- , 2- and 3-blade with 10 degree angle respectively. It is found that while 1- and 2-blade cases still be the under developed flow , at the same distance , 3-blade case is almost complete in developing to the fully developed flow.

Figure 7.5 illustrates the predictions of the centerline mean velocity distribution along flow direction of various dampers with 30 degree angle. At this inclination , all of the characteristic lines can be distinguished in the differences. For 3-blade case , the influence of the flat plates affects to the mean velocity fluctuations less than the other cases that also correspond with the experimental results (in the first part). Moreover , some interesting area which can not be measured in the experiments (due to limitations of the instrument) is demonstrated the details of the velocity vectors as shown in figures 7.16 , 7.17 and 7.18 for 1- , 2- and 3-blade with 30 degree angle respectively. It is interesting to note that the calculations show , as expected , there is a reversed flow region occurs behind a flat plate of 1-blade damper. This phenomena create the velocity profiles like a wake type distortion. While 2-blade damper has the smaller regions of the reversed flow behind each flat plate. Hence , the disturbance to the downstream flow is relieved. For 3-blade damper , there is no any the reversed flow region appears (under the present grid density in the calculation domain) , so the distortion of the velocity profiles is the least and also easily develop to the unchanged profiles at last.

Figures 7.25 , 7.26 and 7.27 confirm the resulting of the above phenomenon of 1- , 2- and 3-blade with 30 degree angle respectively. It is found that , at the distance of L / D = 20 , the development of mean velocity profiles of 3-blade case is faster than the other cases while 1-blade case is slowest due to the influence of the large recirculating zone behind the damper.

Under the present criterion , the length for fully developed flow of the initial conditions such as 30 degree angle and larger , is over than a existent square duct no matter which type of the damper . This meant that the experimental and numerical investigations in the length of the duct are not enough for fully developed flow. However , according to the available information , some useful information of engineering importance can be extracted and then leads to the reasonable conclusions which is discussed later at the end of this subsection.

Figure 7.6 illustrates the predictions of the centerline mean velocity distribution along flow direction of various dampers with 50 degree angle. At this large inclination , all of the characteristic lines can be obviously distinguished in the differences over 10 or 30 degree angle. The trend of the mean velocity fluctuations of 3-blade case still be less than the other cases same as two previous inclinations of the flat plate. Figures 7.19 , 7.20 and 7.21 present the predicted phenomena at the test-section and nearby for 1- , 2- and 3-blade with 50 degree angle respectively. It is found that the size of the reversed flow region in 1-blade case is larger than the other cases and exist around the centerline of the duct to produces wake-distorted velocity

profiles while the multi-blade damper generates asymmetric-distorted velocity profiles that the recirculating zone exist below the centerline of the duct. When increase of the distance until L / D = 20 , the development of the mean velocity profiles still goes on as shown in figures 7.28 , 7.29 and 7.30 for 1- , 2- and 3-blade with 50 degree angle respectively. However , the growth of developing the mean velocity profiles in the multi-blade cases is found to be faster than a single blade case.

In this subsection , effect of the number of flat plates has been studied and is remarked that when the air flow past the flat plate with fixed inclination in a square duct , the development length decreases if the number of the flat plate increases. This can be explained that the flow is separated at the leading and trailing edge of each flat plate of the damper. Thereafter , there are the reversed flow regions occur behind the flat plates (which can be observed easily with the large inclination). The size of those regions depends on the dimension of the flat plate that obstructs the flow. For 1-blade damper , the region of reversed flow is the biggest and this phenomena can strongly affect to the downstream velocity profiles then the length for fully developed flow is longer than the other types of the damper. When number of the blade increases as two blades , although there are more reversed flow regions occur but their size are reduced because the breadth of each flat plate becomes a half of 1-blade case (or D / 2). Therefore , this can relieve the influence of the reversed flow , moreover , the separated flows can easily reattach then begin to redevelop again because there are three allowed pathways of the air

flow past this damper while 1-blade damper has only two allowed pathways (top and bottom gaps of a flat plate). In case of 2-blade damper , the stream of the air that flows through a gap between a upper-blade and a lower-blade can improve the mixing of the adjacent separated flows. Afterwards , such behavior also can interfere the formation of the reversed flow region behind a upper-blade. That are the explanations for the differences in size of the reversed flow regions in case of 2-blade damper although each blade has identical dimension. Accordingly , the length for fully developed flow of this case is shorter than 1-blade case. For 3-blade damper , the size of the reversed flow regions is the smallest due to the breadth of each flat plate becomes D / 3. Moreover , there is the influence of the air stream that flow through the gaps among the blades (or through four allowed pathways). Further explanations of this phenomena can be described as the following step. Beginning from the back of a top-blade which is interfered by the air stream that flows through a gap between a top- and a mid-blade. Next , the back of a mid-blade which also is interfered by the flow past between a mid- and a bottom-blade. Last , the back of a bottom-blade which gets such influence less than the other blades because the air stream must flows through a small gap between a bottom-blade and a bottom-wall. Therefore , the interference to the formation of the reversed flow region is not so effective then the large size of it still be maintained in the downstream flow upon the bottom wall. However , the mean velocity profiles behind this damper get closer to the fully developed flow than the other cases. Therefore , such flow

takes the shortest distance of the development length too. Furthermore , there are some interesting remarks on a blank case compared with 10 degree angle of the various dampers. It is found that at this inclination , when the flow is obstructed by the present obstacles in the duct , the redeveloped profiles reach the fully developed flow earlier than the flow in the blank duct. This can be explained that in the duct without any obstacle has nothing to enforce the movement of the air flow in the different directions such as the mixing , recirculating , or even fluctuating. These types of the flow let the momentum transfer to be faster than the natural developing flow in a blank duct.

7.1.2 EFFECT OF THE INCLINATION OF FLAT PLATES

Figure 7.7 illustrates the predictions of the centerline mean velocity distribution along flow direction of 1-blade damper with various inclinations. For any degree angle of a flat plate , all of the characteristic lines indicate the same trend but different in the amplitude around the test-section area. Moreover , figures 7.13 , 7.16 and 7.19 show the flow patterns at the test-section and nearby for 10 , 30 and 50 degree angle of 1-blade damper respectively. It is found that at the smallest inclination as 10 degree angle , the downstream mean velocity profiles are distorted from the undisturbed flow less than the other cases. The available numerical results predicted the length for fully developed flow about 18 diameters of the duct. While the larger inclinations as 30 and 50 degree angle require such length over 40 diameters of the duct behind the damper. Figures 7.22 , 7.25 and 7.28 present the mean

velocity profiles of 1-blade damper in the developing zone about L / D = 20 for 10 , 30 and 50 degree angle respectively. These informations confirm the above mentions on the development length of each case. For 10 degree angle , the developing of the velocity profiles to be the fully developed flow is progressed rapidly than 30 degree angle and much more than 50 degree angle because the influence of the reversed flow behind a flat plate increases with its size.

Figure 7.8 illustrates the predictions of the centerline mean velocity distribution along flow direction of 2-blade damper with various inclinations. A characteristic line of 10 degree angle is quite similar to a blank case and the length for fully developed flow is predicted about 13 diameters of the duct. When the inclinations become as larger as 30 and 50 degree , the predictions of the development length must take the distance not less than 40 diameters of the duct due to the large fluctuations of the mean velocity which are resultant from the reversed flow behind the flat plates. Figures 7.14 , 7.17 and 7.20 show the velocity vector profiles at the test-section and nearby for 10 , 30 and 50 degree angle of 2-blade damper respectively. It is found that the size of the reversed flow regions is enlarged if the slope of the blades against to the upstream flow is increased and that surely affects to the distance for fully developed flow. Moreover , figures 7.23 , 7.26 and 7.29 present the developing mean velocity profiles of 2-blade damper about L / D = 20 for 10 , 30 and 50 degree angle respectively. The flow patterns in case of the smallest inclination are the symmetric-velocity profiles and get close to the fully

.developed flow more than the cases of the larger inclinations that the flow patterns just redevelop from the asymmetric-velocity profiles.

Figure 7.9 illustrates the predictions of the centerline mean velocity distribution along flow direction of 3-blade damper with various inclinations. It is found that although the trend of the characteristic lines at any inclination is similar but some differences of the velocity fluctuations still be identified and corresponding with the experimental results. Moreover , the unmeasurable regions nearby the damper in the experiments are demonstrated the details of the velocity vectors as shown in figures 7.15 , 7.18 and 7.21 for 10 , 30 and 50 degree angle of 3-blade damper respectively. At the smallest inclination , the mean velocity profiles behind the flat plates are almost the same as the undisturbed flow. This confirms that such flow requires the shortest distance for fully developed flow if compares with the other inclinations. According to the numerical results , it is approximately 11 diameters of the duct. While the cases of 30 and 50 degree angle are predicted that the development length is longer than of 10 degree angle case and also the available length of 40 diameters behind the damper in the present study is not long enough for recovering the separated boundary-layers then redeveloping the flow patterns until finally reaching the fully developed flow. Figures 7.24 , 7.27 and 7.30 present the mean velocity profiles in the developing flow region about L / D = 20 of 3-blade damper with 10 , 30 and 50 degree angle respectively. At this same distance behind the damper , the flow patterns with the small and moderate inclinations as 10 and 30 degree angle can develop to be faster

than the large inclination as 50 degree angle and such behaviors lead the under developed flow to reach the fully developed flow earlier.

In this subsection , effect of the inclination of flat plates has been studied and is remarked that when the air flow past the flat plate with varied inclinations in a square duct , the development length extends if the inclination of the flat plate increases. This can be explained that the flow is separated at the sharp edges of each flat plate of the damper. Thereafter , there are the reversed flow regions occur behind the flat plates (which can be observed easily in a single blade damper). Their size of those regions depend on the degree angle of attack to the undisturbed flow which also is proportional to the separation distance (the perpendicular distance between the adjacent separated flow behind any flat plate). For 10 degree angle , the separation distance is so short then the influence of the reversed flow can not strongly disturb the developing of the flow patterns. Hence , the length for fully developed flow of this case is shorter than the other cases. When the inclination increases as 30 degree angle , the regions of the reversed flow also enlarges due to the separation distance becomes longer than the former case. Therefore , till the adjacent separated flows reattach together again for the transference of the momentum of the air then developing to the unchanged velocity profiles at last , such process requires the longer development length. At the largest inclination of 50 degree angle , the separation distance much more extends and this surely affects to the enlargements of the reversed flow regions which directly disturb to the

downstream velocity profiles and produce the extreme velocity fluctuations , accordingly , the required distance for fully developed flow is the longest too.

By the way , the additional information of the total pressure value , that is predicted for each geometry , also is available here.

Figure 7.31 illustrates the pressure distribution in the blank duct. It is found that the pressure value continually drops over the length of the duct (from the inlet) due to the friction loss at the wall.

Figure 7.32 , 7.33 and 7.34 illustrate the pressure distribution in the region nearby the damper for 1- , 2- and 3-blade respectively. It is found that there is a pressure difference between the high pressure over the upstream surface of the flat plate and the low pressure on the downstream surface of the flat plate in the near wake thus causing a pressure drag force on the flat plate in the direction of air flow. Consequently , this behavior also let the loss of momentum at the flat plate beyond at the wall only as the air flow in the blank duct. Such pressure difference is the largest in case of 1-blade damper thus the largest size of the reversed flow region occurs behind the flat plate while a pressure difference in 2- and 3-blade damper becomes small and smaller respectively , therefore , their regions of the reversed flow also occupy the smaller size than a single blade damper.

7.2 APPLICATION OF THE PREDICTIONS

For the real practice of air-handling systems , some factors have been set such as the type of the damper that involves with number of the flat plate , or

even the adjustment of the open-closed position for controlling the flow that involves with inclination of the flat plate. The studies of these both factors have been done in subsection 7.1.1 and 7.1.2 respectively. Consequently , in this section , the other factors are studied such as the dimension of the duct and the velocity of the air that are in the parts of Reynolds number definition and be able to use for reference in the case of the dynamics similarity.

In order to be corresponding with the actual conditions , thus the dimension of the duct must be changed into the large scale but still having the square crosssectional area by using the hydraulic diameter (D_h) equals to 0.8 m (equivalent to the normal diameter of the duct , D) to follow the real industrial design (or about 5 times of the test-section in chapter VI) and 40 m in length of the duct. The damper is located at the position of L / D = 6 behind the inlet of the duct.

Study on the air flow with the uniform inlet velocity past various types of the damper : 1- , 2- and 3-blade with fixed inclination at 30 degree angle and including another case of the blank duct , is performed. Here Reynolds number (Re) is varied for each initial condition. In the engineering application , Re is in the range of 10^4 - 10^5 as usual (the average velocity in the duct is about 10 m/s). In the present study , the range of Re is extended to cover the high-velocity duct system from 2.6×10^5 to 1.0×10^6.

The grid density in the calculation domain must be changed from the previous section become $3 \times 30 \times 70$ for $N_x \times N_y \times N_z$ respectively due to

suitability of the real geometry and the computer limitations. While the boundary conditions still maintain the same except the inlet velocity that is varied for 5 , 10 and 20 m / s and the external pressure becomes 210 N / m^2. The presentation of the numerical results in this section will be separated for two aspects :

The first is the illustration of the characteristic line of the centerline mean velocity over the length of the duct for each initial condition with various Re as shown in figures 7.35 to 7.38.

The second is the illustration of the mean velocity vectors around the damper and some interesting areas as shown in figures 7.39 to 7.50.

7.2.1 EFFECT OF HIGH REYNOLDS NUMBER

Figure 7.35 illustrates the predictions of the centerline mean velocity distribution along flow direction in a blank duct with various Reynolds numbers. The trend of all characteristic lines gradually change from the inlet to the outlet of the duct. The further details as figures 7.39 , 7.40 and 7.41 present the vector profiles of the mean-longitudinal-velocity in a blank duct around the position of L / D =18 under Reynolds number of 2.6×10^5 , 5.1×10^5 and 1.0×10^6 respectively. It is found that the developing of the core flow is shifted to the downstream side when Reynolds number is increased. This meant that the growing of boundary-layers of the lower Re case is naturally faster than the higher Re case at the same distance. Therefore , it can be reasonably concluded that the length for fully developed

flow in the blank case is extended as increase of Re which is corresponding with the former empirical relation (3.5) of basic knowledge in chapter III.

Figure 7.36 illustrates the predictions of the centerline mean velocity distribution along flow direction of 1-blade damper with various Reynolds numbers. It is remarked that the air velocity in the upstream section is decelerated due to the influence of a flat plate (its size equals to the diameter of the duct , D) which hardly obstructs the flow around the center of cross-sectional area of the duct then the velocity drop occurs particularly in case of high Reynolds number. Subsequently , the flow is separated at the leading and trailing edge of a flat plate then forms the region of the reversed flow as shown in figures 7.42 , 7.43 and 7.44 for Reynolds number of 2.6×10^5 , 5.1×10^5 and 1.0×10^6 respectively. It is found that when Re is increased , the size of the wake behind a flat plate is enlarged and such phenomena surely more disturbs to the development of the downstream flow in case of higher Re.

Figure 7.37 illustrates the predictions of the centerline mean velocity distribution along flow direction of 2-blade damper with various Reynolds numbers. It is remarked that the air velocity in the upstream section is accelerated due to the influence of a gap between the both parallel flat plates because the flow is squeezed through this narrow area. Hence , the mean-longitudinal-velocity is increased to conserve the mass flow rate to be constant over the length of the duct. Thereafter , the separations of the flows are occured at the edges of each flat plate then produce the recirculating flow

regions as shown in figures 7.45 , 7.46 and 7.47 for Reynolds number of 2.6×10^5 , 5.1×10^5 and 1.0×10^6 respectively. It is found similarly as 1-blade damper case that the air flow at higher Re requires the distance for developing the flow patterns , to be longer than the lower Re case.

Figure 7.38 illustrates the predictions of the centerline mean velocity distribution along flow direction of 3-blade damper with various Reynolds numbers. It is remarked that the air velocity in the upstream section is decelerated but not strongly as 1-blade damper case because the breadth of a middle flat plate which obstructs the flow , is decreased to be only D / 3. Moreover , all of characteristic lines does not show in differences of the mean velocity fluctuations for any Reynolds number with significantly as two previously mentioned dampers. When the flow is separated at the sharp edges of the flat plates as shown in figures 7.48 , 7.49 and 7.50 for Reynolds number of 2.6×10^5 , 5.1×10^5 and 1.0×10^6 respectively , the downstream flow patterns begin to redevelop the boundary-layers again , according to the numerical results of this damper , the differences of the flow patterns between the higher and lower Re cases can be obviously observed in the far wake region that the trend of the development to be fully developed flow at the lower Re case progress rapidly than the higher Re case.

In this subsection , effect of high Reynolds number has been studied and is remarked that when the air flow past the flat plate with fixed inclination in a square duct , the development length extends if Reynolds number of the air flow increases. This can be explained that the separated flows left from the

leading and trailing edge of each flat plate with the lower velocity in case of lower Re as 2.6×10^5. Thereafter , the adjacent separated flows reattach again at some distance in the downstream flow then begin to redevelop the velocity profiles until finally become the fully developed flow (which still be over the whole length of the present duct). However , the available information is sufficient to indicate that the trend of the development length in case of higher Re as 5.1×10^5 is extended due to the adjacent separated flows carry the higher momentum at the separation points. Consequently , such flow must takes the longer distance for reattaching , recovering and redeveloping to the unchanged velocity profiles and also the longest distance for fully developed flow surely requires with the highest Re as 1.0×10^6 of the air flow.

By the way , the additional information of the total pressure drop , that is predicted for each geometry , also is available here.

According to the numerical results , total pressure drop across the inlet and outlet of the square duct at the same Re , approximately are 33 , 24 and 18 N / m^2 for 1- , 2- and 3-blade damper cases respectively as shown in figures 7.51 , 7.52 and 7.53. This indicates that the pressure drop reduces when the number of flat plates increases. Due to the pathways of air flow are increased and the obstructed surface areas are decreased , thus causing the momentum loss is relieved then total pressure along the length of the duct gradually drops too.

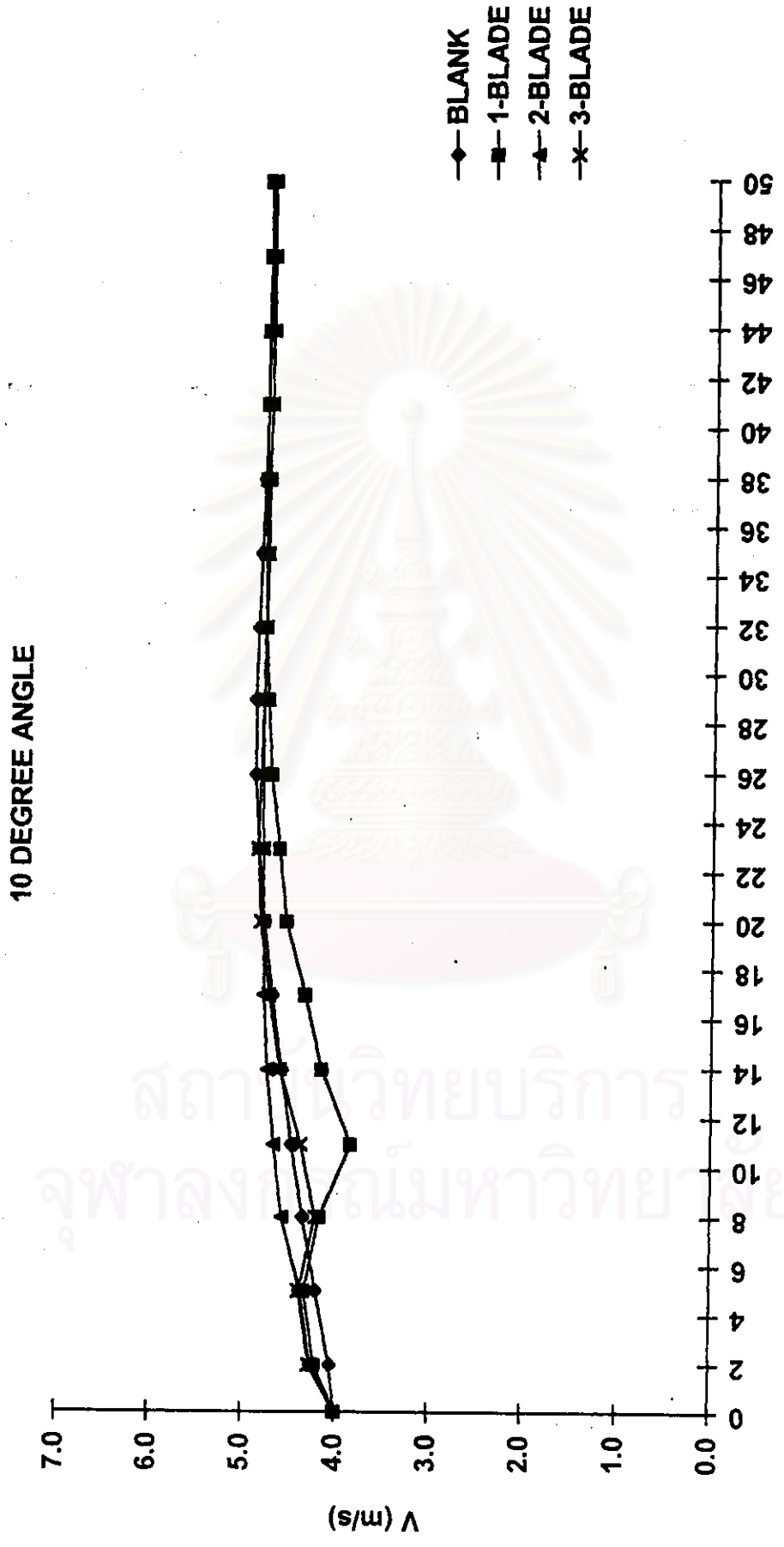

Figure 7.4 Centerline mean-longitudinal-velocity distribution of various dampers with 10 degree angle.

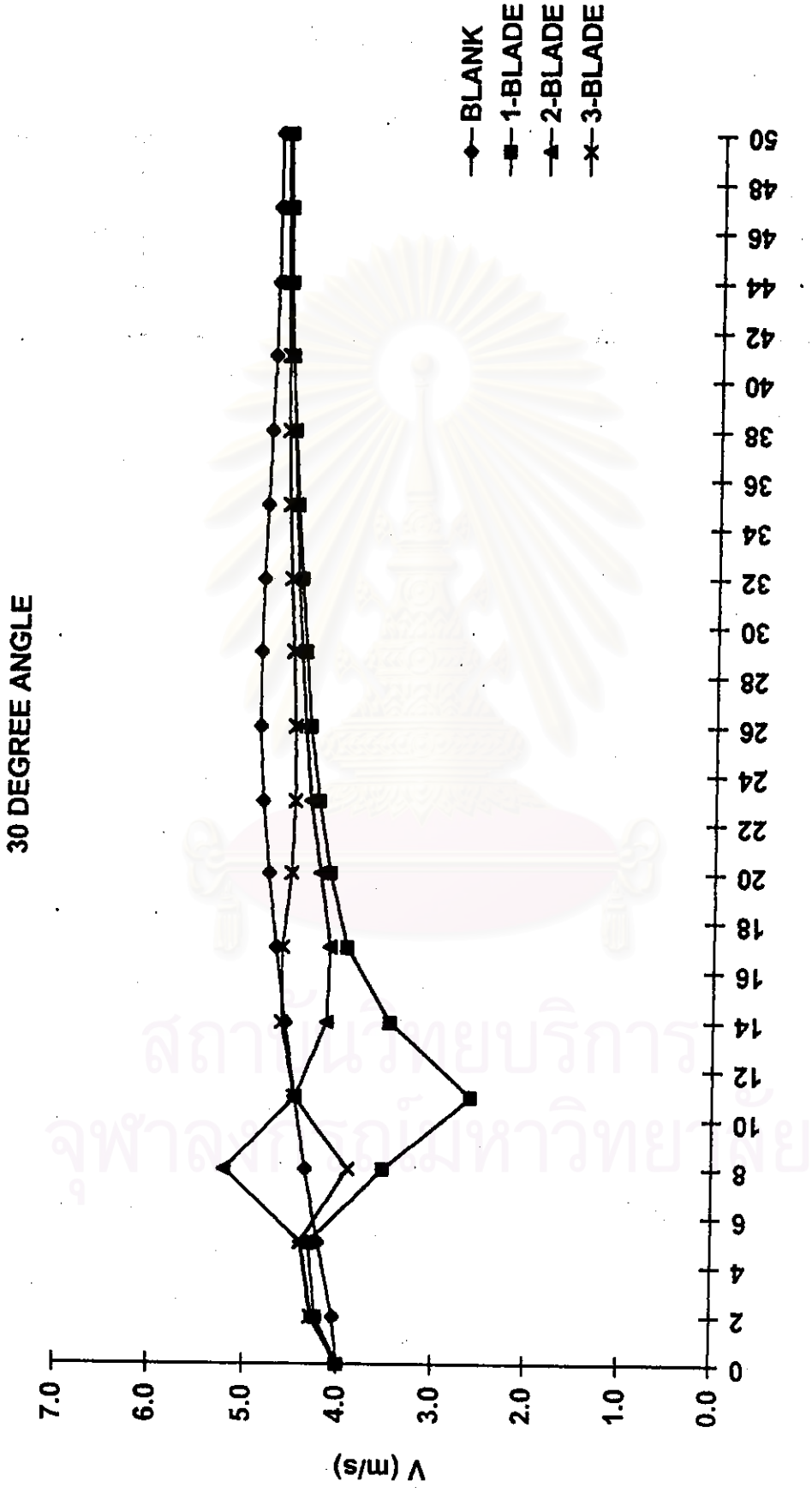

Figure 7.5 Centerline mean-longitudinal-velocity distribution of various dampers with 30 degree angle.

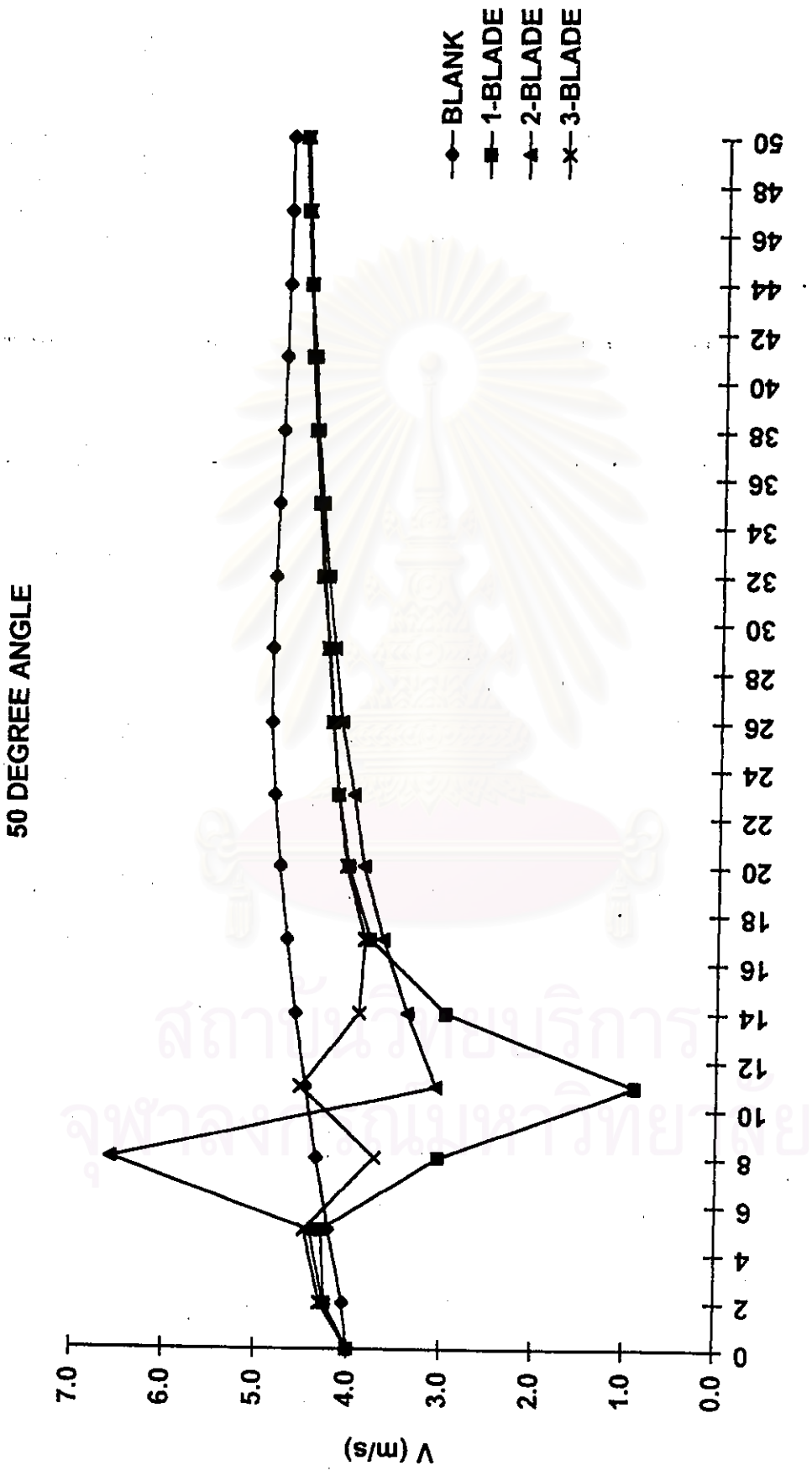

Figure 7.6 Centerline mean-longitudinal-velocity distribution of various dampers with 50 degree angle.

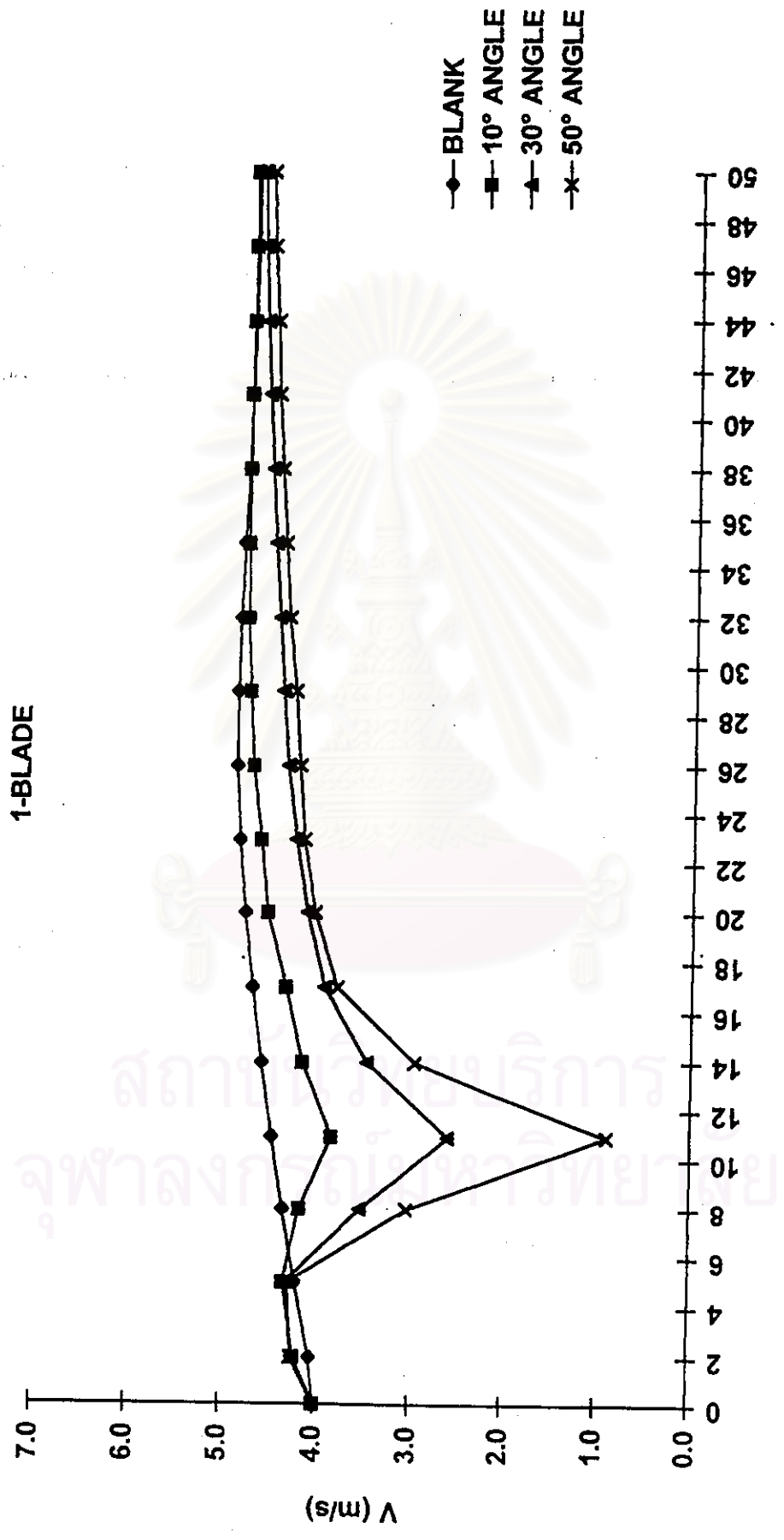

Figure 7.7 Centerline mean-longitudinal-velocity distribution of 1-blade damper with various inclinations.

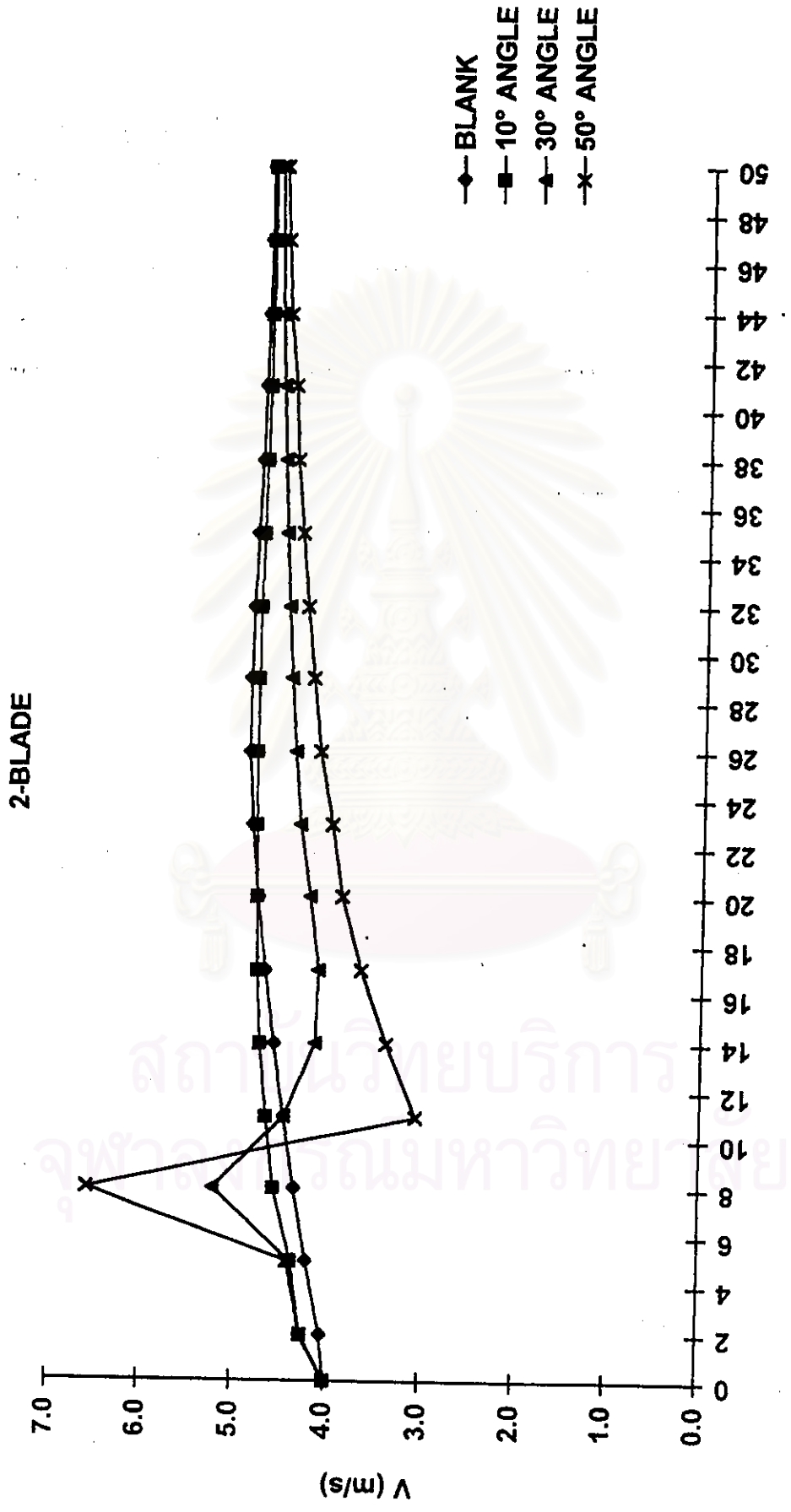

Figure 7.8 Centerline mean-longitudinal-velocity distribution of 2-blade damper with various inclinations.

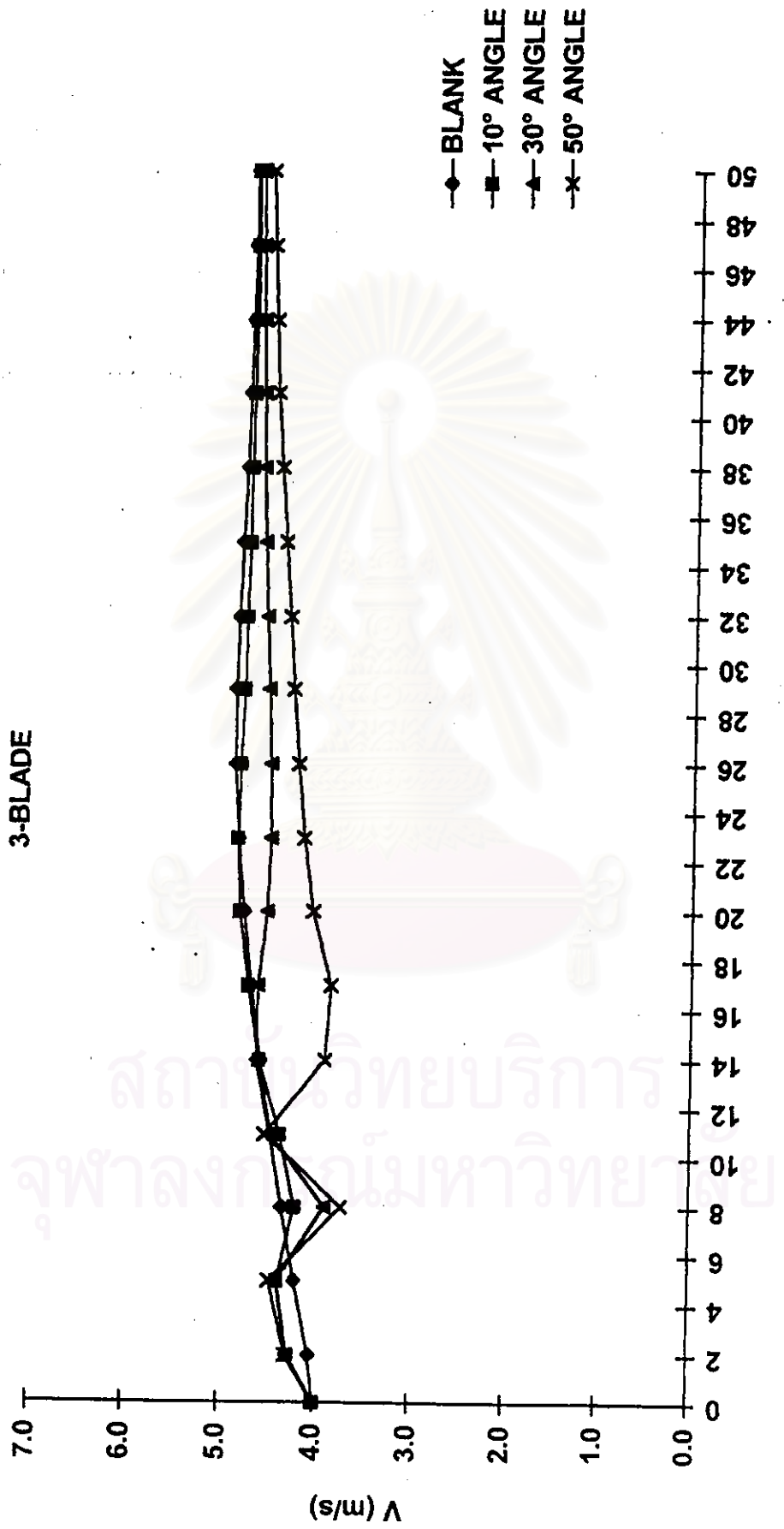

Figure 7.9 Centerline mean-longitudinal-velocity distribution of 3-blade damper with various inclinations.

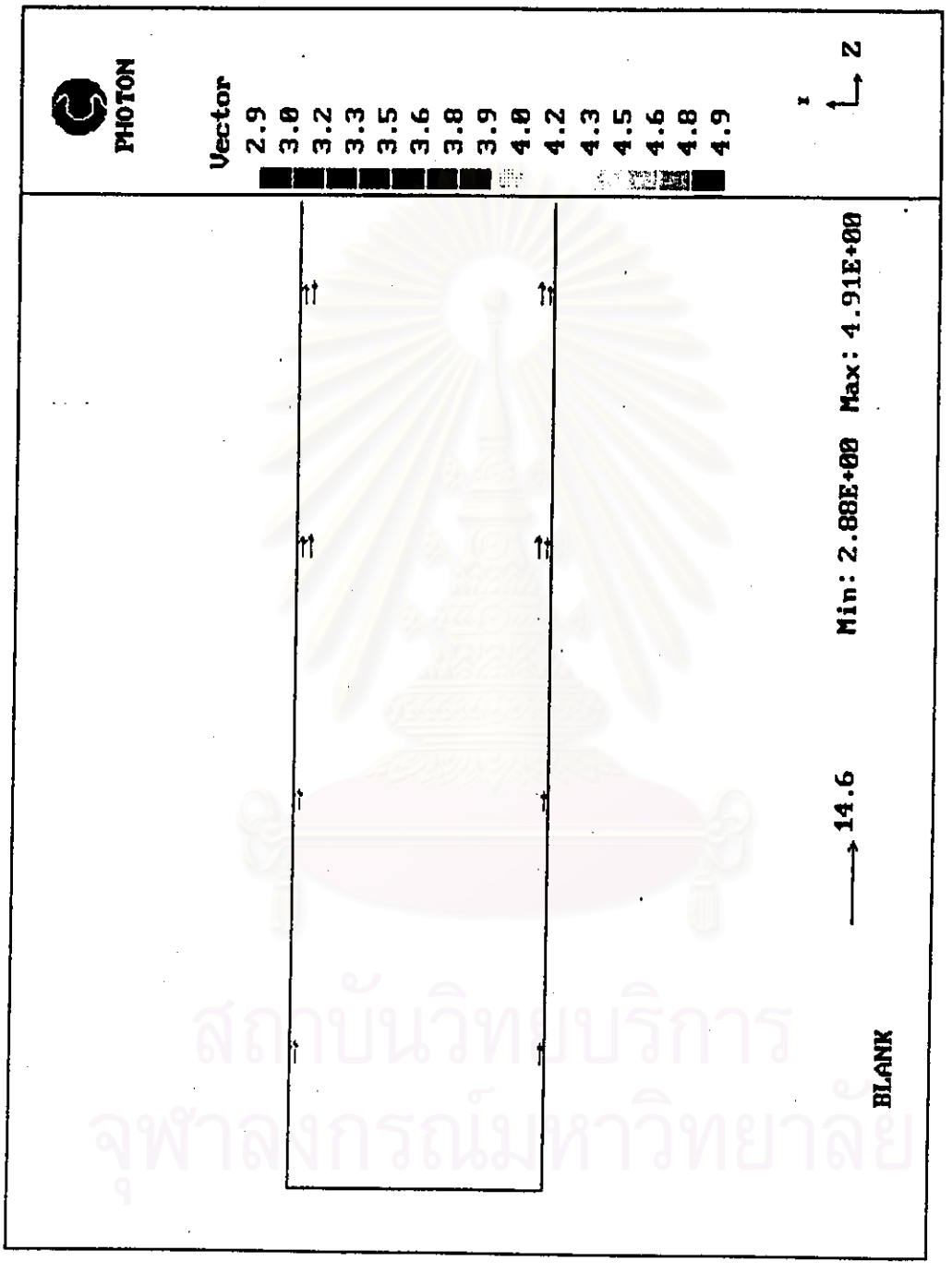

Figure 7.10 Mean velocity profiles at the inlet of a blank duct.

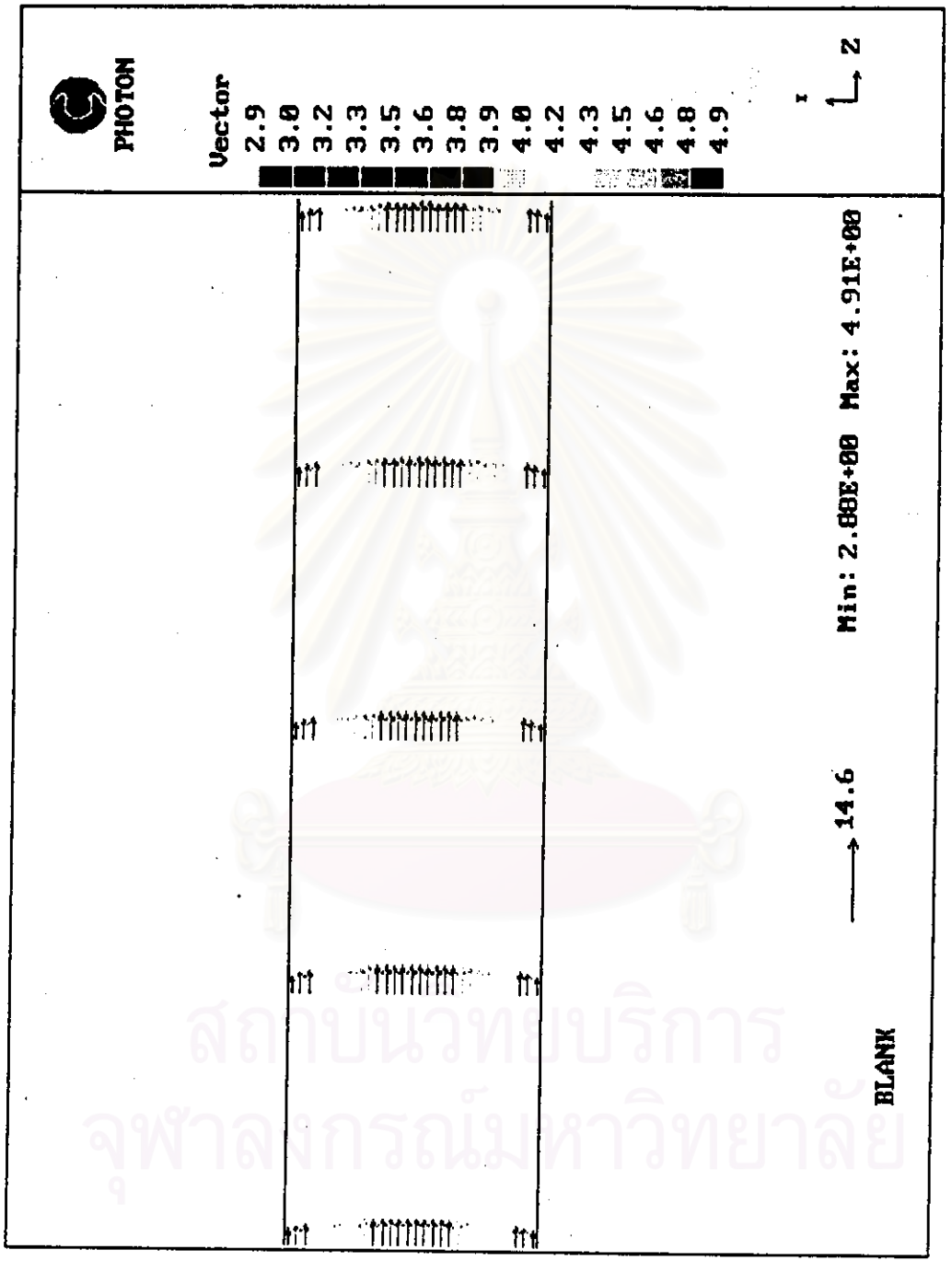

Figure 7.11 Fully developed flow in a blank duct for y-z plane (about L / D = 22).

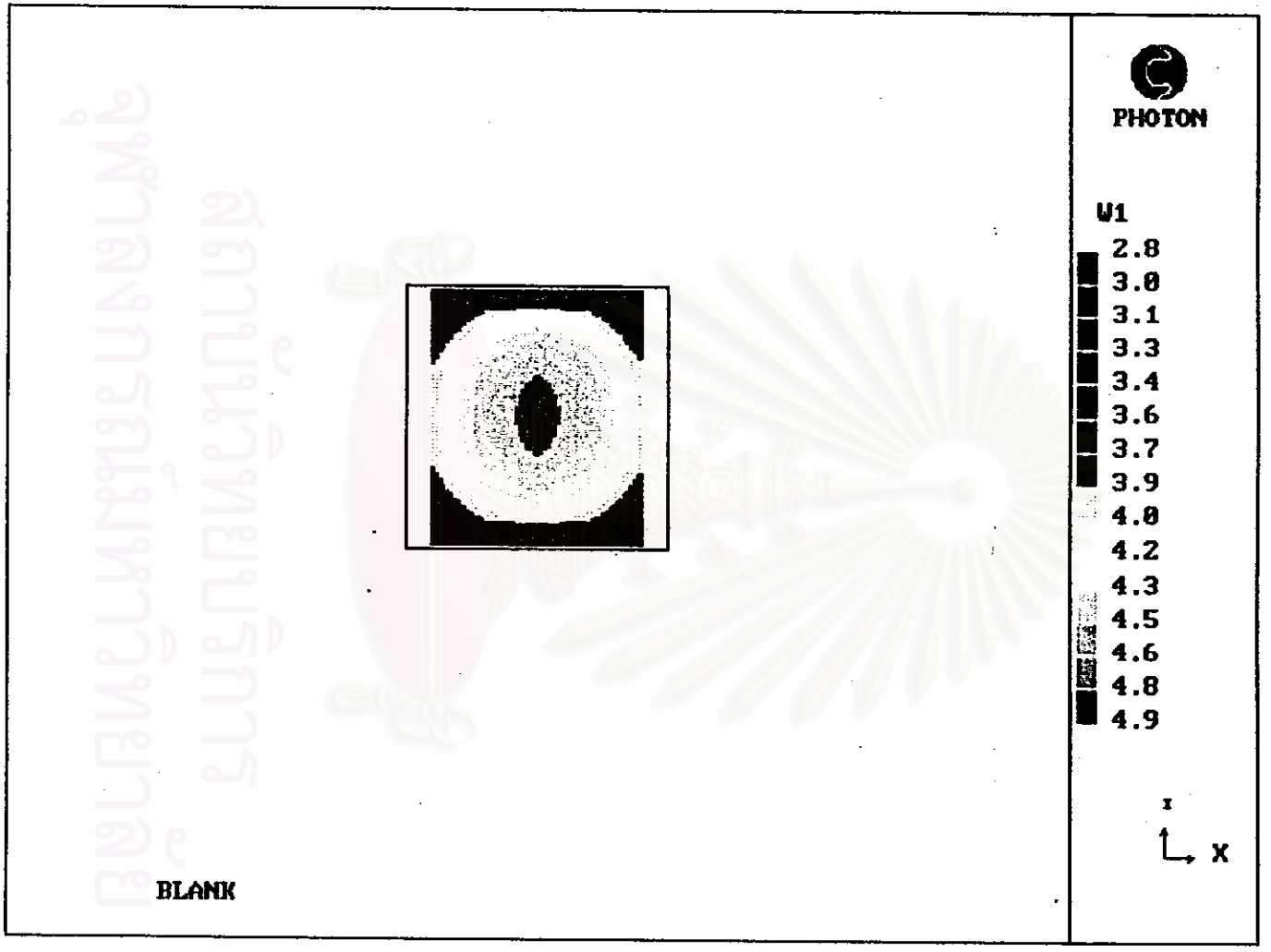

Figure 7.12 Fully developed flow in a blank duct for x-y plane (at L / D = 22).

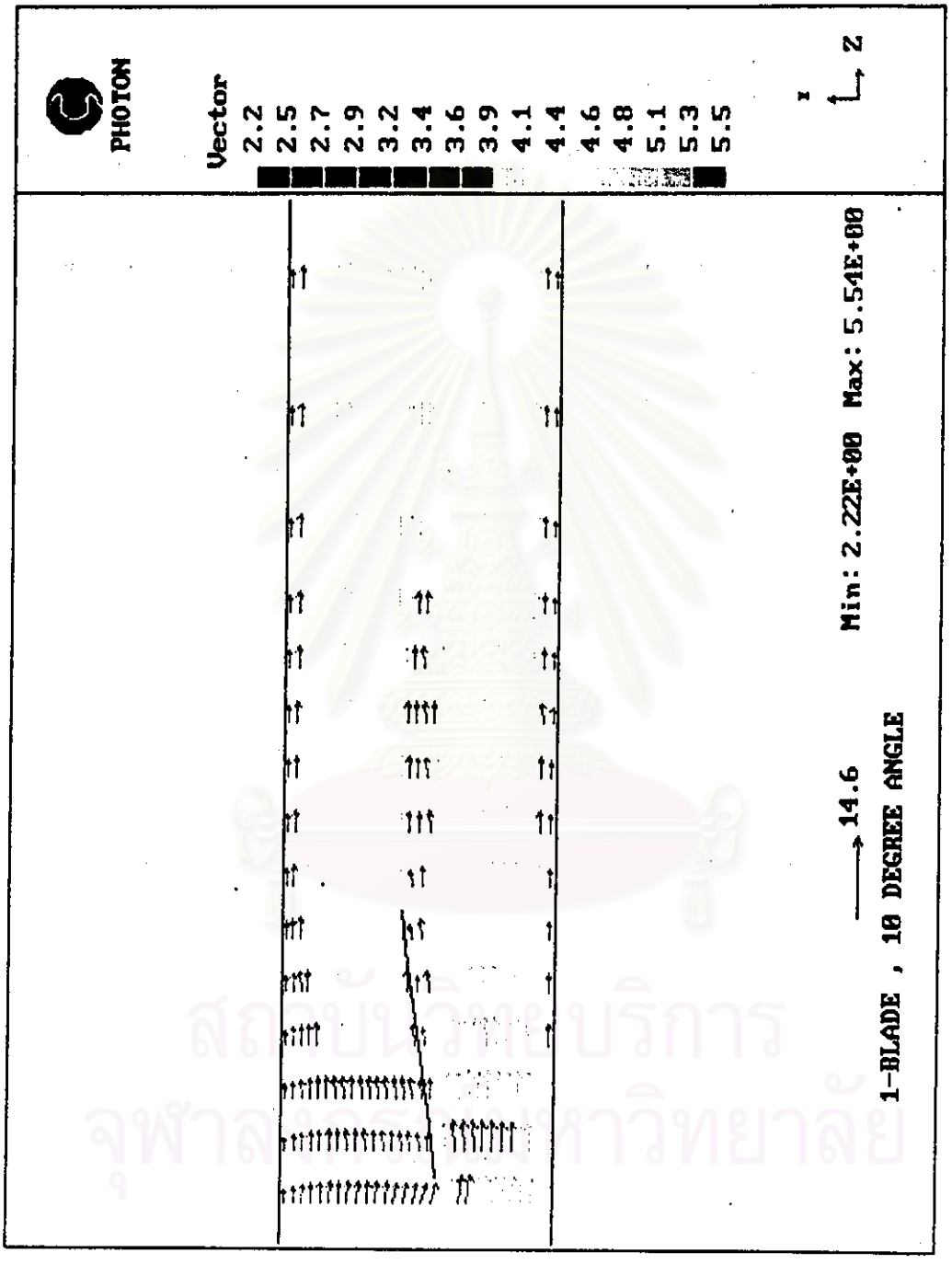

Figure 7.13 Mean velocity vectors of air flow past 1-blade damper with 10 degree angle.

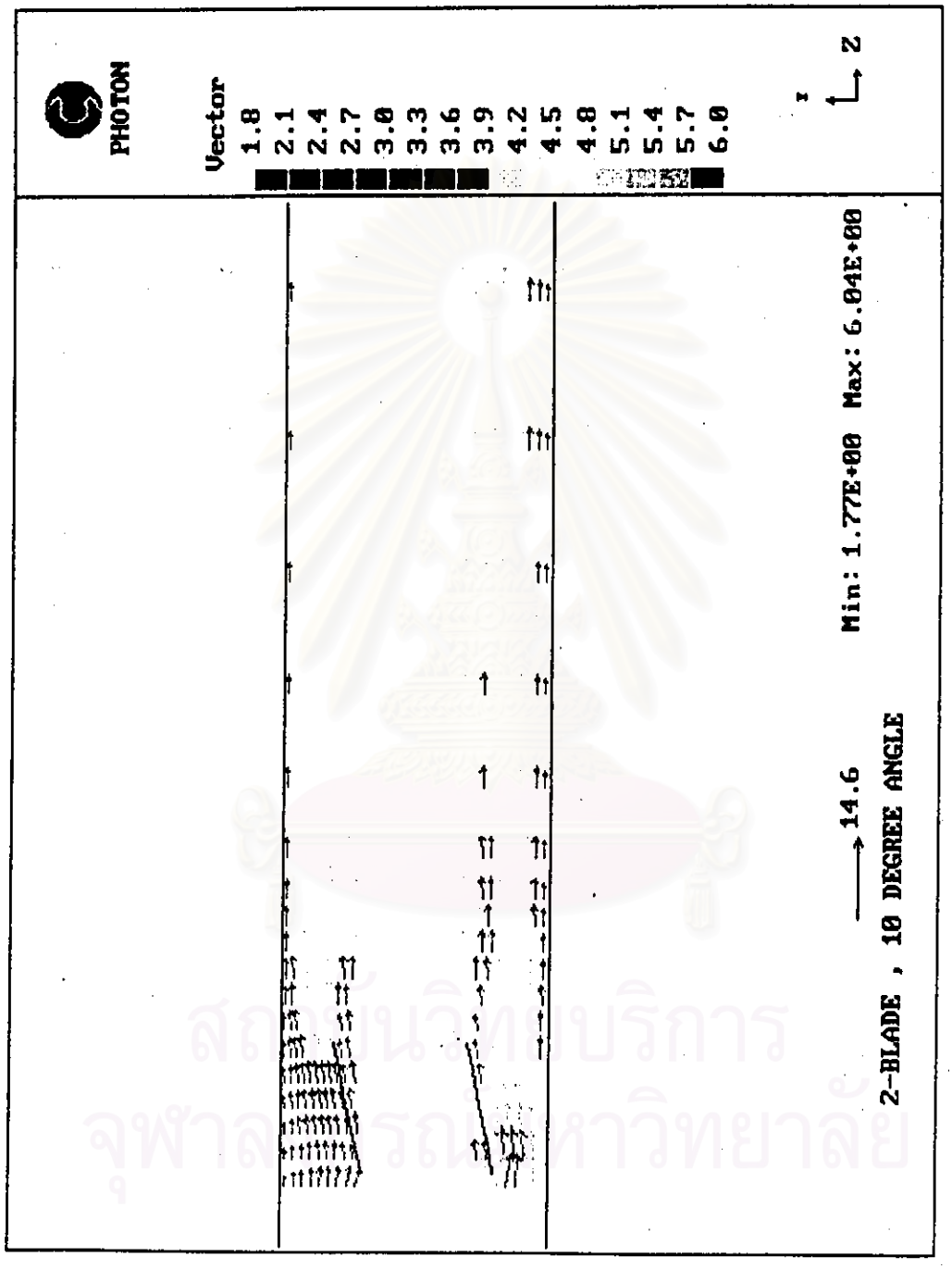

Figure 7.14 Mean velocity vectors of air flow past 2-blade damper with 10 degree angle.

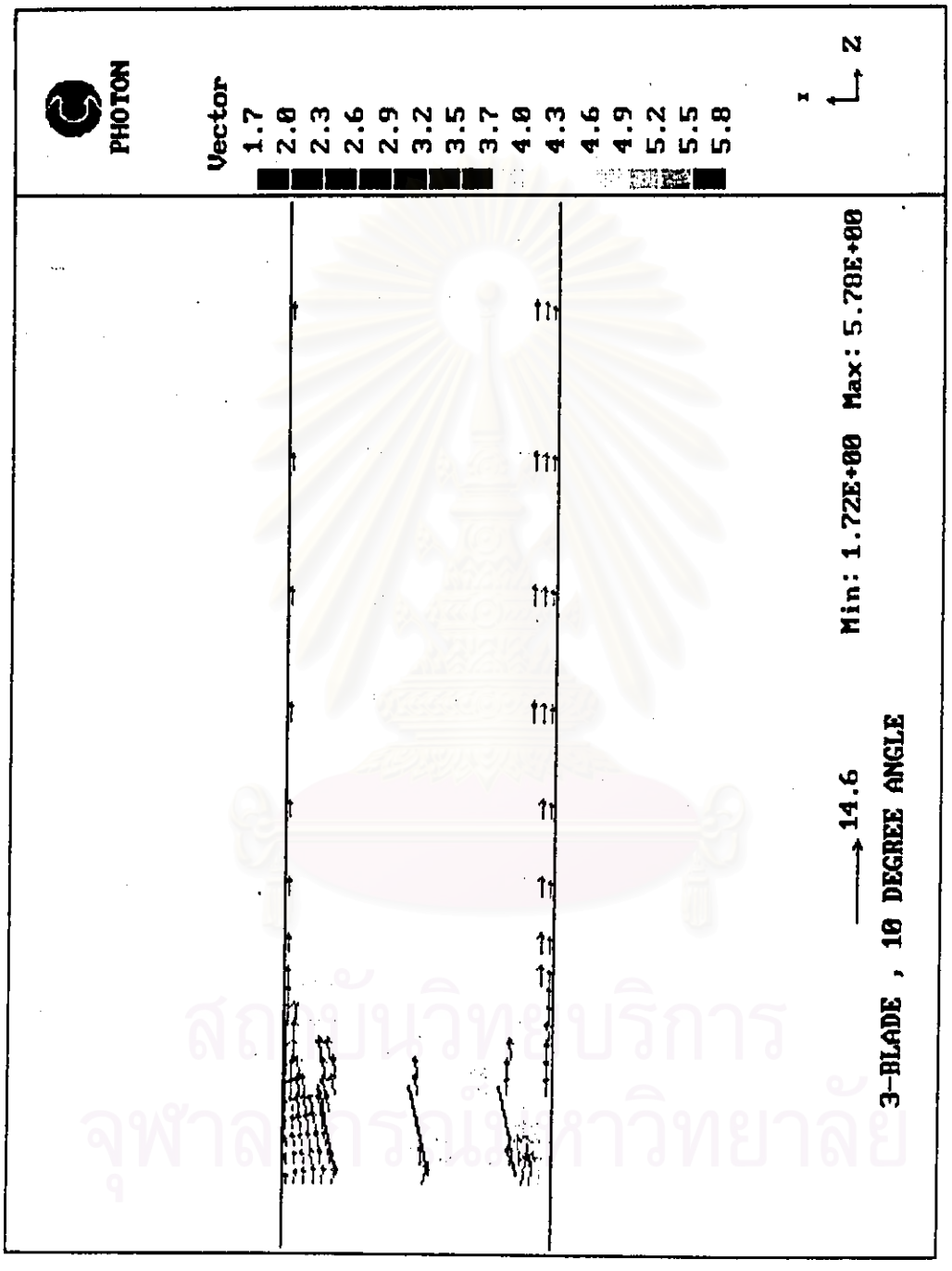

Figure 7.15 Mean velocity vectors of air flow past 3-blade damper with 10 degree angle.

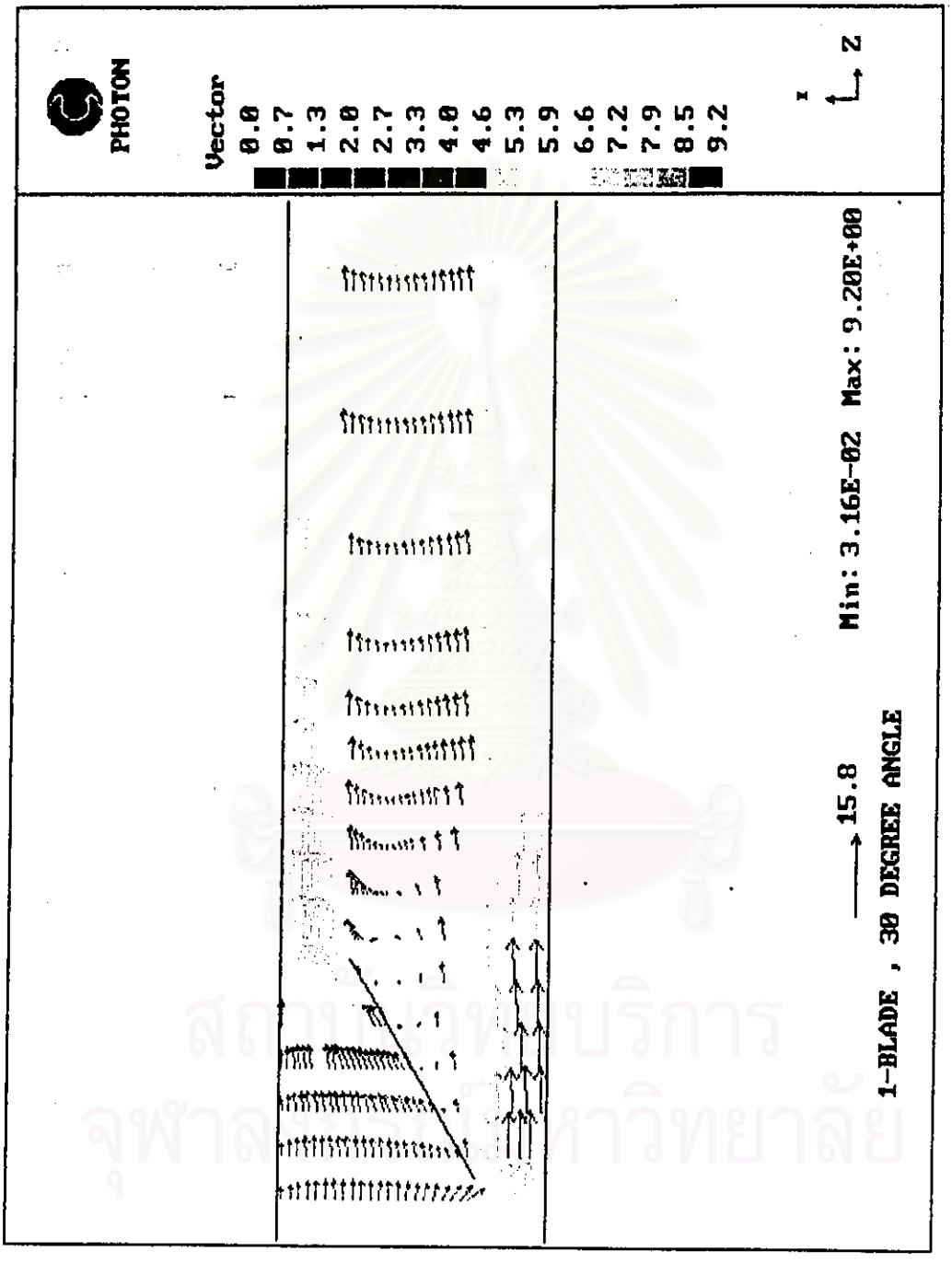

Figure 7.16 Mean velocity vectors of air flow past 1-blade damper with 30 degree angle.

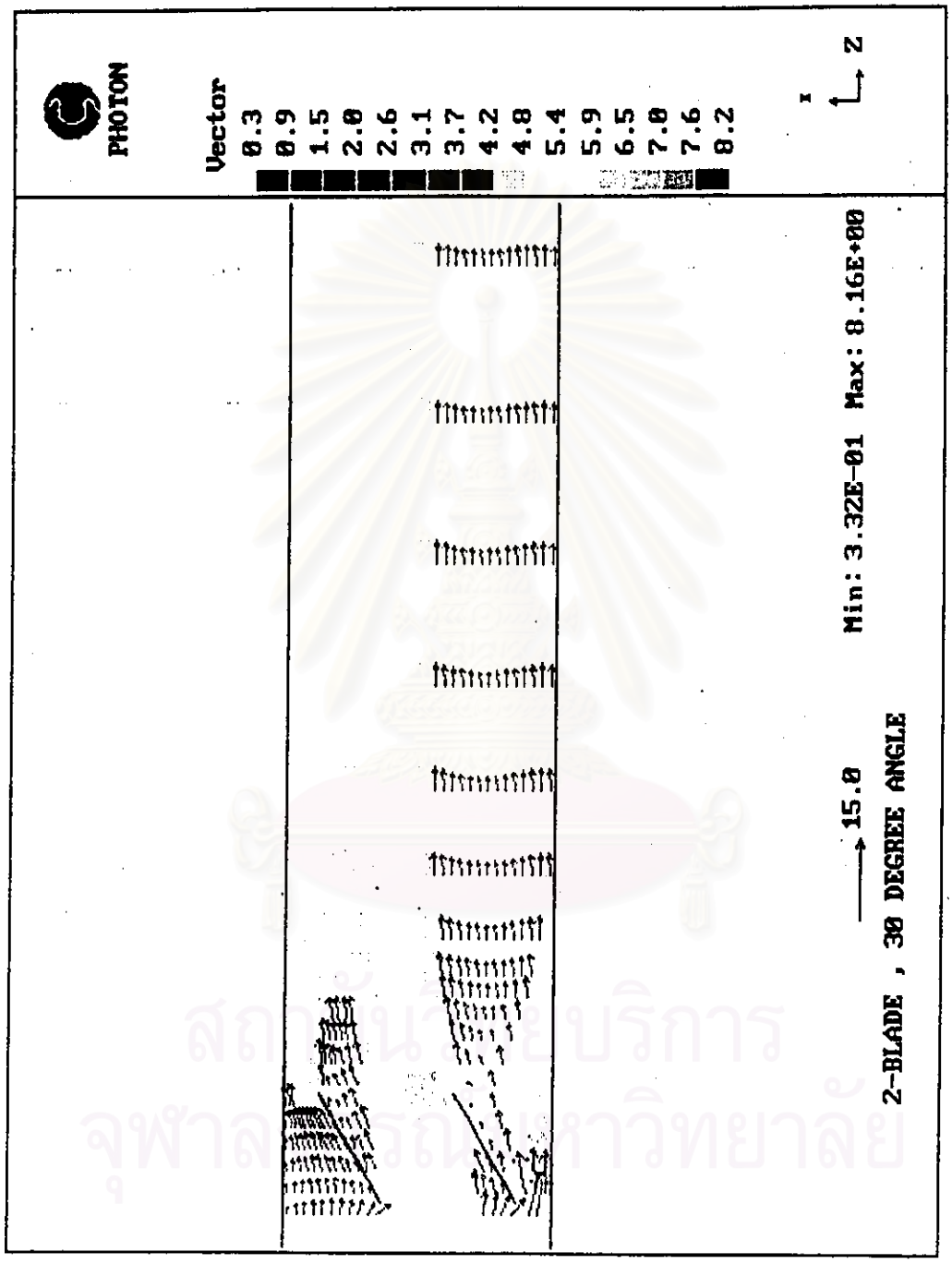

Figure 7.17 Mean velocity vectors of air flow past 2-blade damper with 30 degree angle.

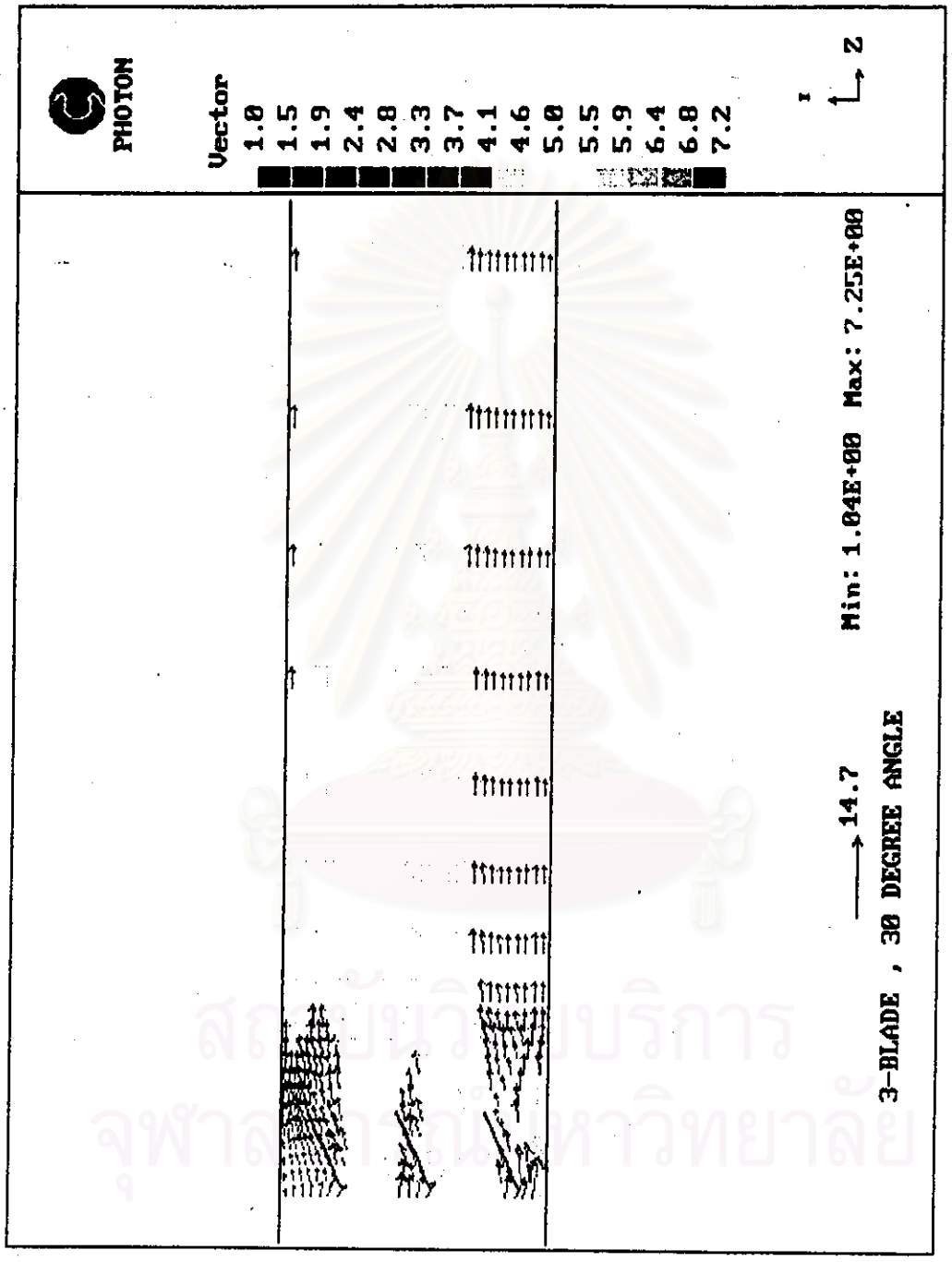

Figure 7.18 Mean velocity vectors of air flow past 3-blade damper with 30 degree angle.

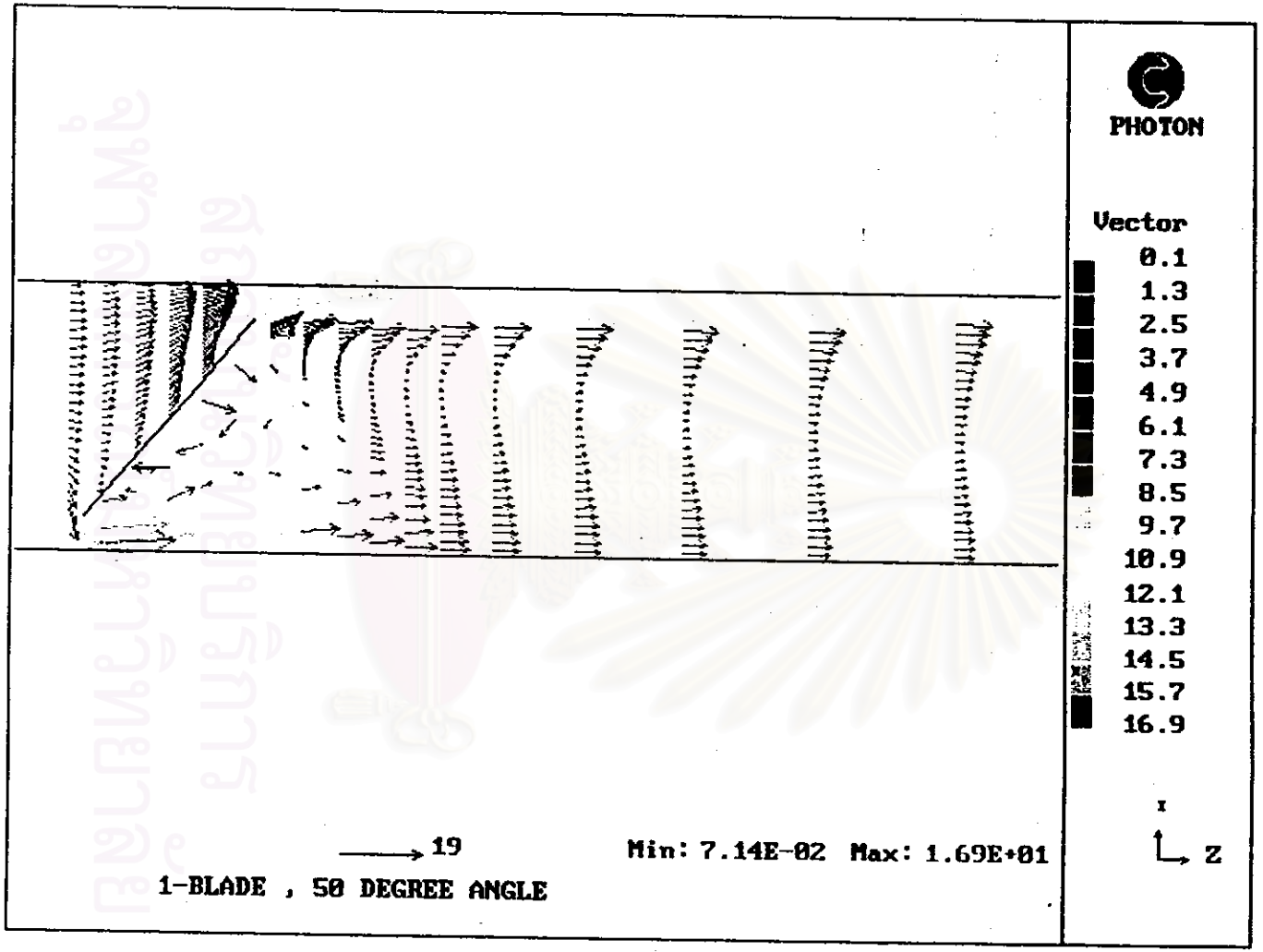

Figure 7.19 Mean velocity vectors of air flow past 1-blade damper with 50 degree angle.

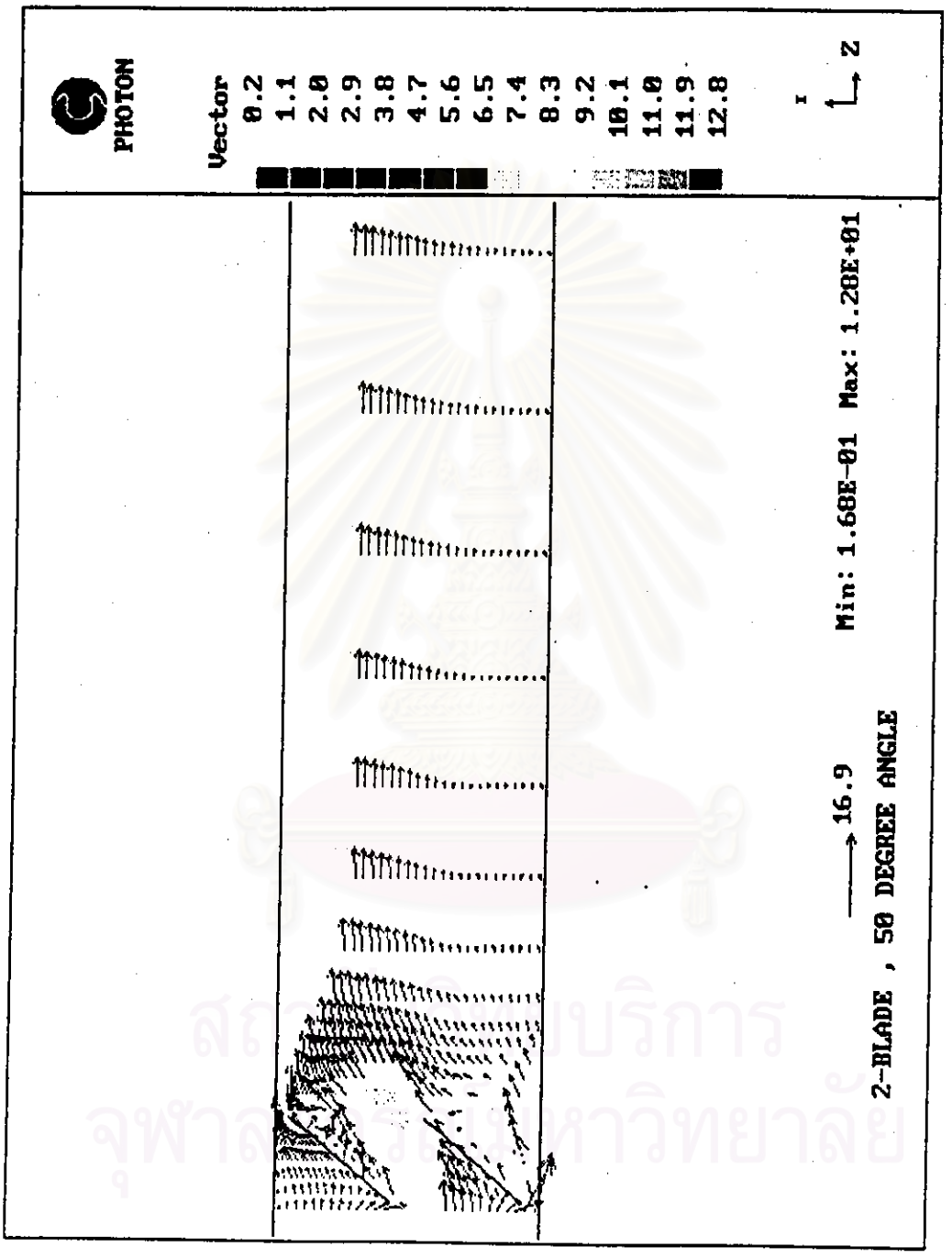

Figure 7.20 Mean velocity vectors of air flow past 2-blade damper with 50 degree angle.

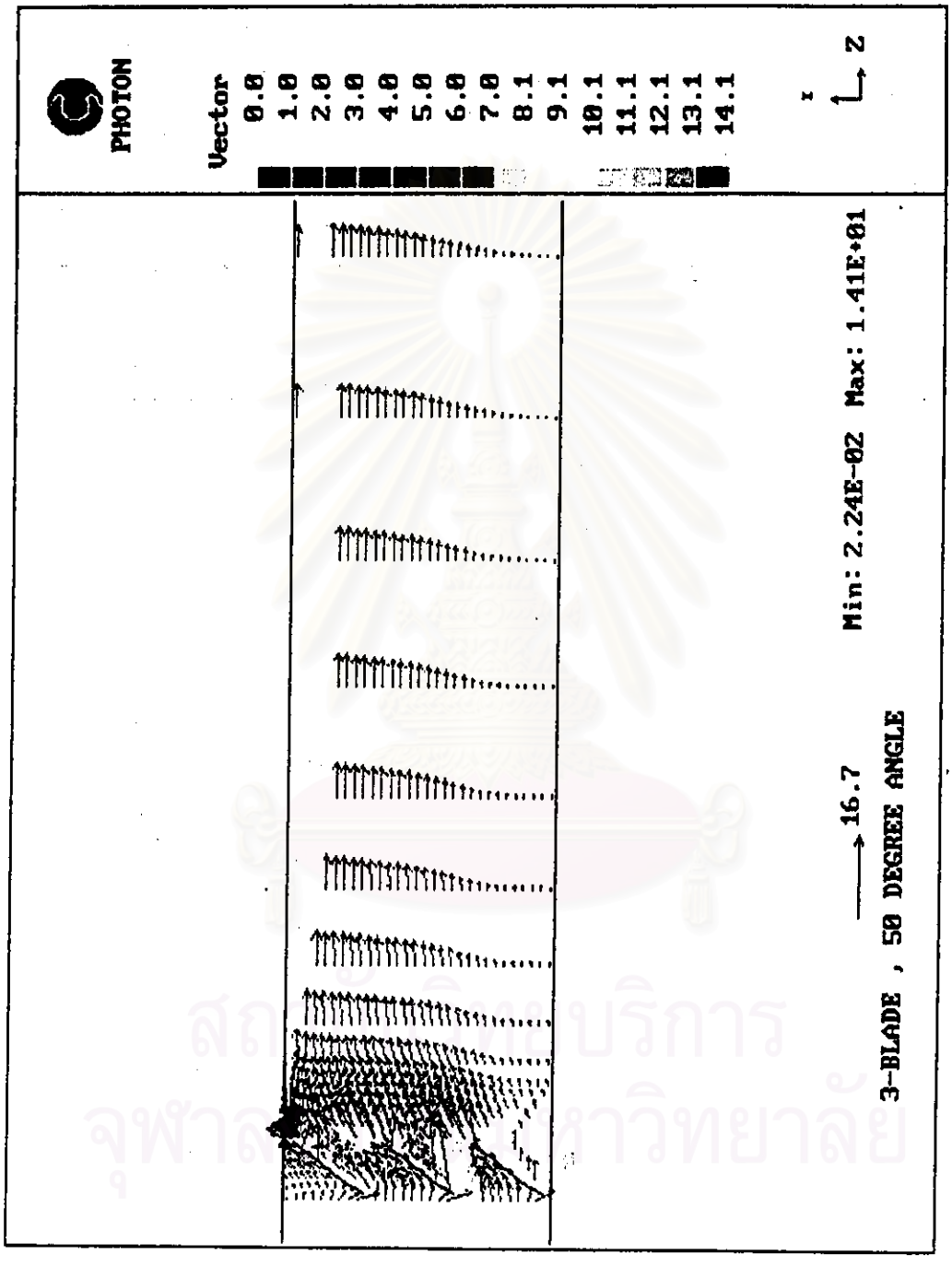

Figure 7.21 Mean velocity vectors of air flow past 3-blade damper with 50 degree angle.

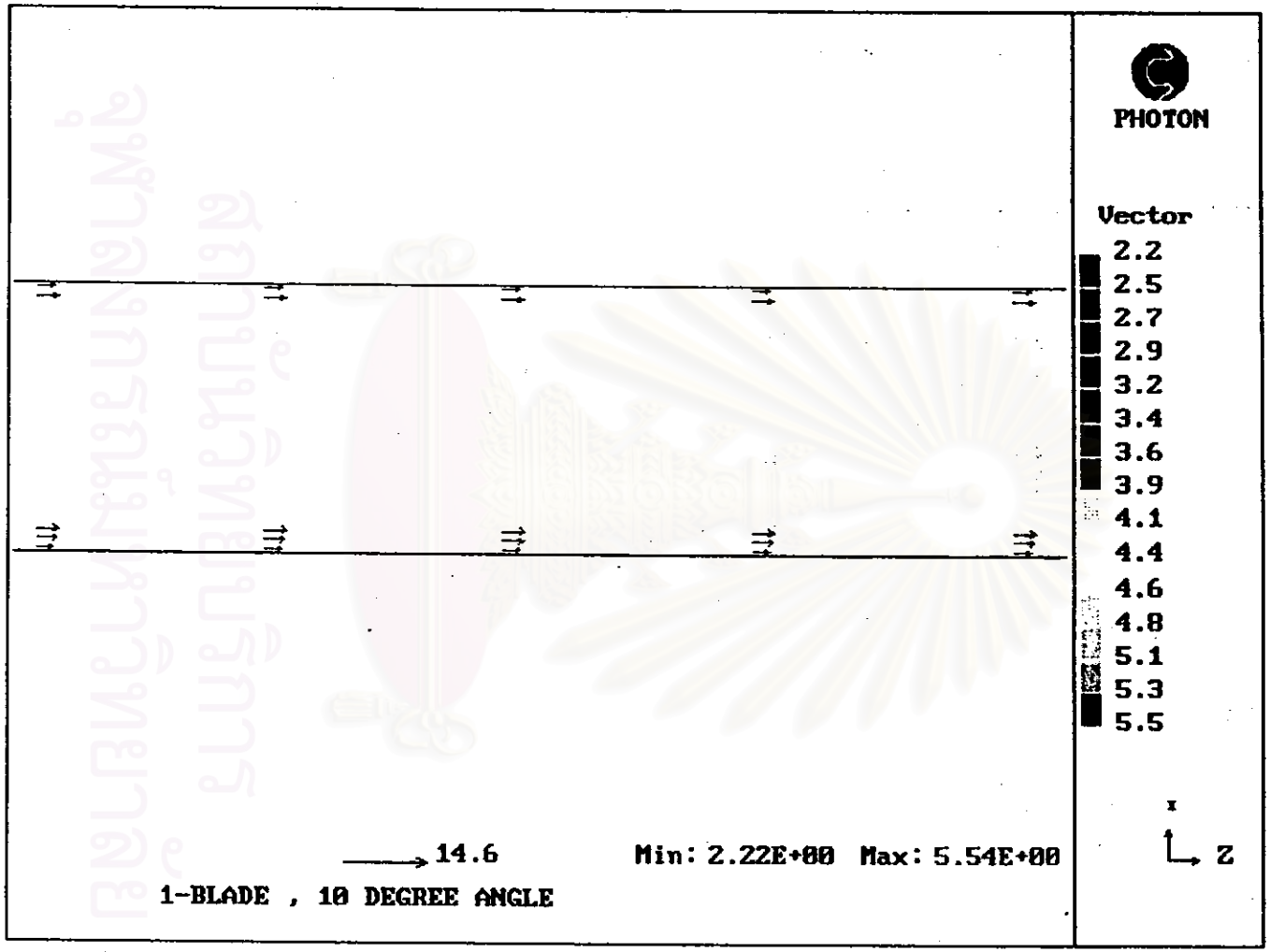

Figure 7.22 Mean velocity profiles in the developing flow region of 1-blade damper with 10 degree angle (about L / D = 20).

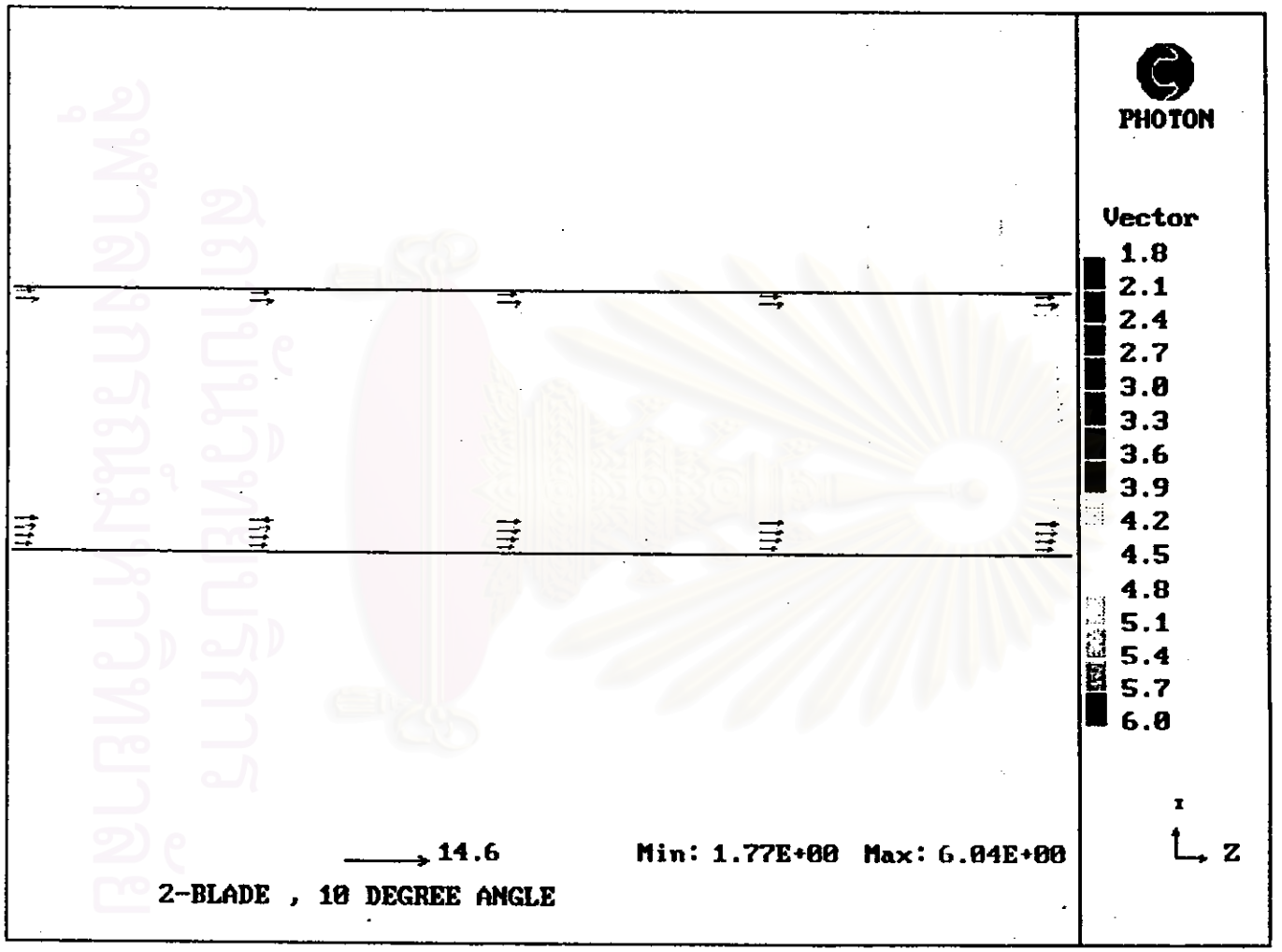

Figure 7.23 Mean velocity profiles in the developing flow region of 2-blade damper with 10 degree angle (about L / D = 20).

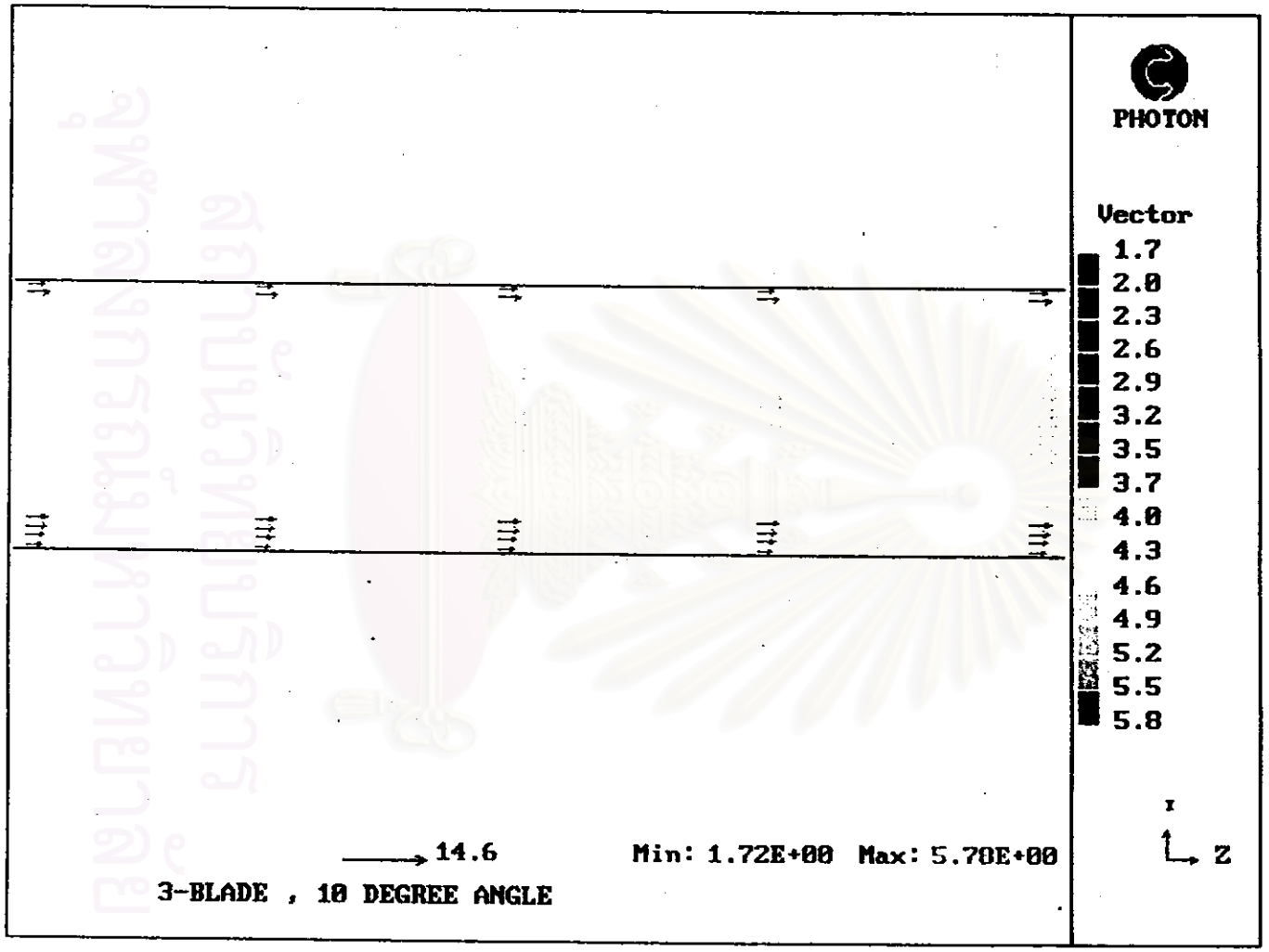

Figure 7.24 Mean velocity profiles in the developing flow region of 3-blade damper with 10 degree angle (about L / D = 20).

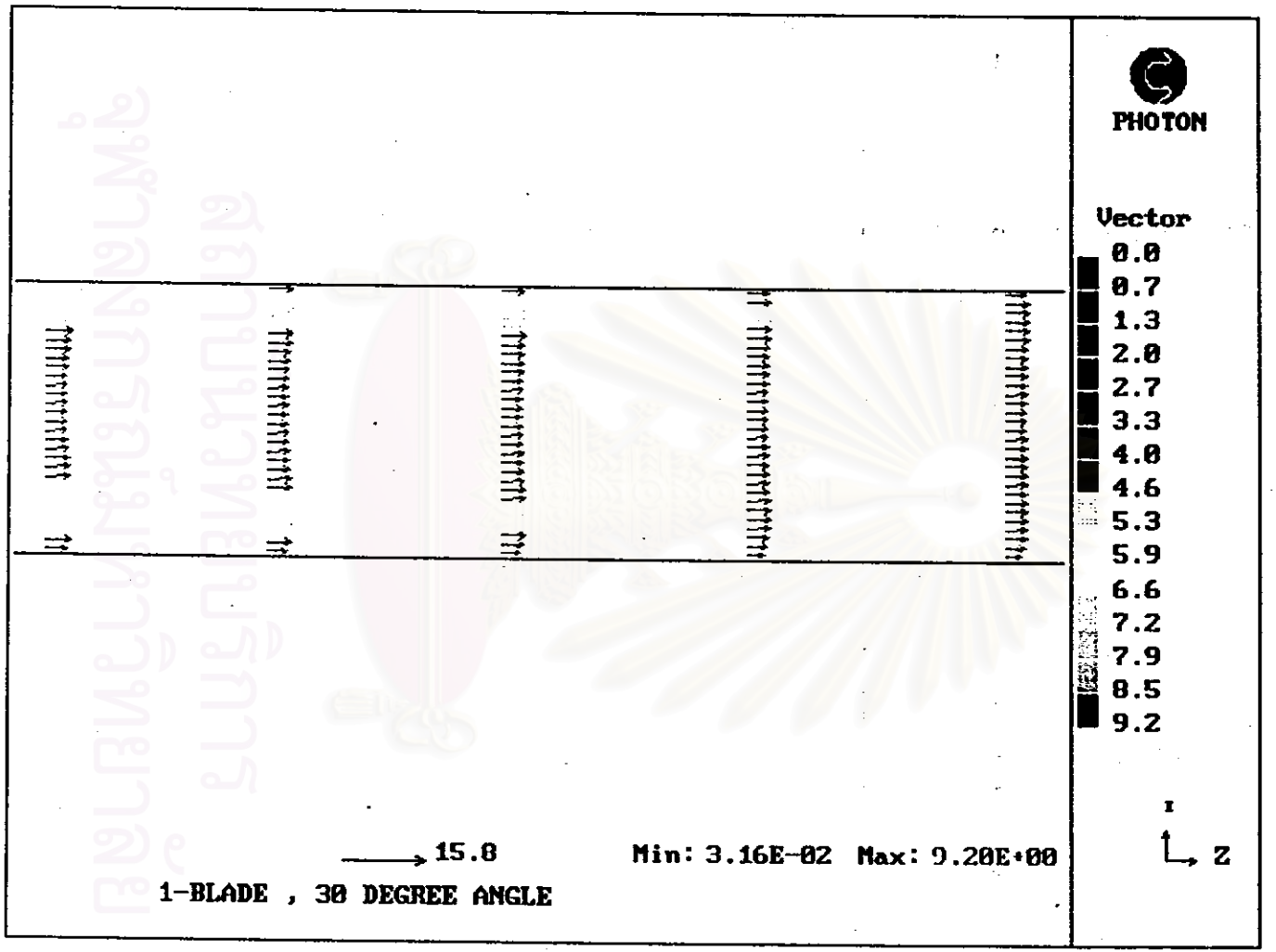

Figure 7.25 Mean velocity profiles in the developing flow region of 1-blade damper with 30 degree angle (about L / D = 20).

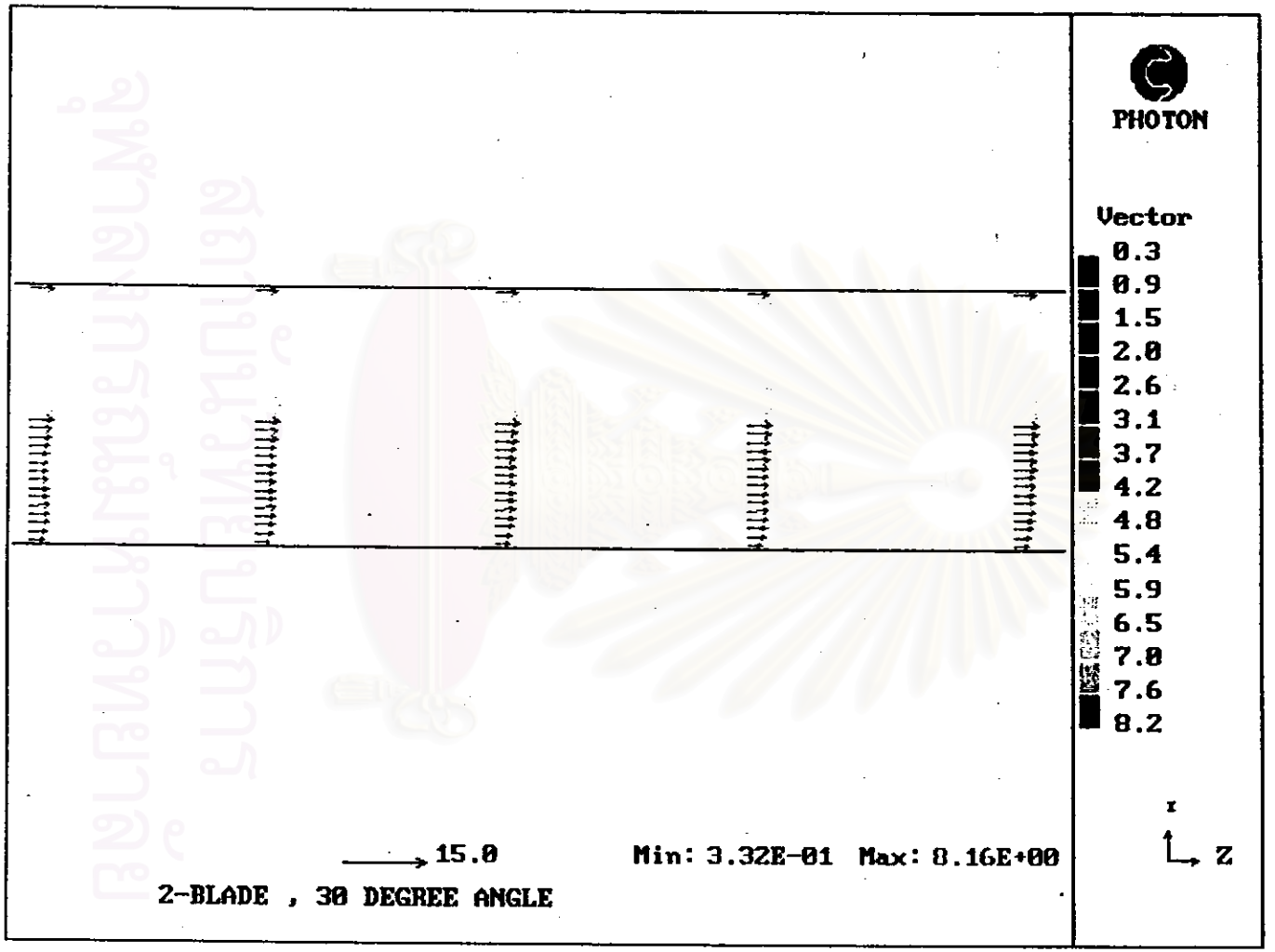

Figure 7.26 Mean velocity profiles in the developing flow region of 2-blade damper with 30 degree angle (about L / D = 20).

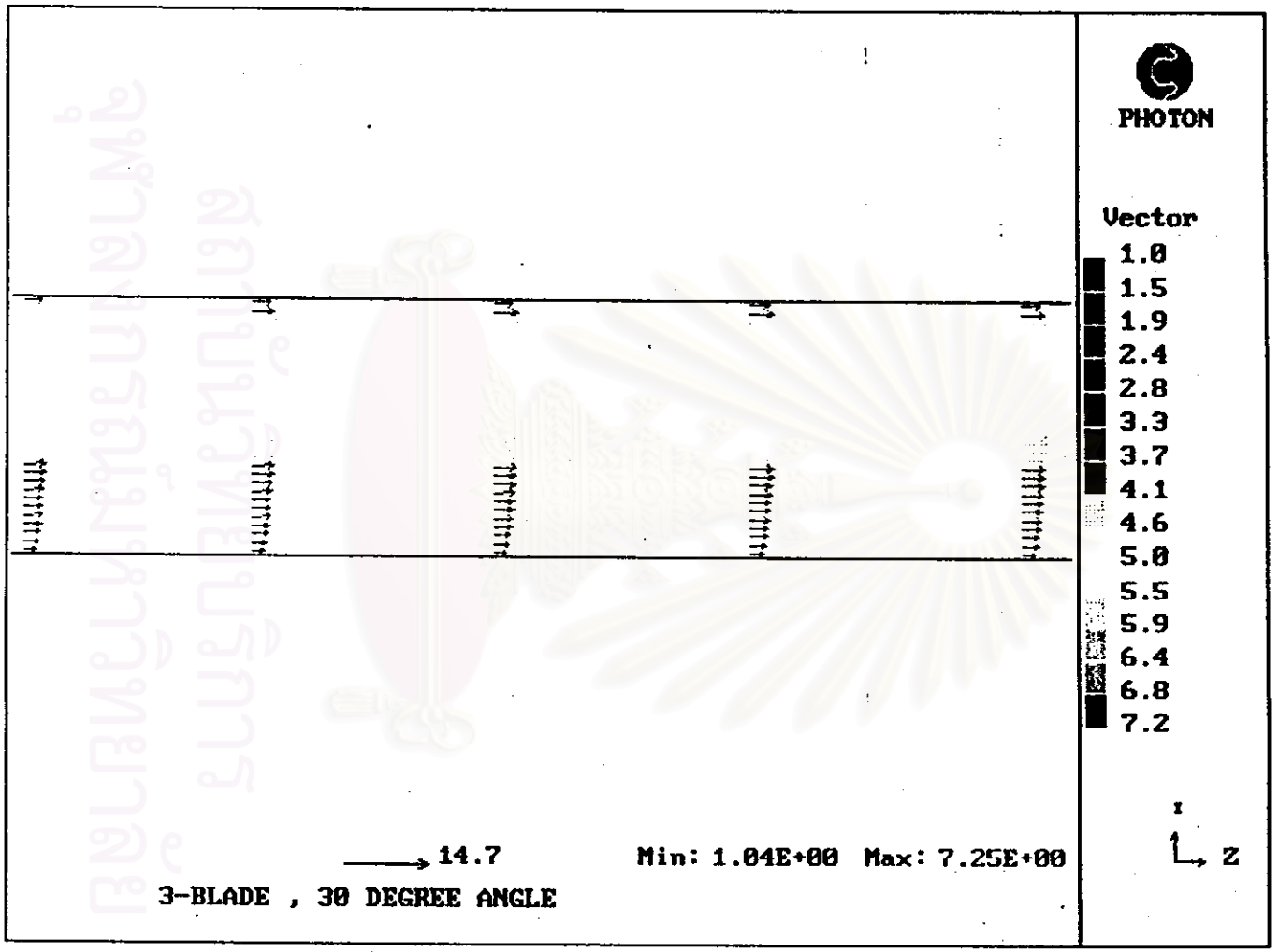

Figure 7.27 Mean velocity profiles in the developing flow region of 3-blade damper with 30 degree angle (about L / D = 20).

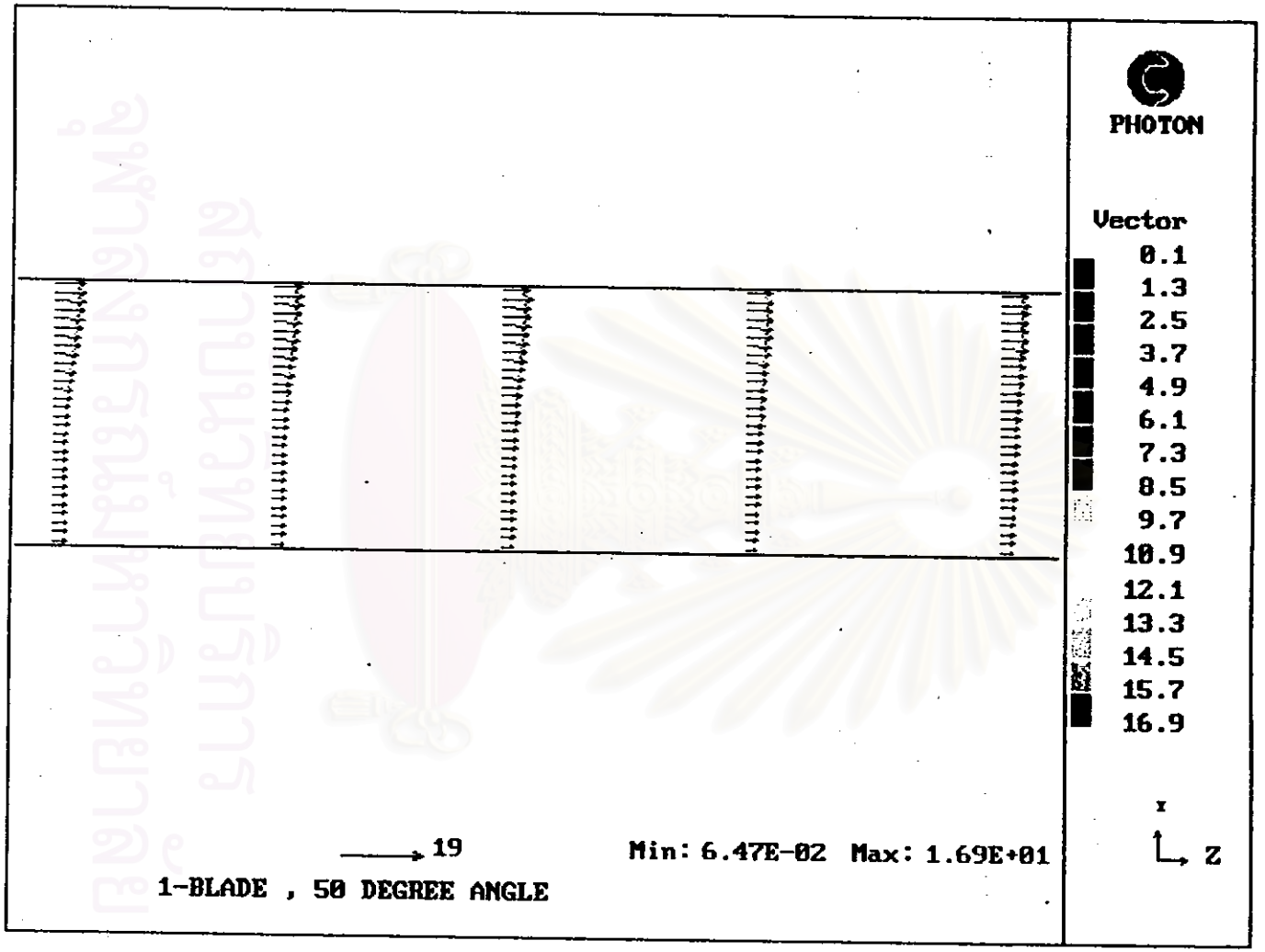

Figure 7.28 Mean velocity profiles in the developing flow region of 1-blade damper with 50 degree angle (about L / D = 20).

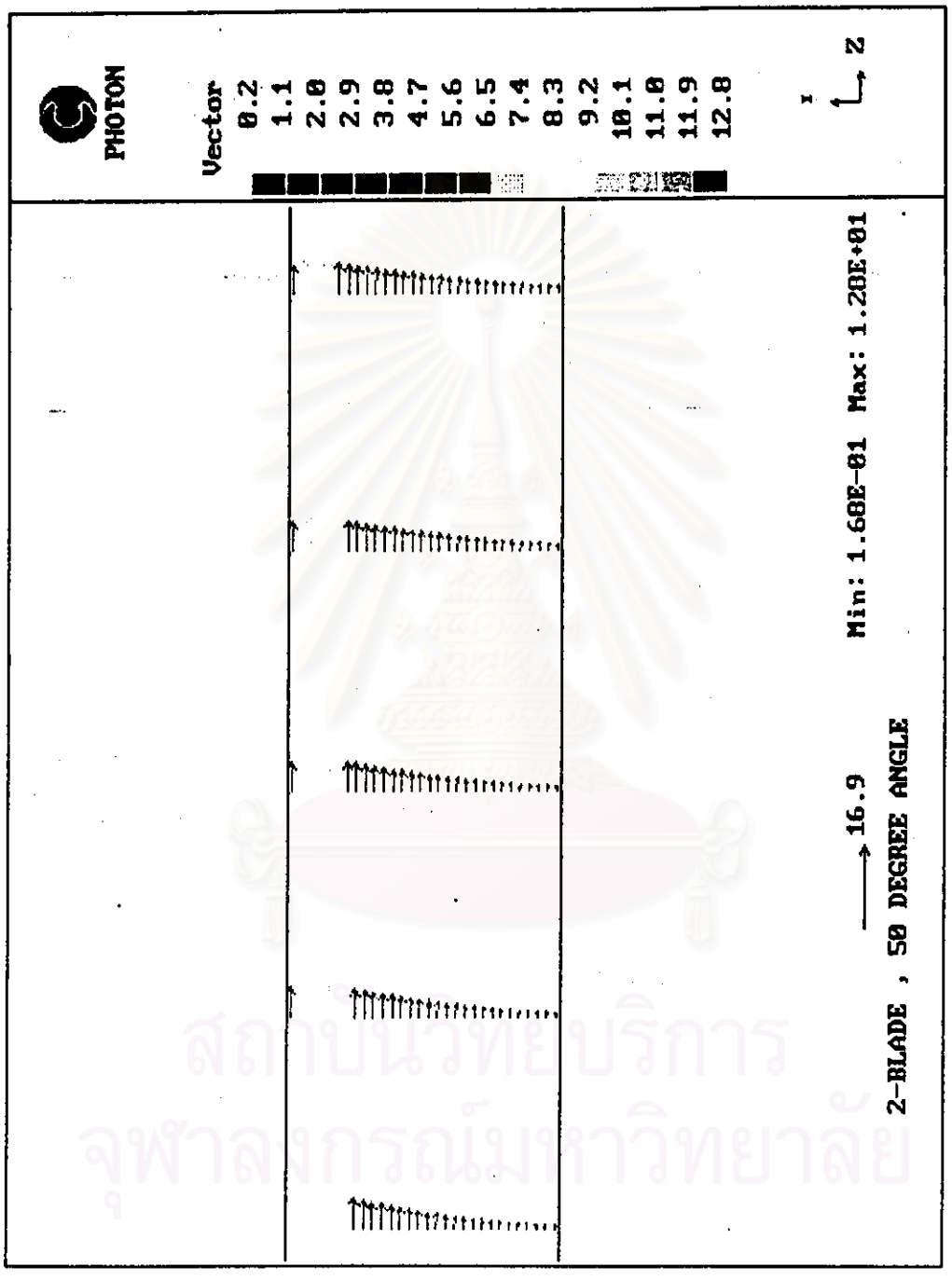

Figure 7.29 Mean velocity profiles in the developing flow region of 2-blade damper with 50 degree angle (about L / D = 20).

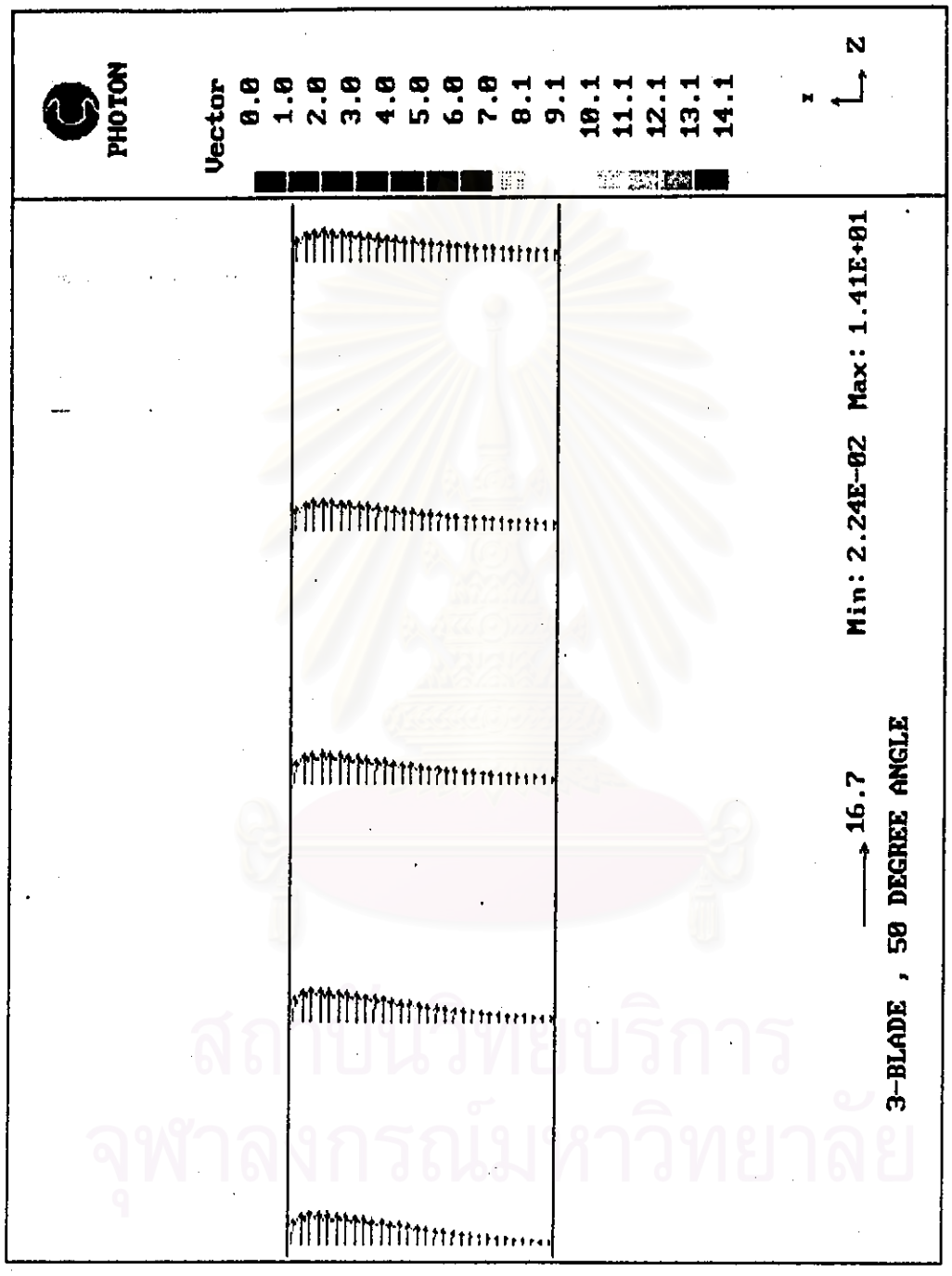

Figure 7.30 Mean velocity profiles in the developing flow region of 3-blade damper with 50 degree angle (about L / D = 20).

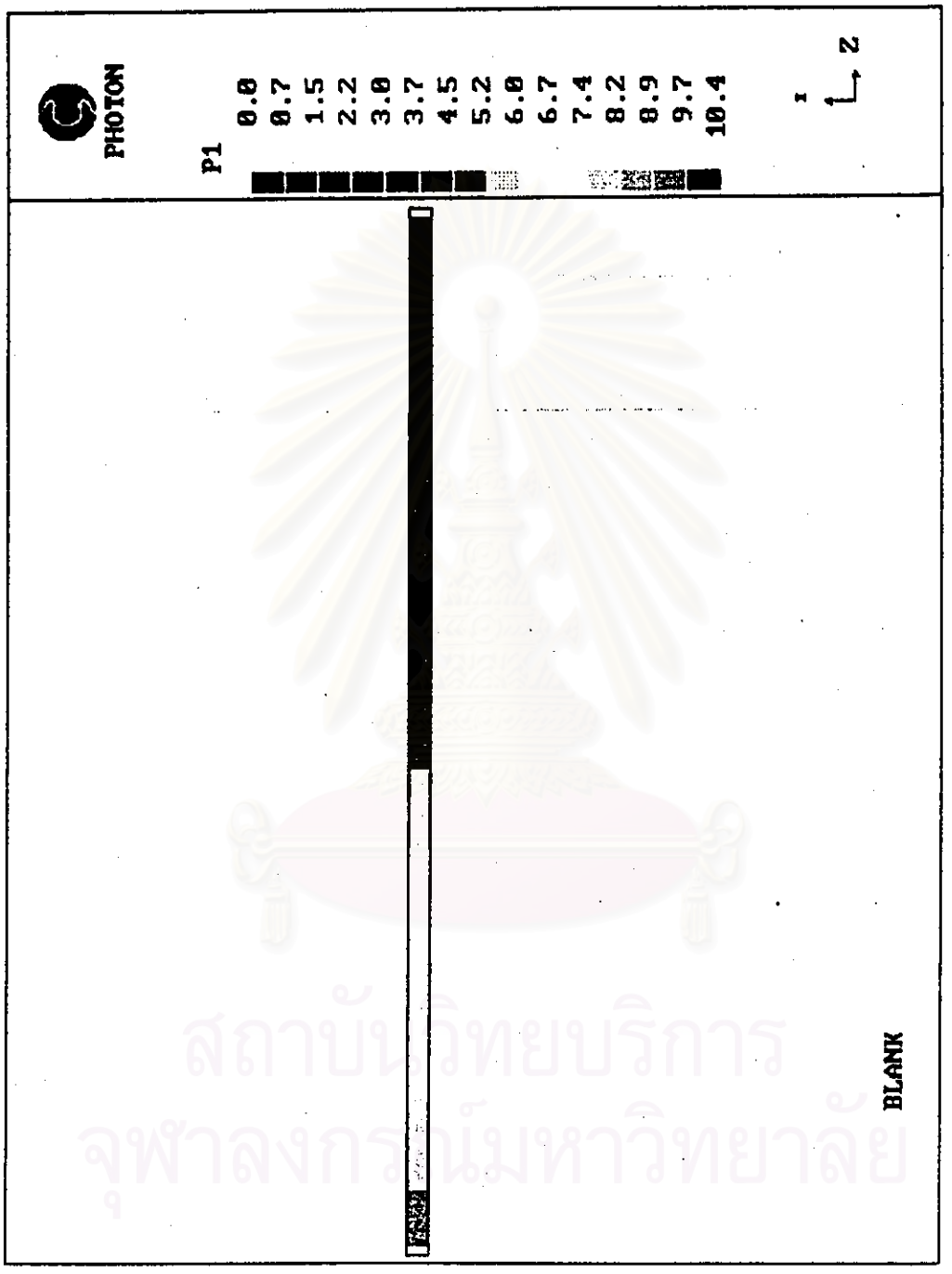

Figure 7.31 Pressure contours in a blank duct.

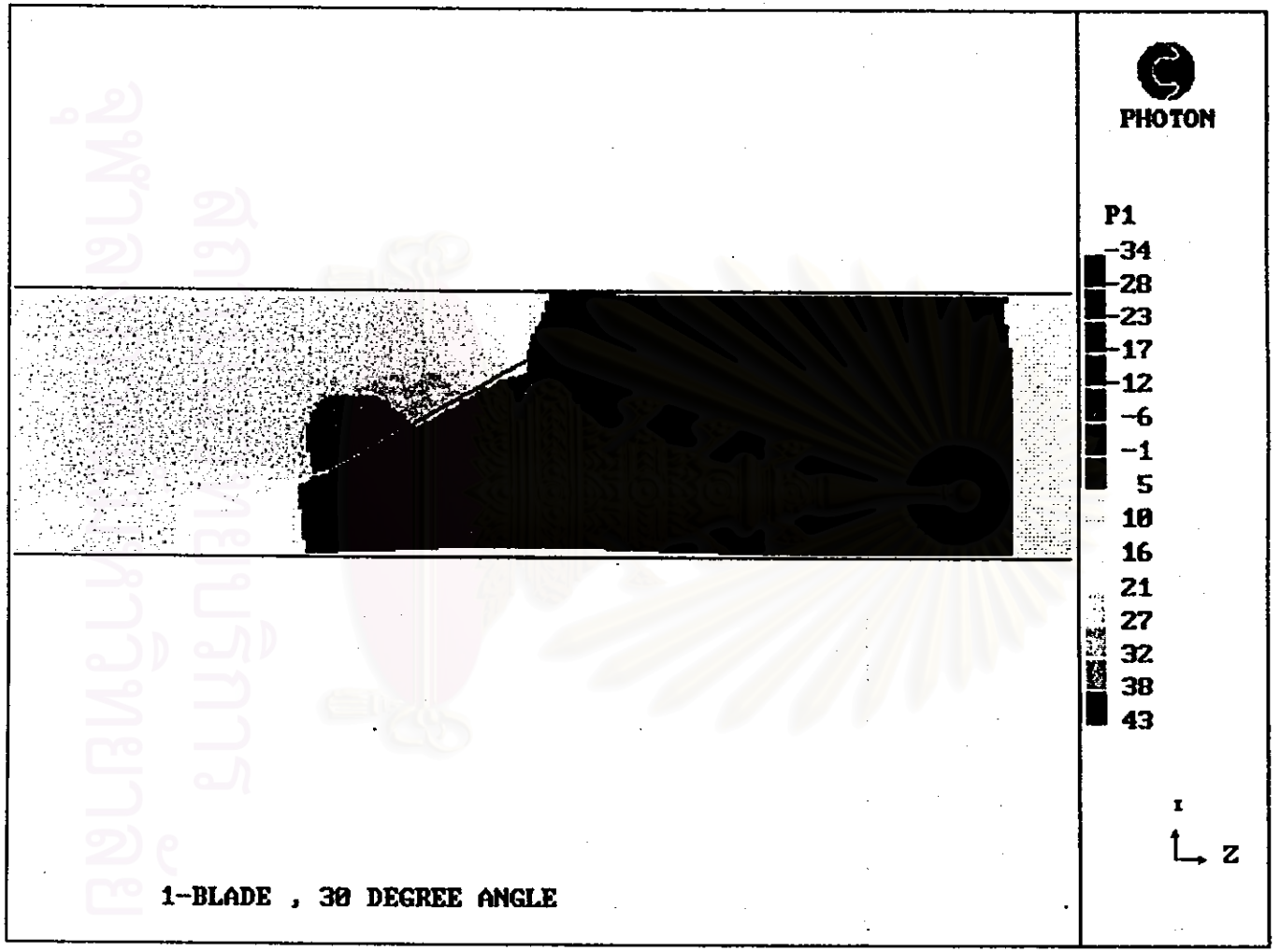

Figure 7.32 Pressure contours of air flow past 1-blade damper.

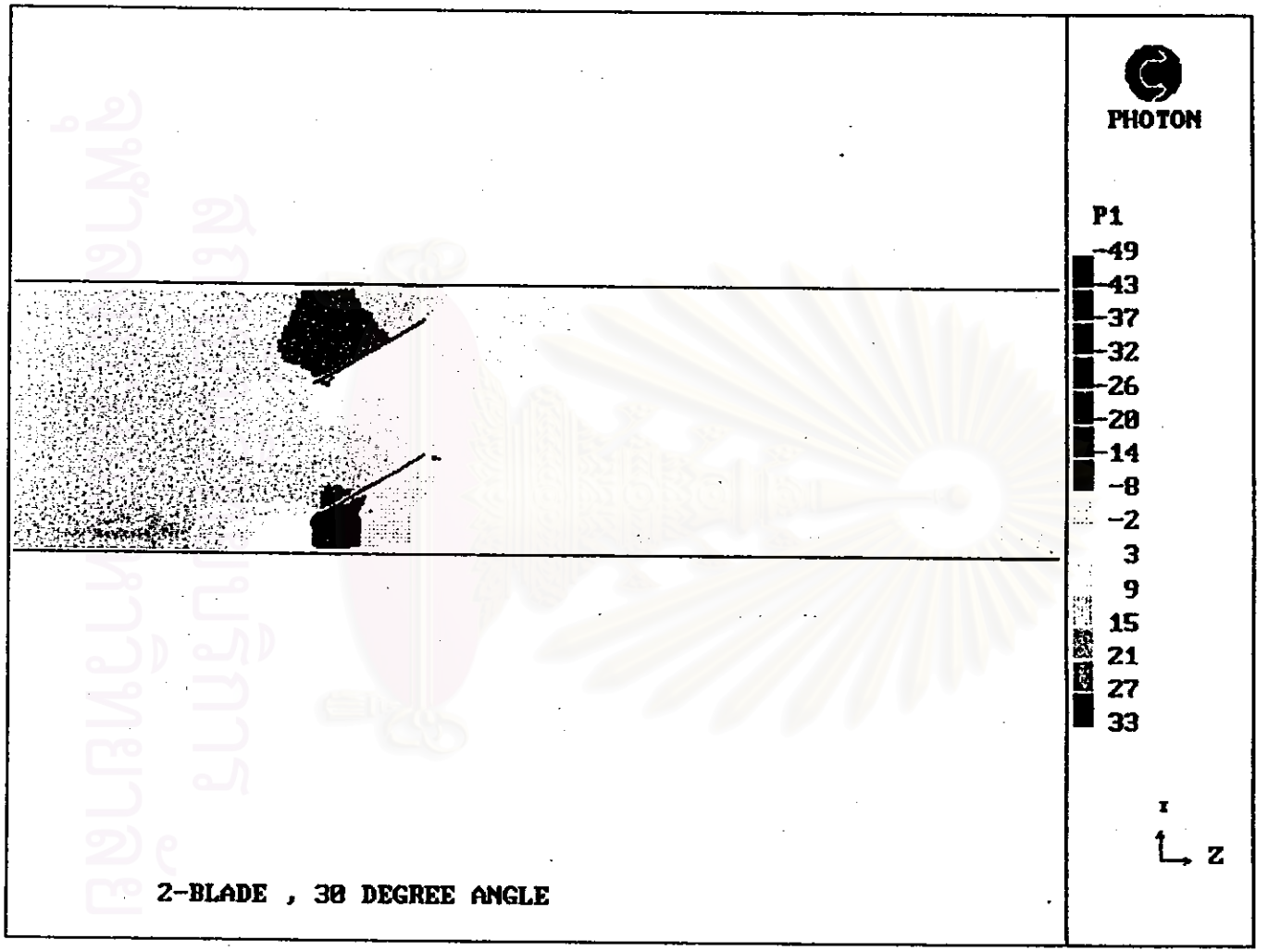

Figure 7.33 Pressure contours of air flow past 2-blade damper.

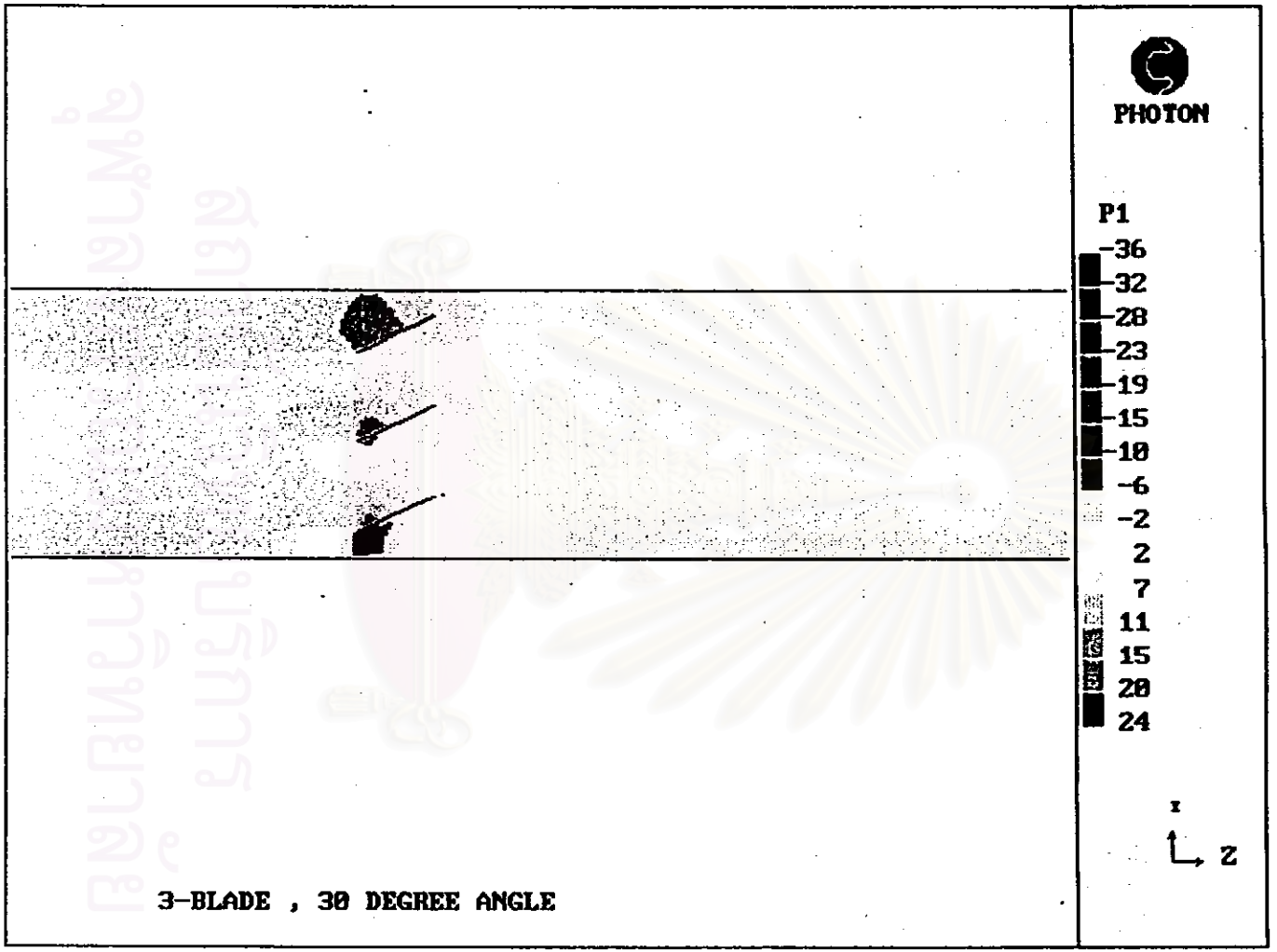

Figure 7.34 Pressure contours of air flow past 3-blade damper.

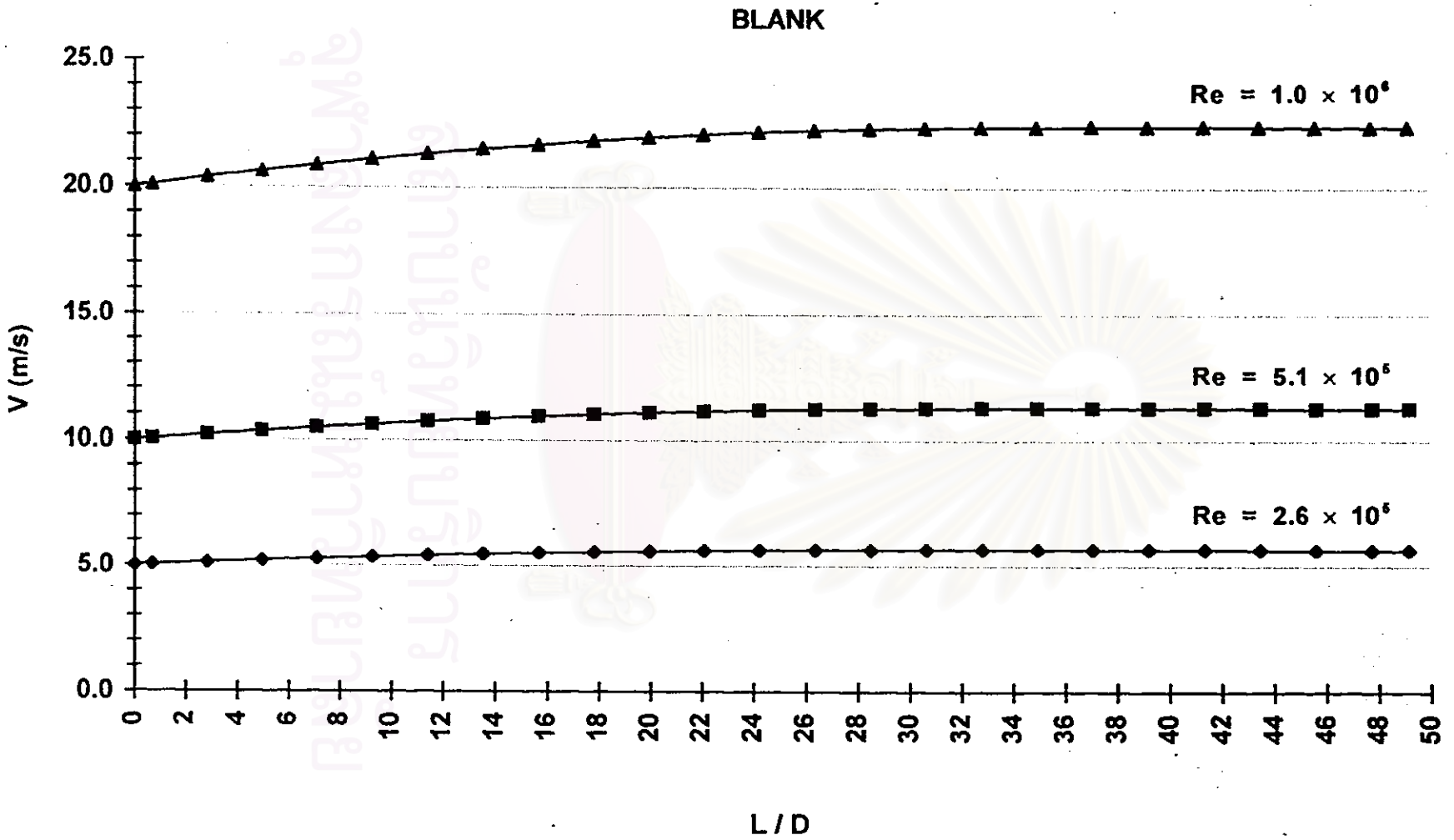

Figure 7.35 Centerline mean-longitudinal-velocity distribution in a blank duct with various Reynolds numbers.

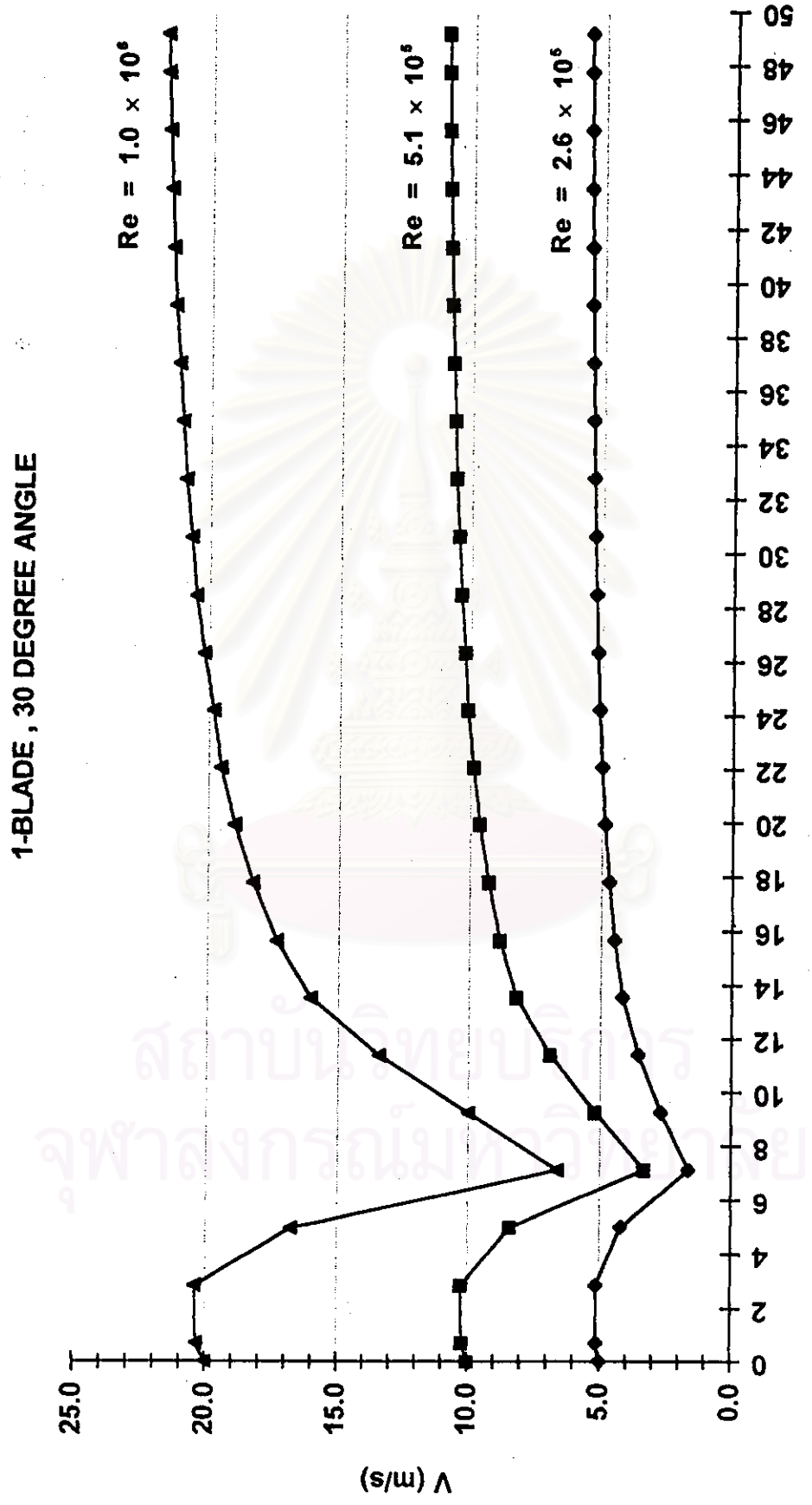

Figure 7.36 Centerline mean-longitudinal-velocity distribution of 1-blade damper with various Reynolds numbers.

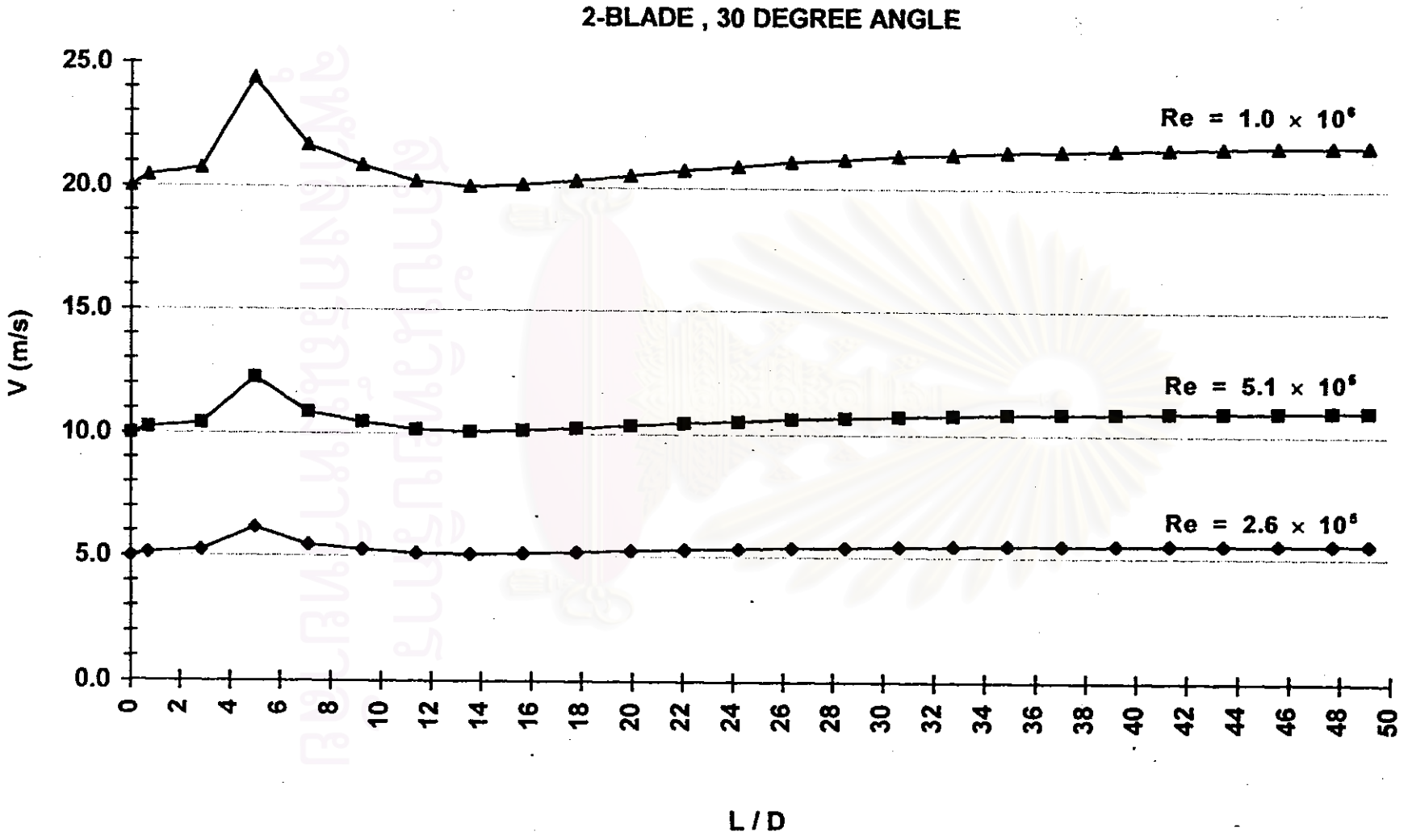

Figure 7.37 Centerline mean-longitudinal-velocity distribution of 2-blade damper with various Reynolds numbers.

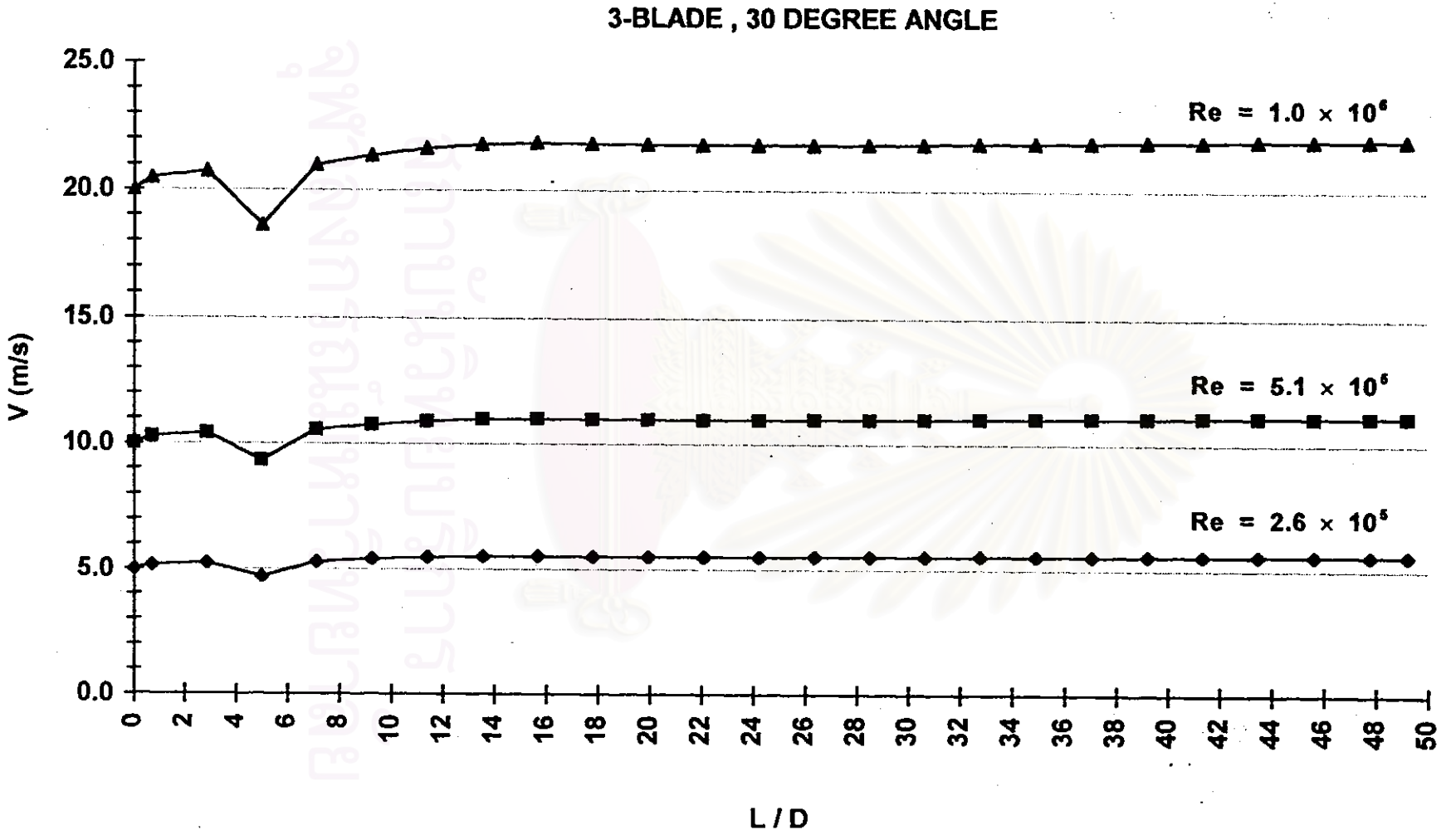

Figure 7.38 Centerline mean-longitudinal-velocity distribution of 3-blade damper with various Reynolds numbers.

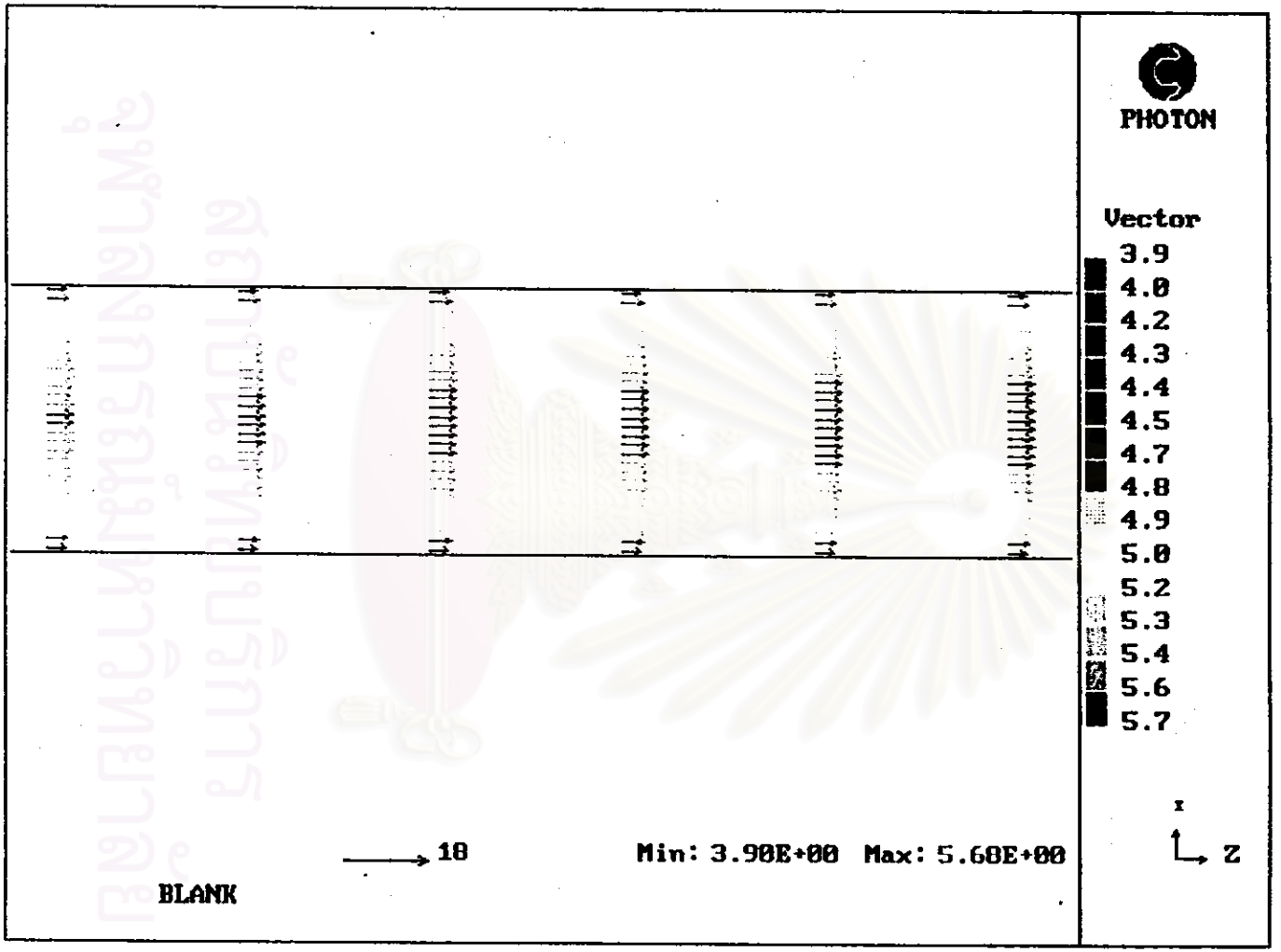

Figure 7.39 Mean velocity vectors in a blank duct at Re = 2.6 × 10^5 (about L / D = 18).

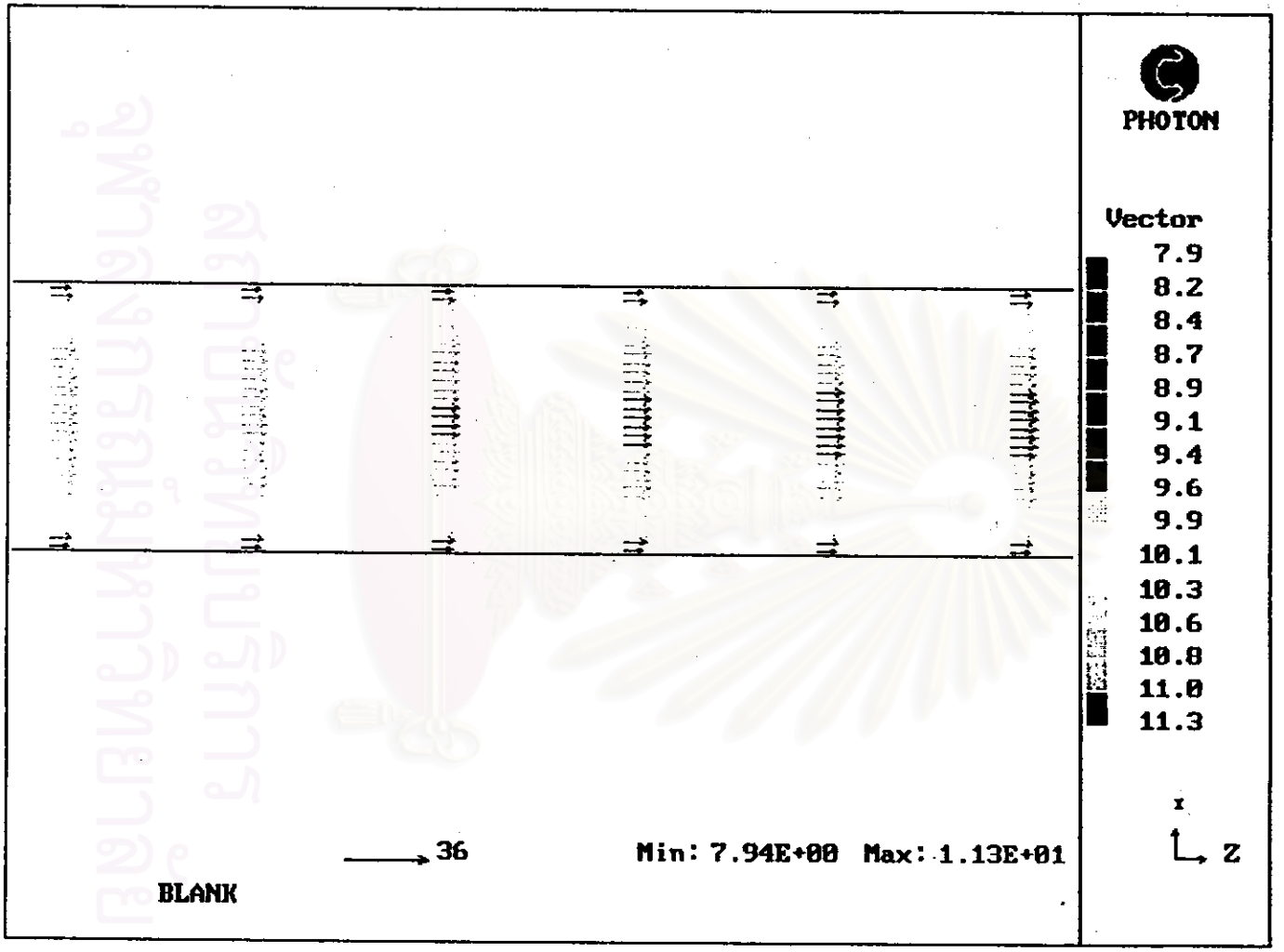

Figure 7.40 Mean velocity vectors in a blank duct at Re = 5.1 × 10^5 (about L / D = 18).

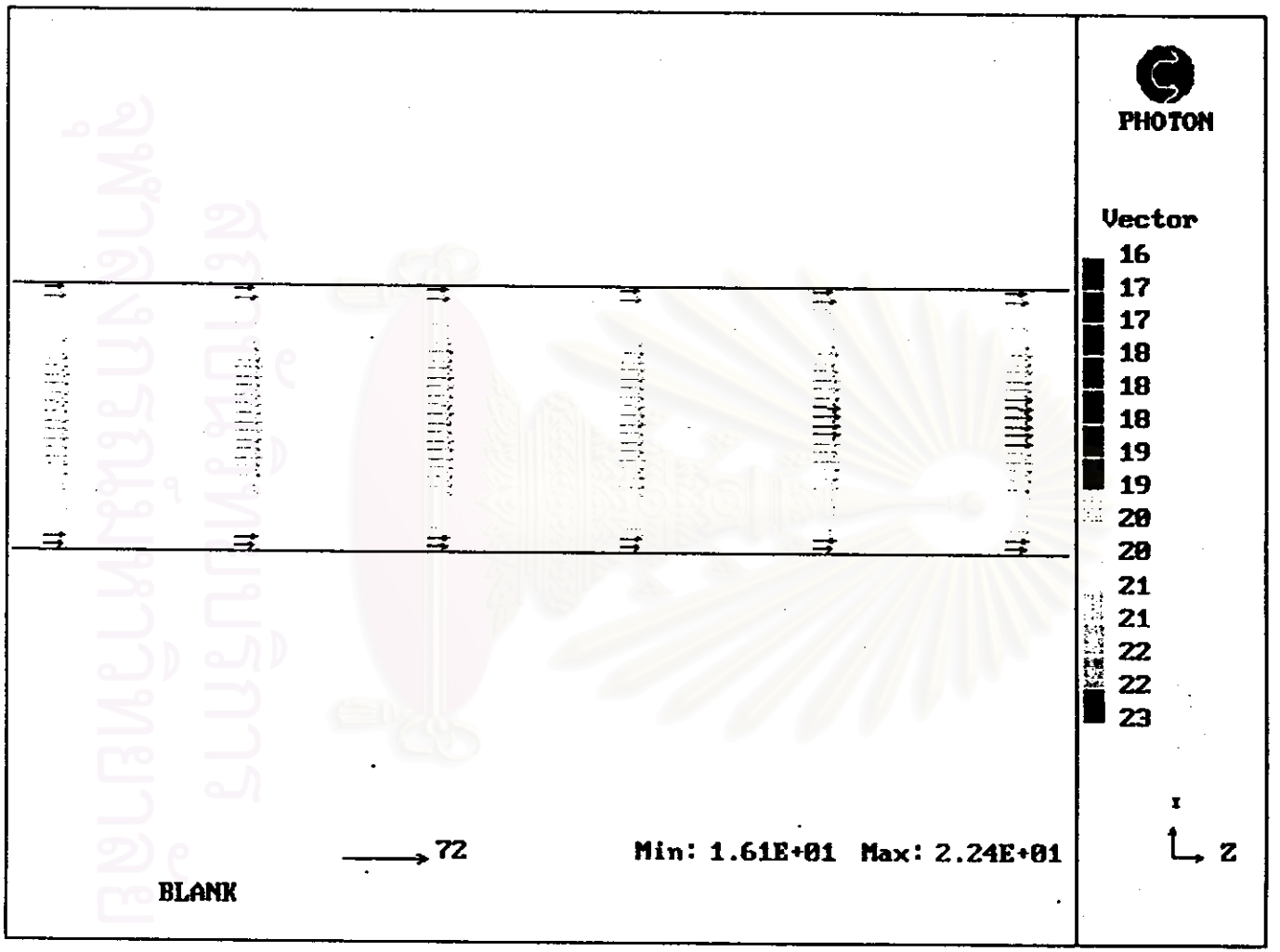

Figure 7.41 Mean velocity vector in a blank duct at Re = 1.0×10^6 (about L / D = 18).

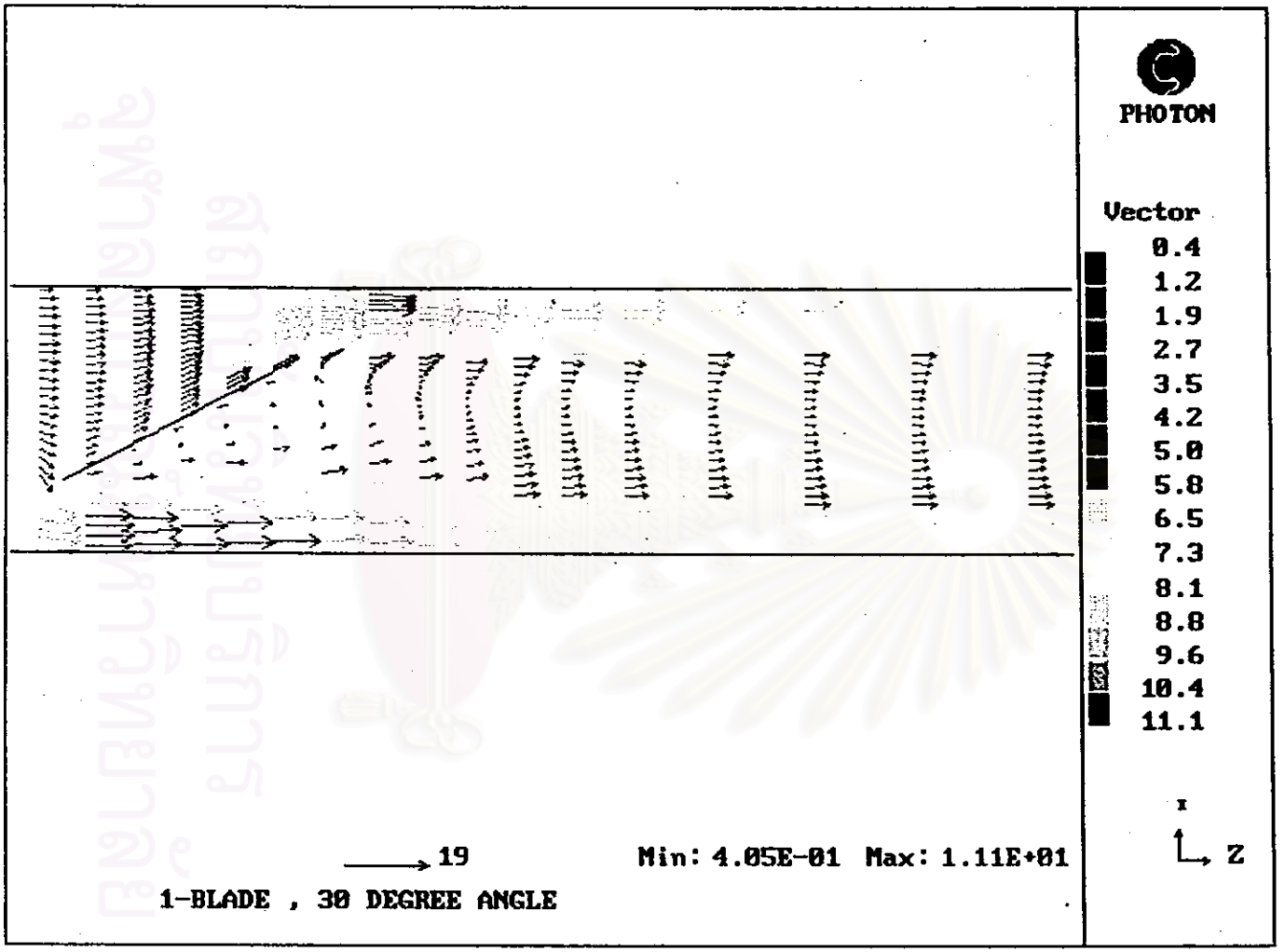

Figure 7.42(a) Mean velocity vectors around the separated-flow region of 1-blade damper at Re = 2.6 × 10^5.

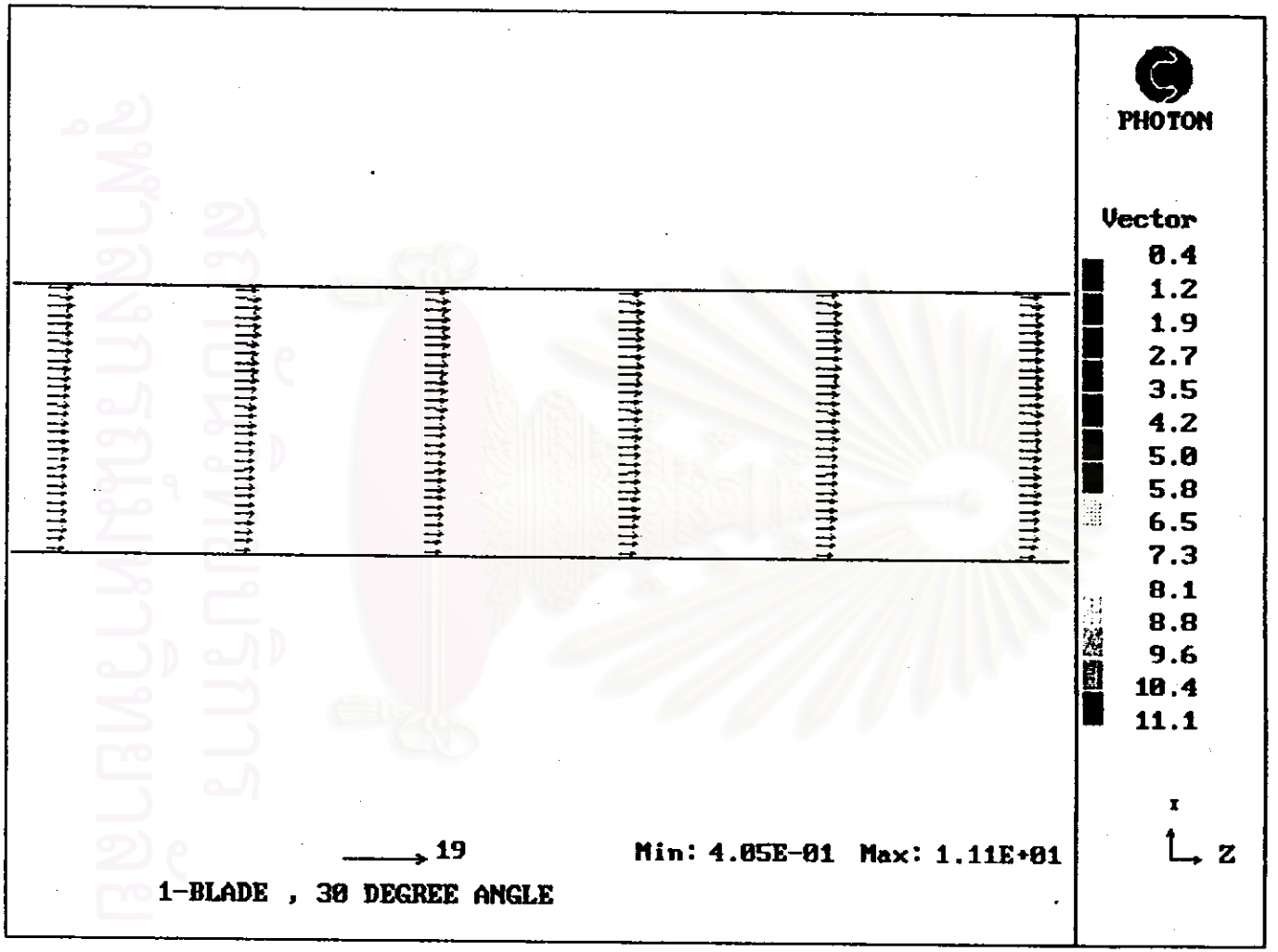

Figure 7.42(b) Mean velocity profiles in the developing flow region of 1-blade damper at Re = 2.6 × 10^5 (about L / D = 20).

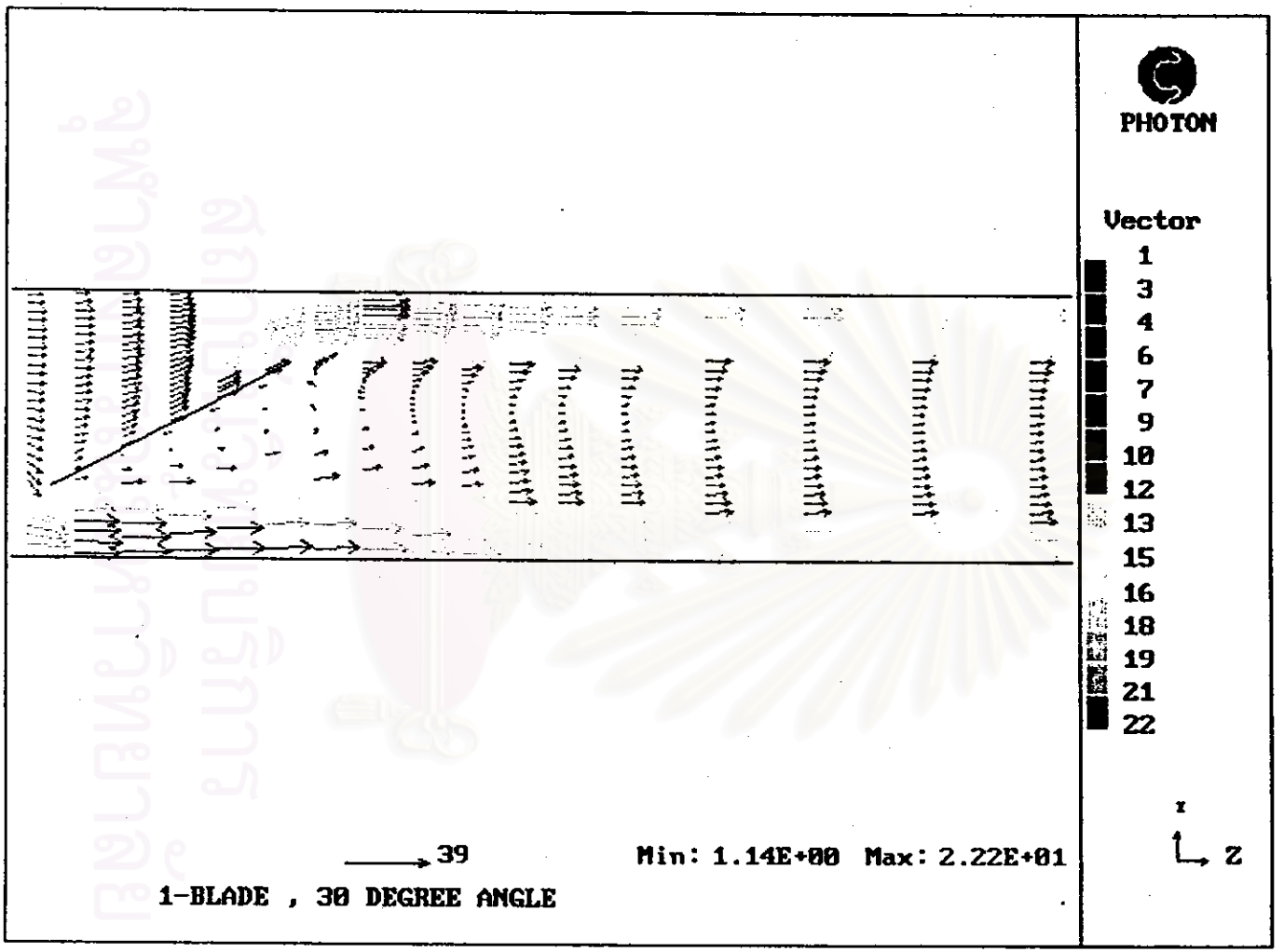

Figure 7.43(a) Mean velocity vectors around the separated-flow region of 1-blade damper at Re = 5.1 × 10^5.

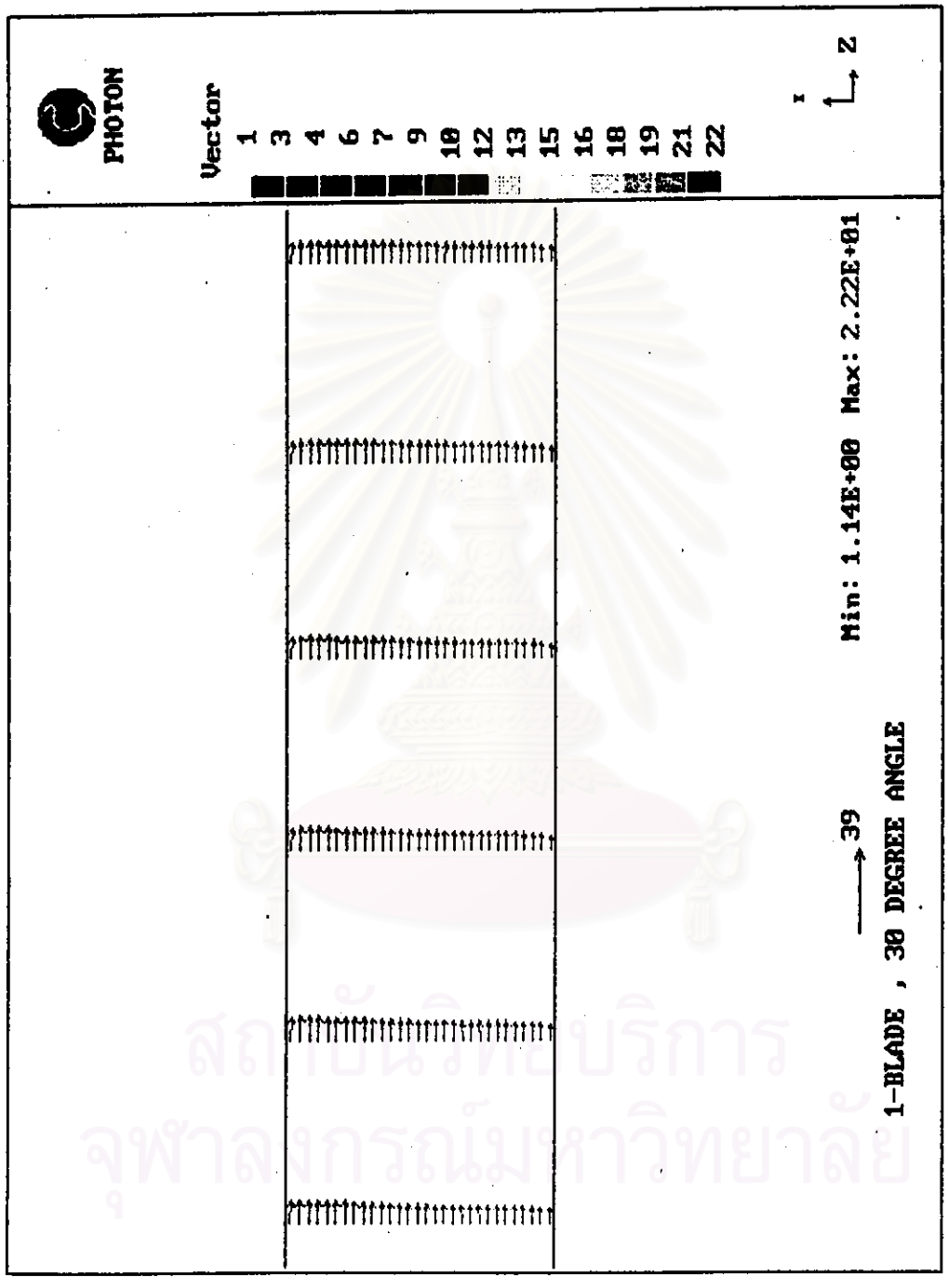

Figure 7.43(b) Mean velocity profiles in the developing flow region of 1-blade damper at Re = 5.1 × 10^5 (about L / D = 20).

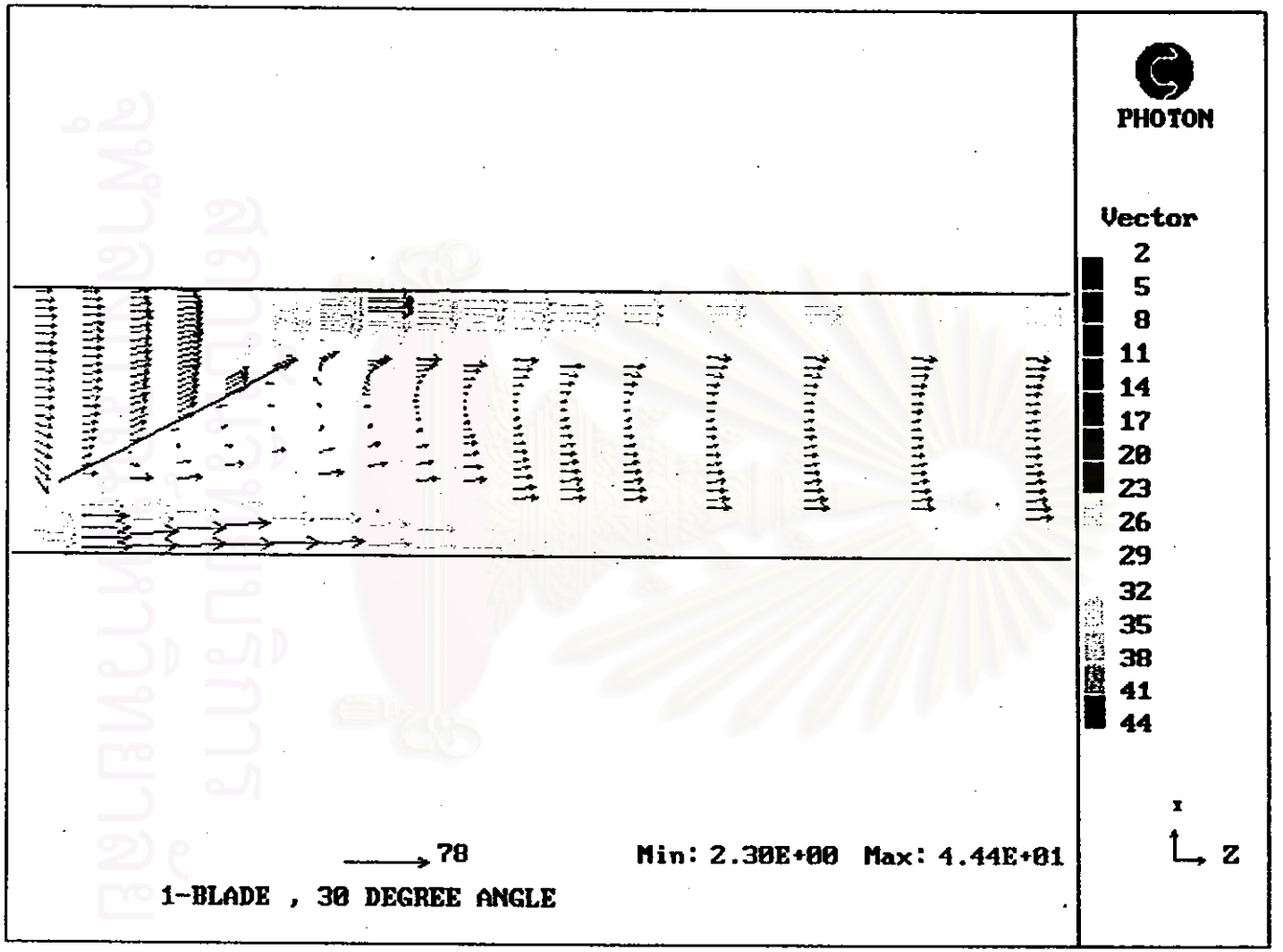

Figure 7.44(a) Mean velocity vectors around the separated-flow region of 1-blade damper at Re = 1.0×10^6.

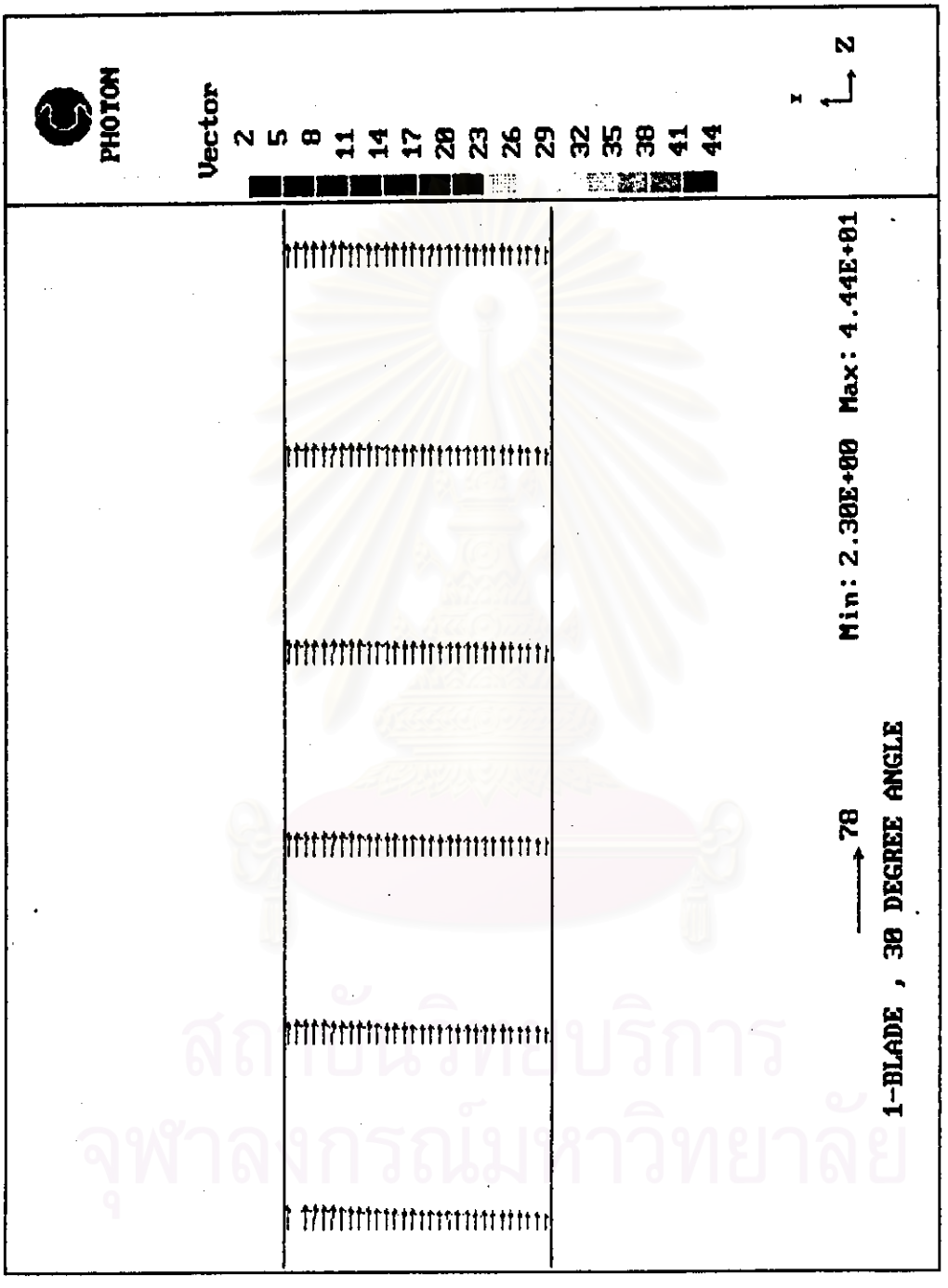

Figure 7.44(b) Mean velocity profiles in the developing flow region of 1-blade damper at Re = 1.0×10^6 (about L / D = 20).

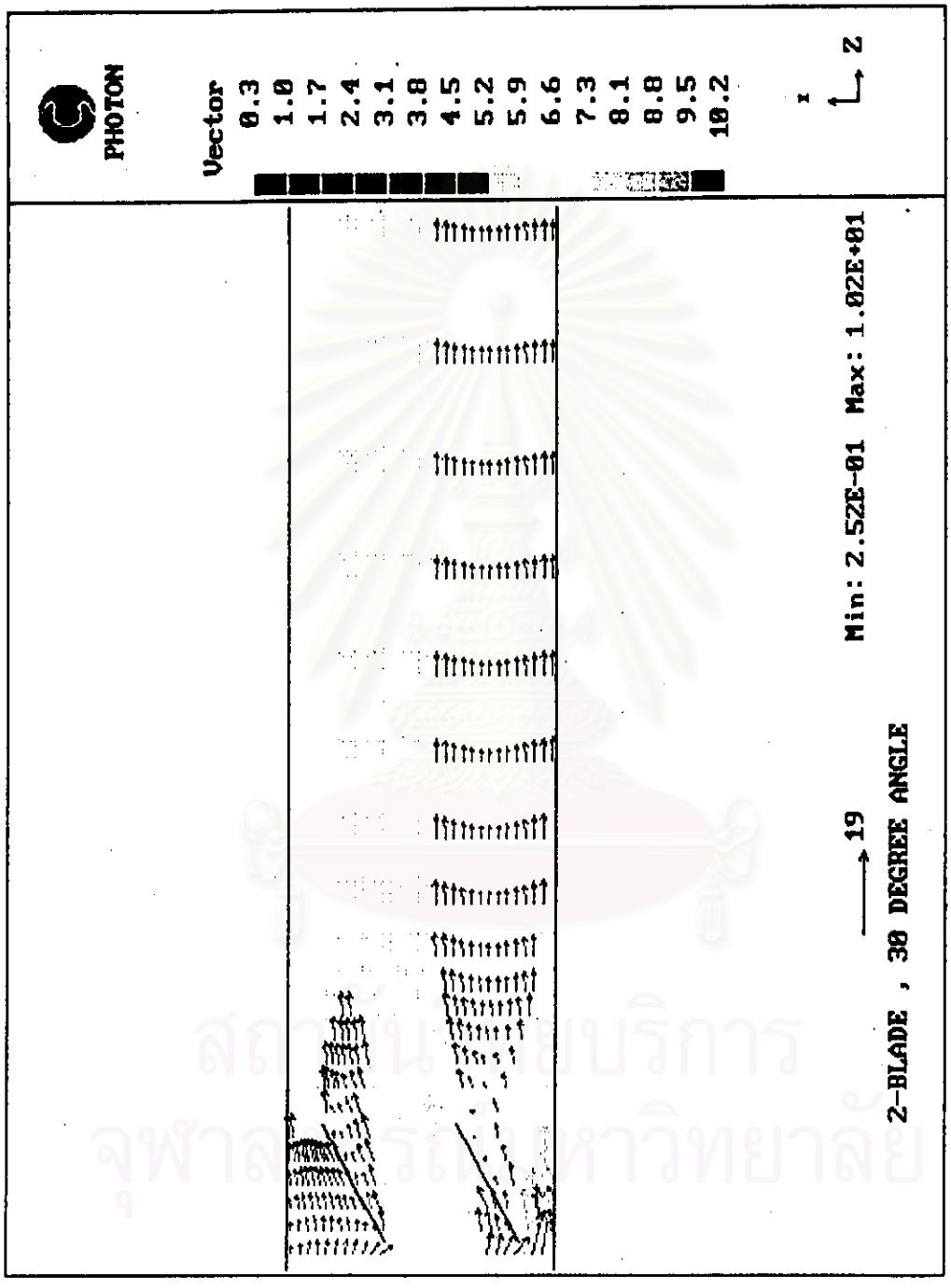

Figure 7.45(a) Mean velocity vectors around the separated-flow region of 2-blade damper at Re = 2.6 × 10^5.

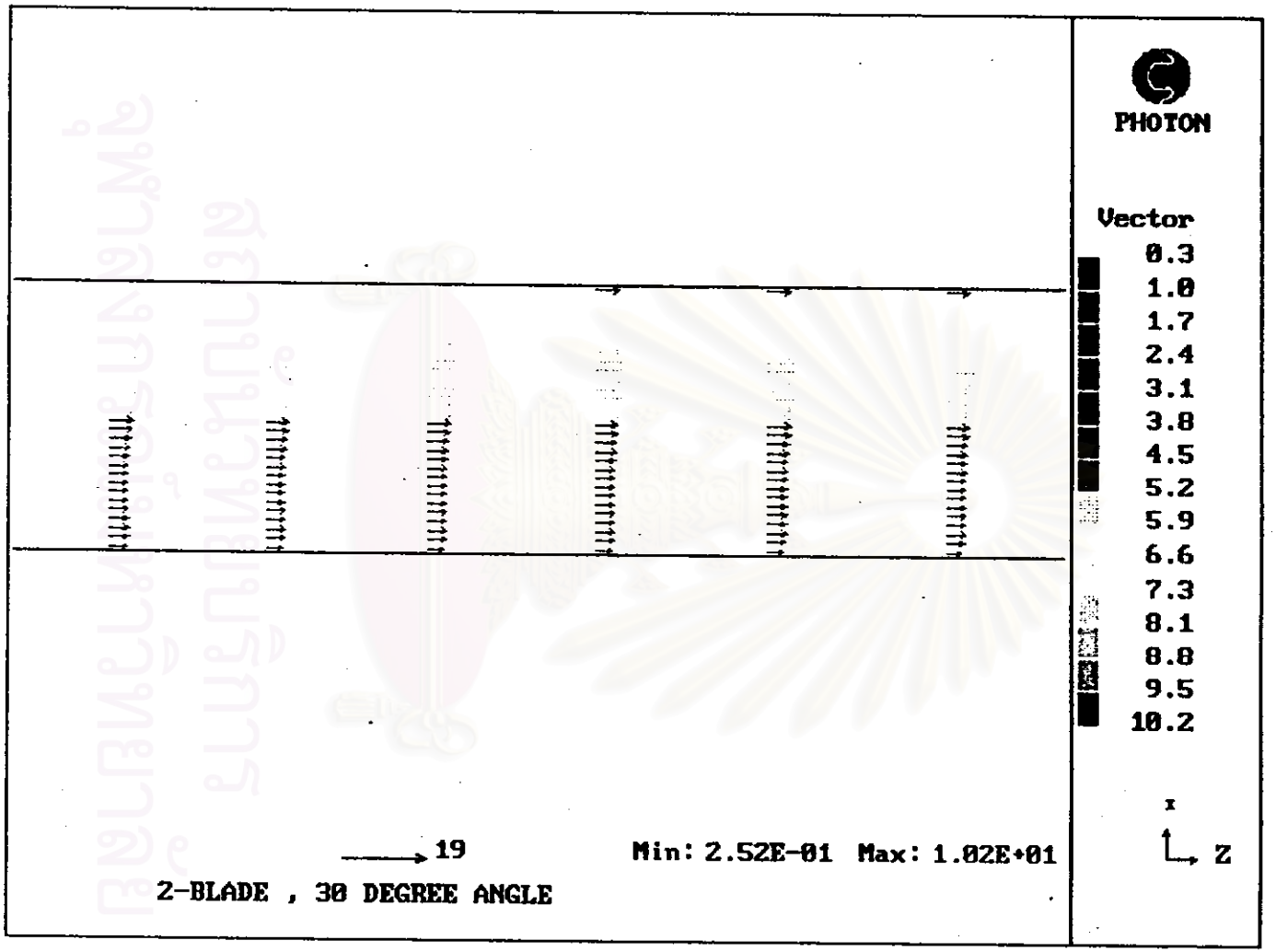

Figure 7.45(b) Mean velocity profiles in the developing flow region of 2-blade damper at Re = 2.6 × 10^5 (about L / D = 16).

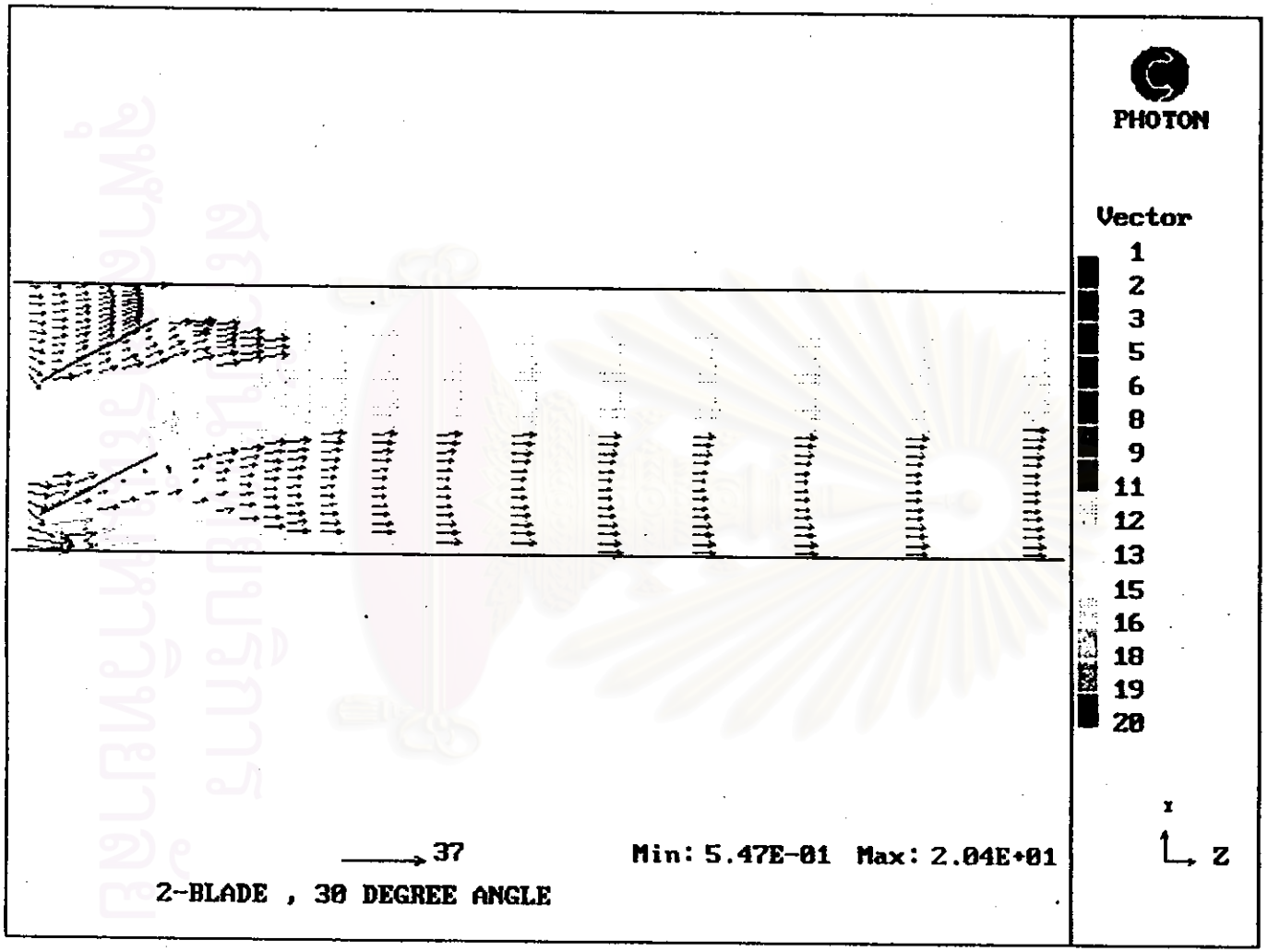

Figure 7.46(a) Mean velocity vectors around the separated-flow region of 2-blade damper at Re = 5.1 × 10^5.

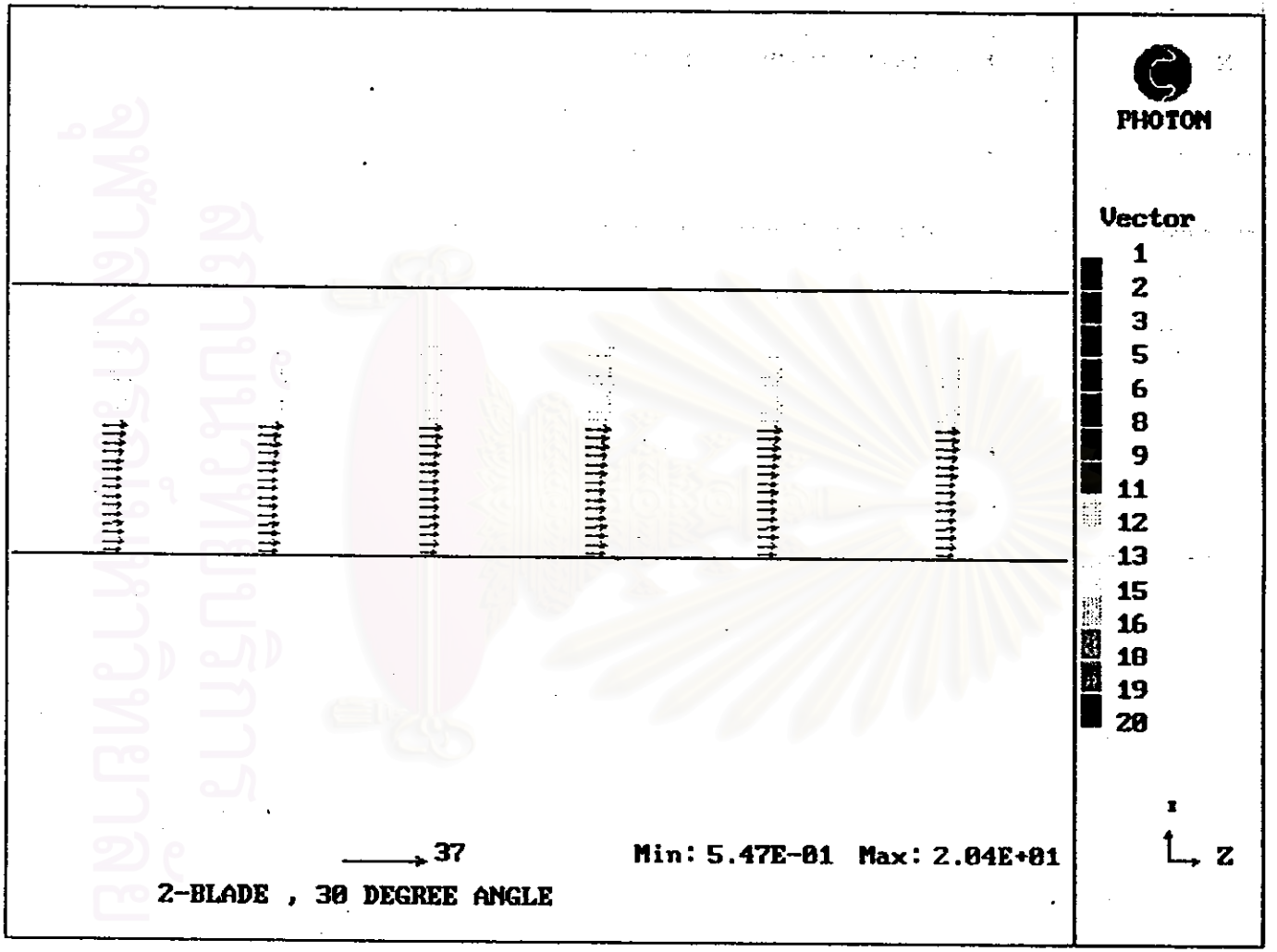

Figure 7.46(b) Mean velocity profiles in the developing flow region of 2-blade damper at Re = 5.1 × 10^5 (about L / D = 16).

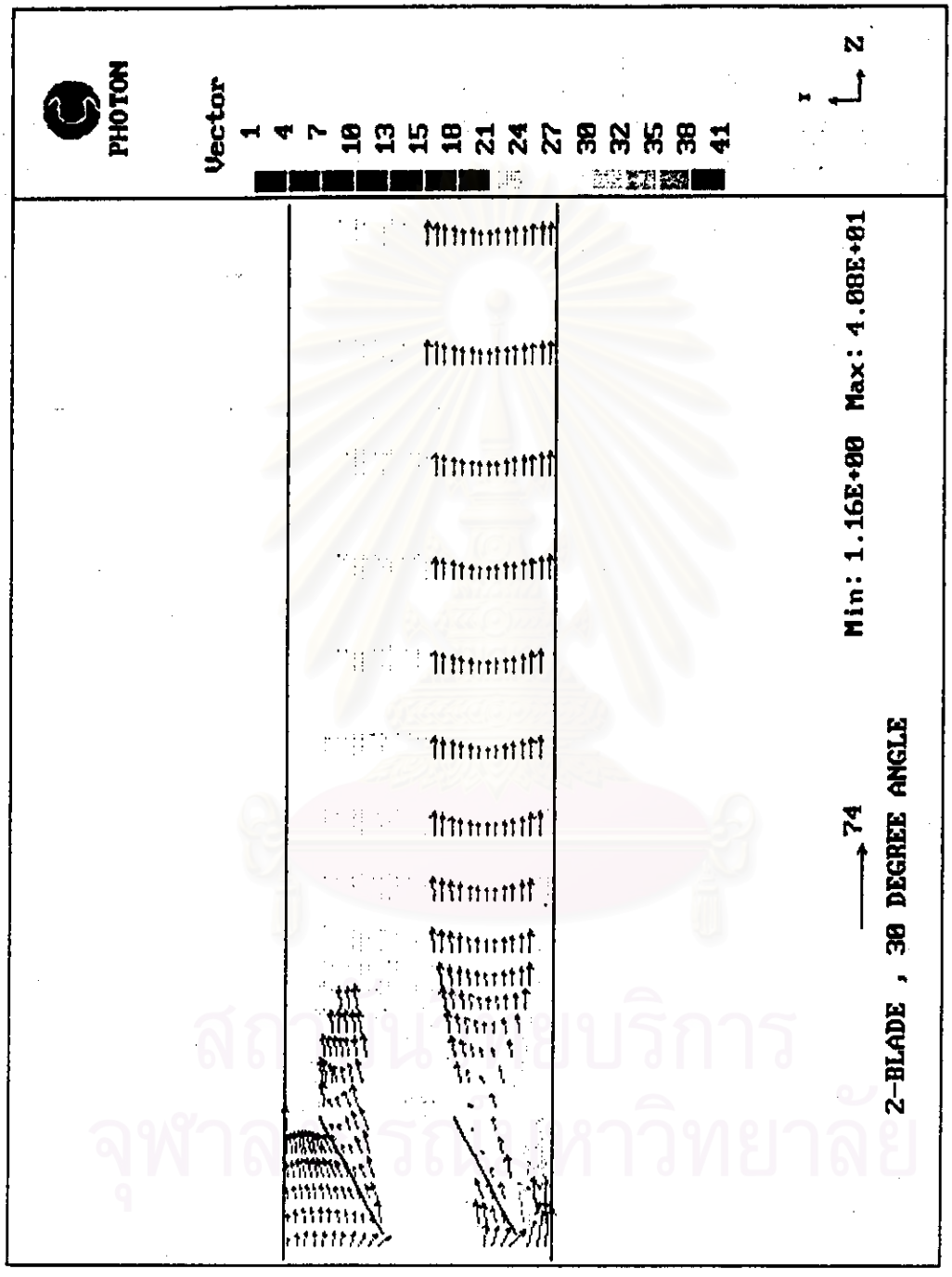

Figure 7.47(a) Mean velocity vectors around the separated-flow region of 2-blade damper at Re = 1.0 x 10^6.

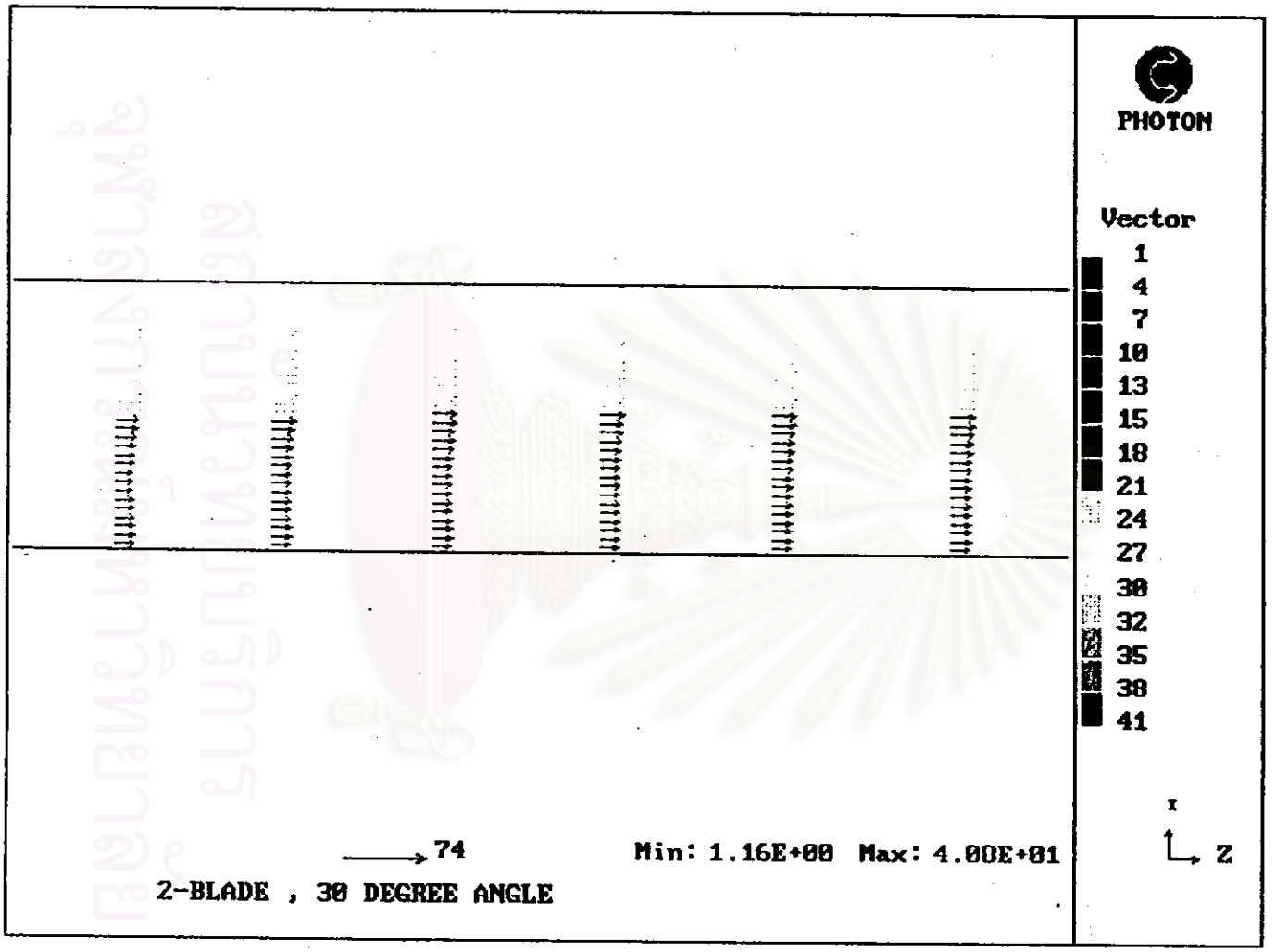

Figure 7.47(b) Mean velocity profiles in the developing flow region of 2-blade damper at Re = 1.0 x 10^6 (about L / D = 16).

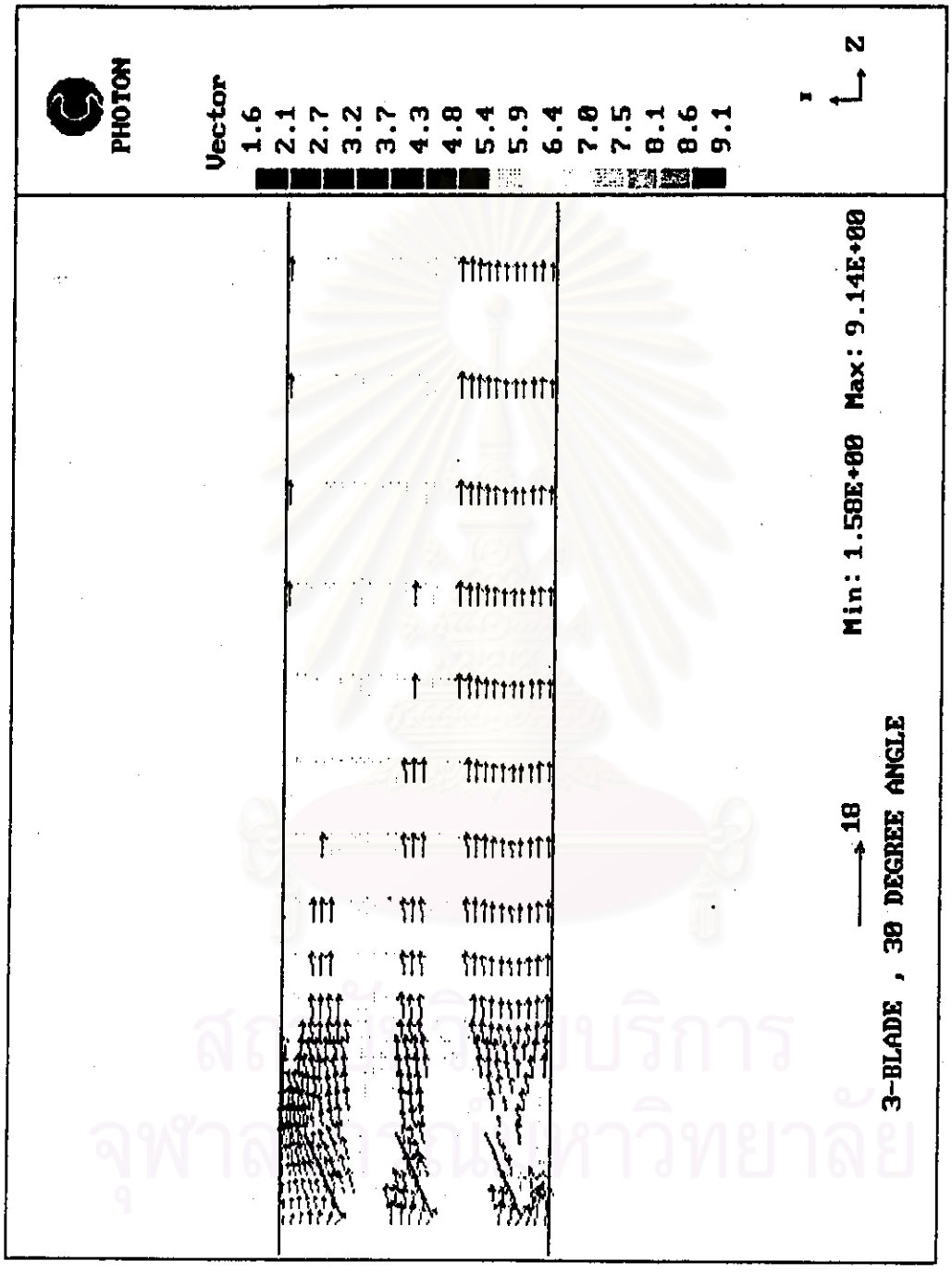

Figure 7.48(a) Mean velocity vectors around the separated-flow region of 3-blade damper at Re = 2.6 × 10^5.

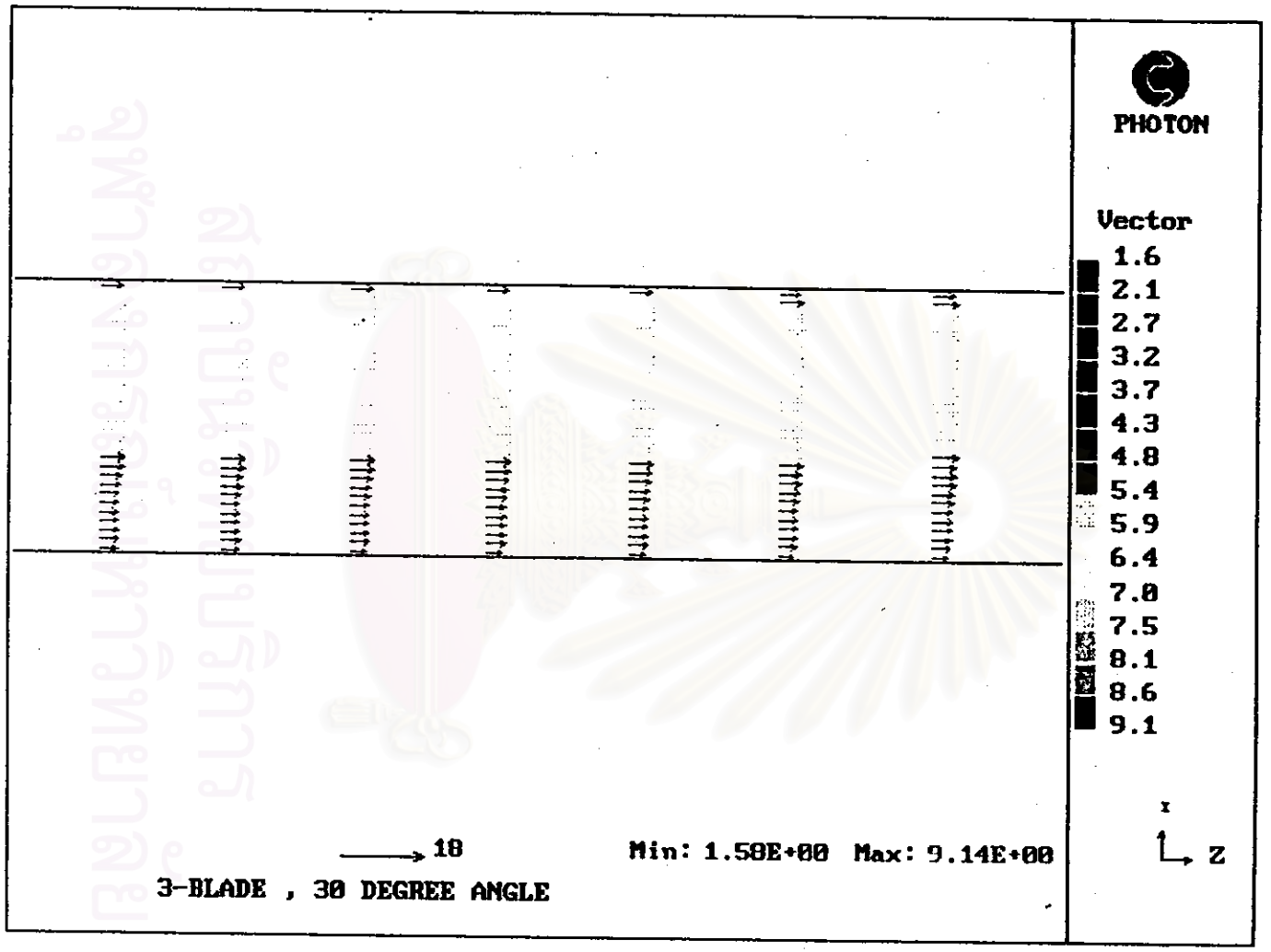

Figure 7.48(b) Mean velocity profiles in the developing flow region of 3-blade damper at Re = 2.6 x 10^5 (about L / D = 14).

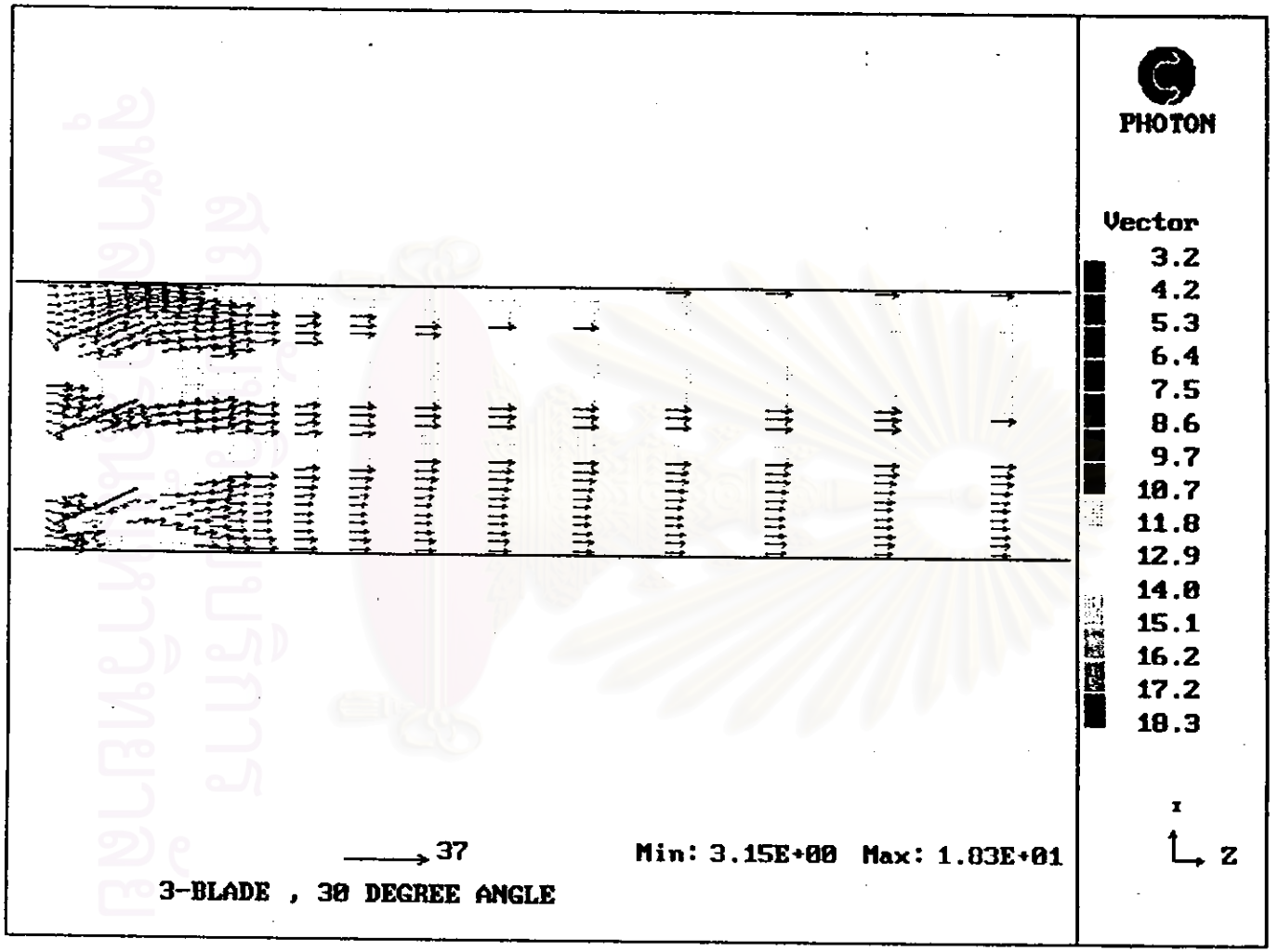

Figure 7.49(a) Mean velocity vectors around the separated-flow region of 3-blade damper at Re = 5.1 × 10^5.

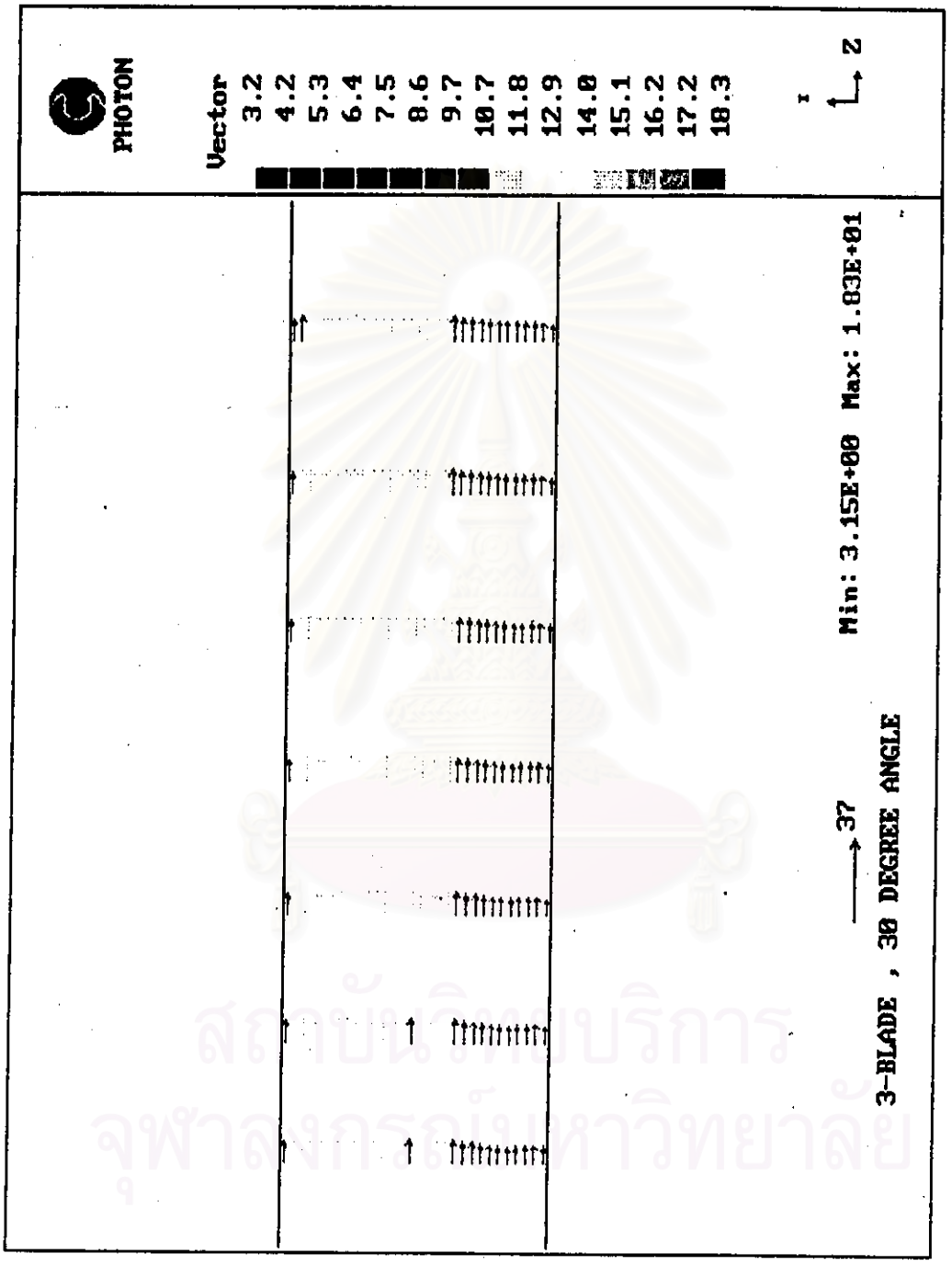

Figure 7.49(b) Mean velocity profiles in the developing flow region of 3-blade damper at Re = 5.1 × 10^5 (about L / D = 14).

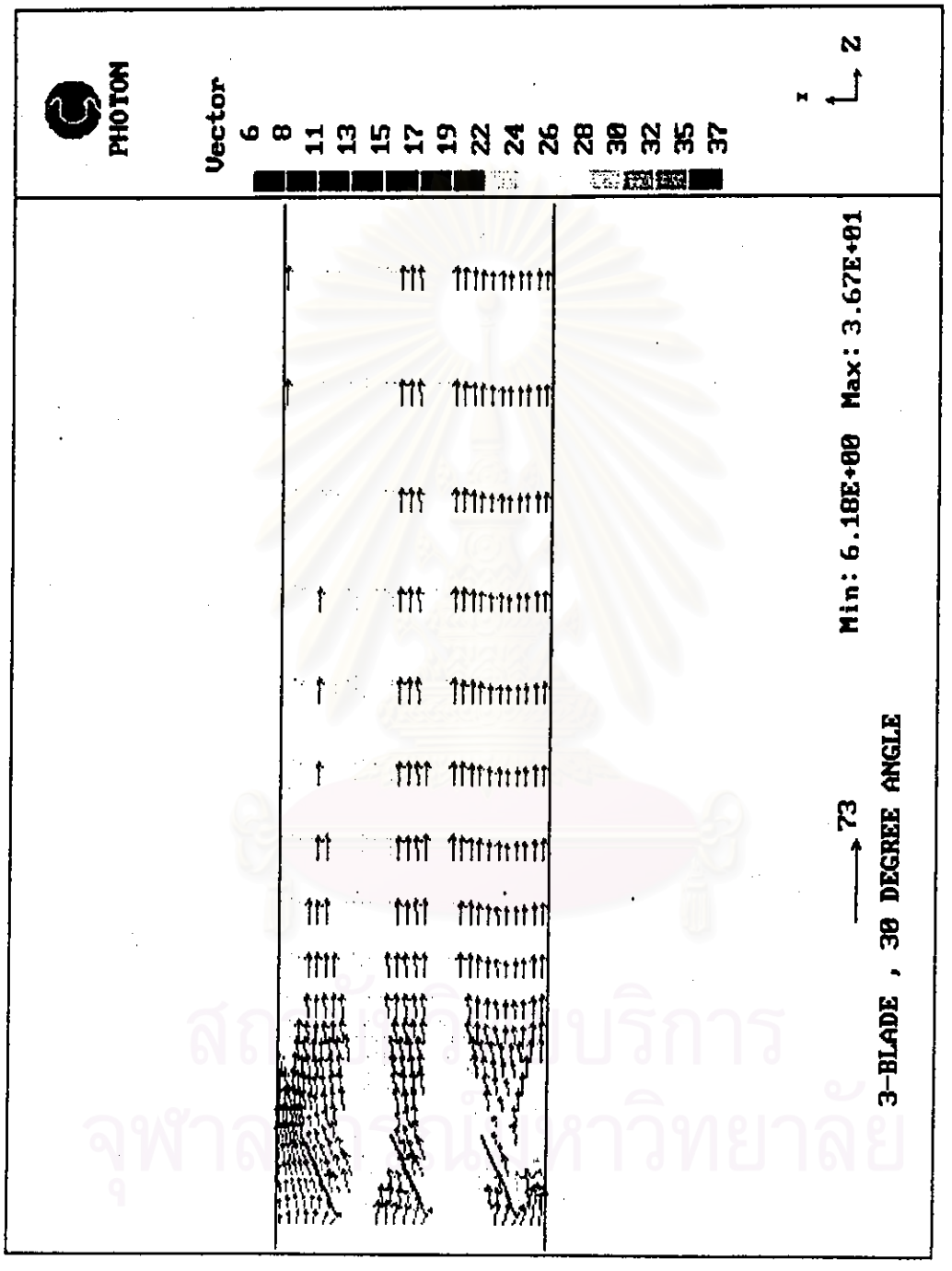

Figure 7.50(a) Mean velocity vectors around the separated-flow region of 3-blade damper at Re = 1.0×10^6.

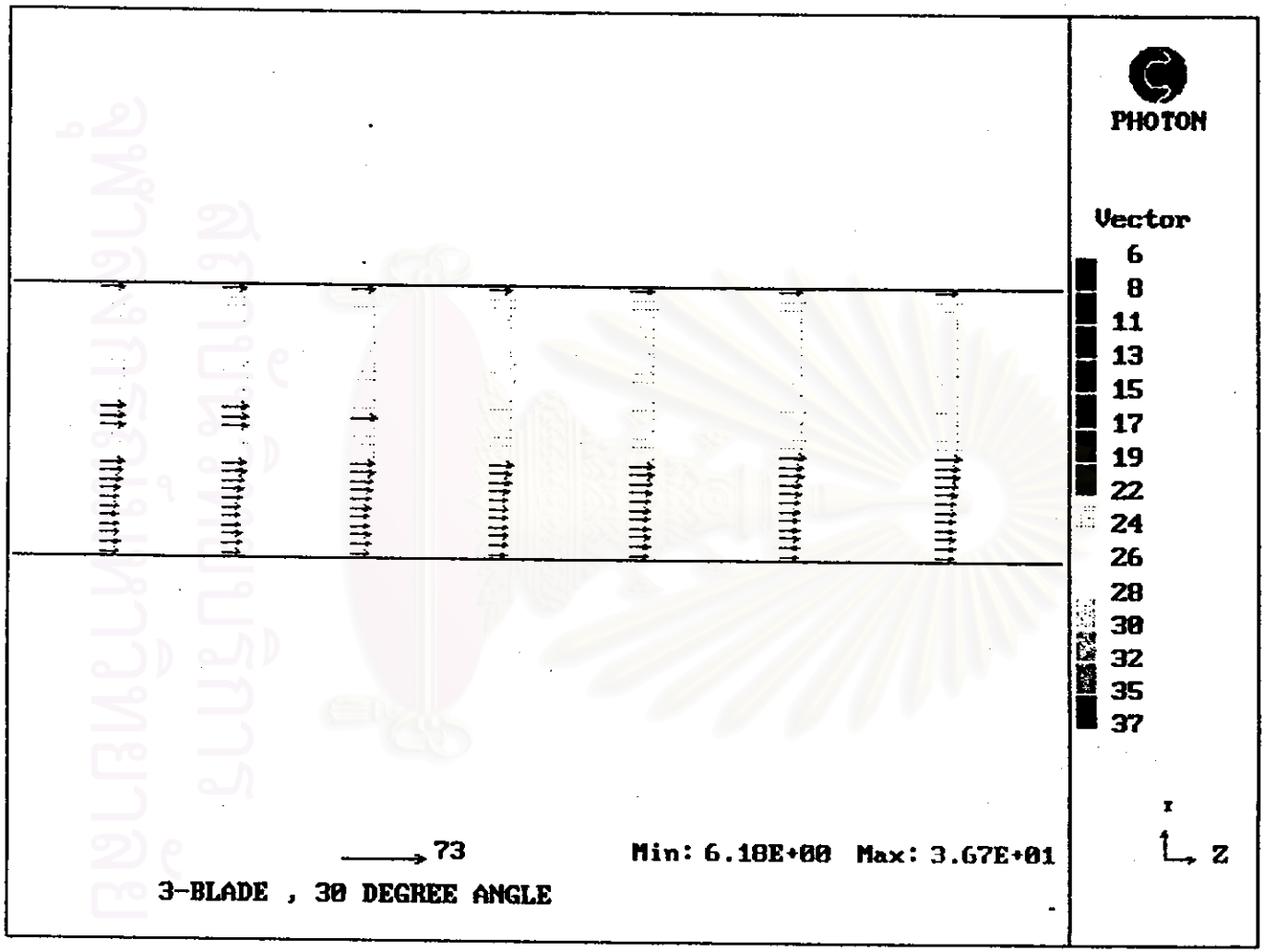

Figure 7.50(b) Mean velocity profiles in the developing flow region of 3-blade damper at Re = 1.0 × 10^6 (about L / D = 14).

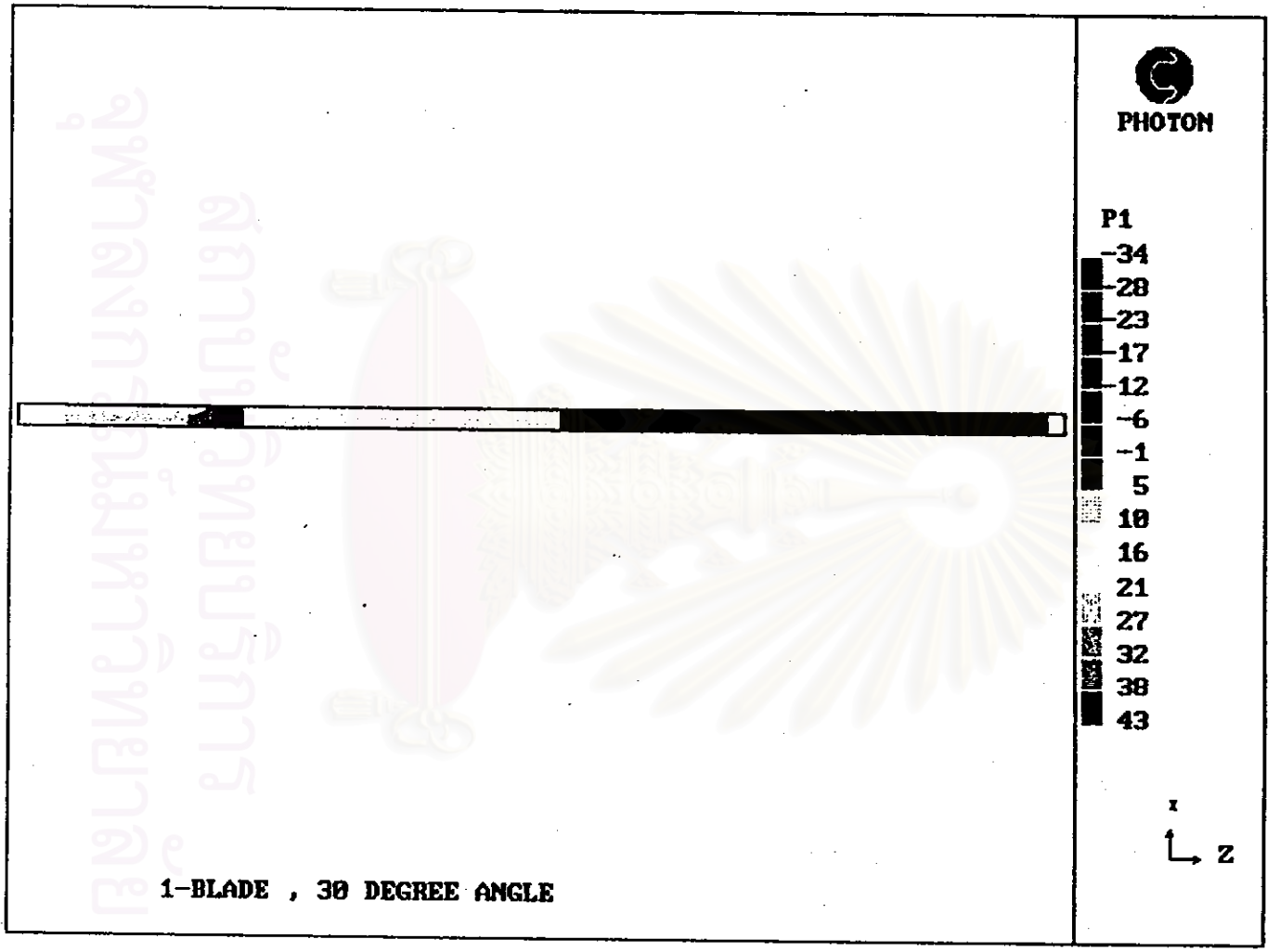

Figure 7.51 Pressure distribution of 1-blade damper with 30 degree angle.

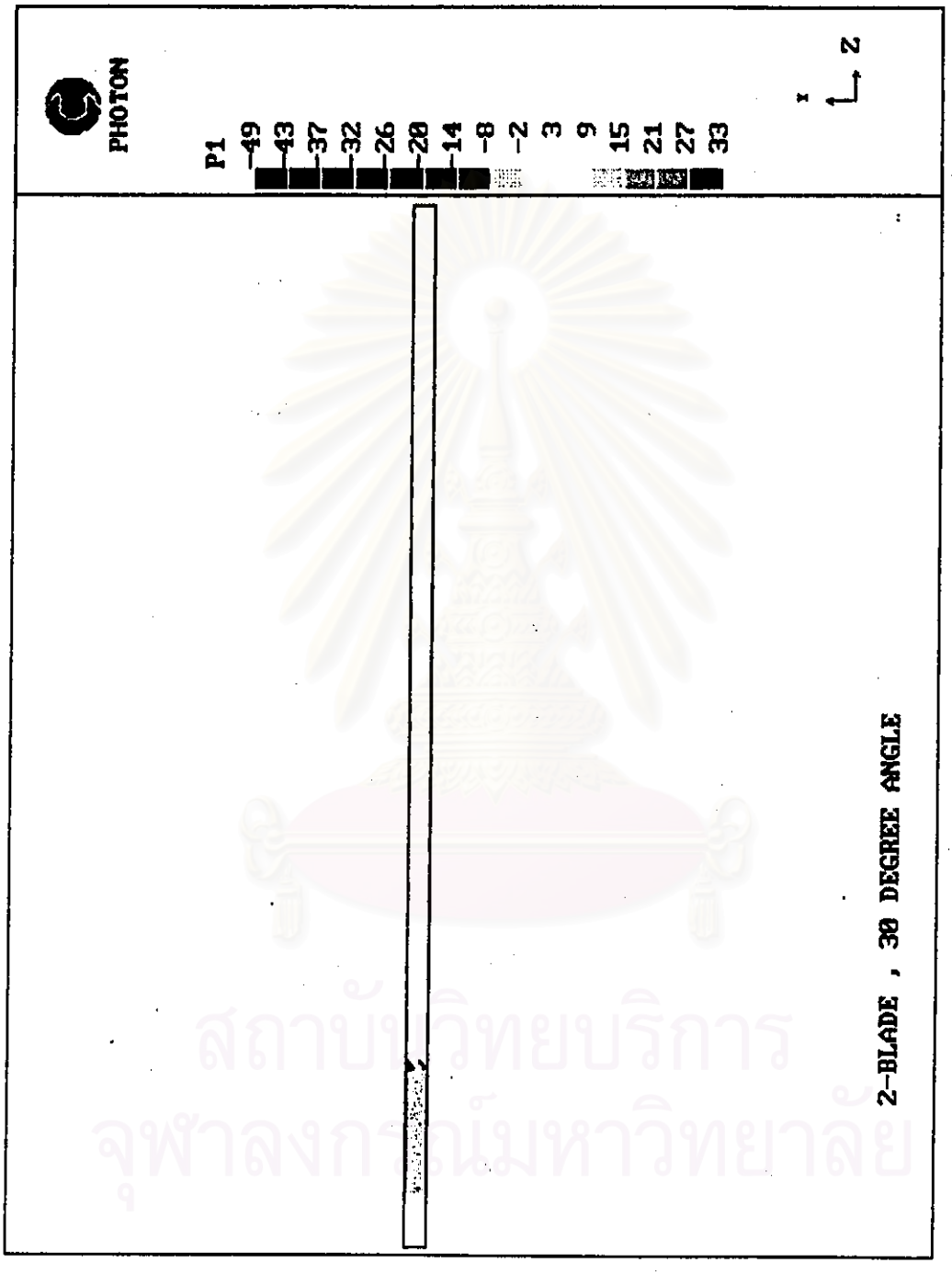

Figure 7.52 Pressure distribution of 2-blade damper with 30 degree angle.

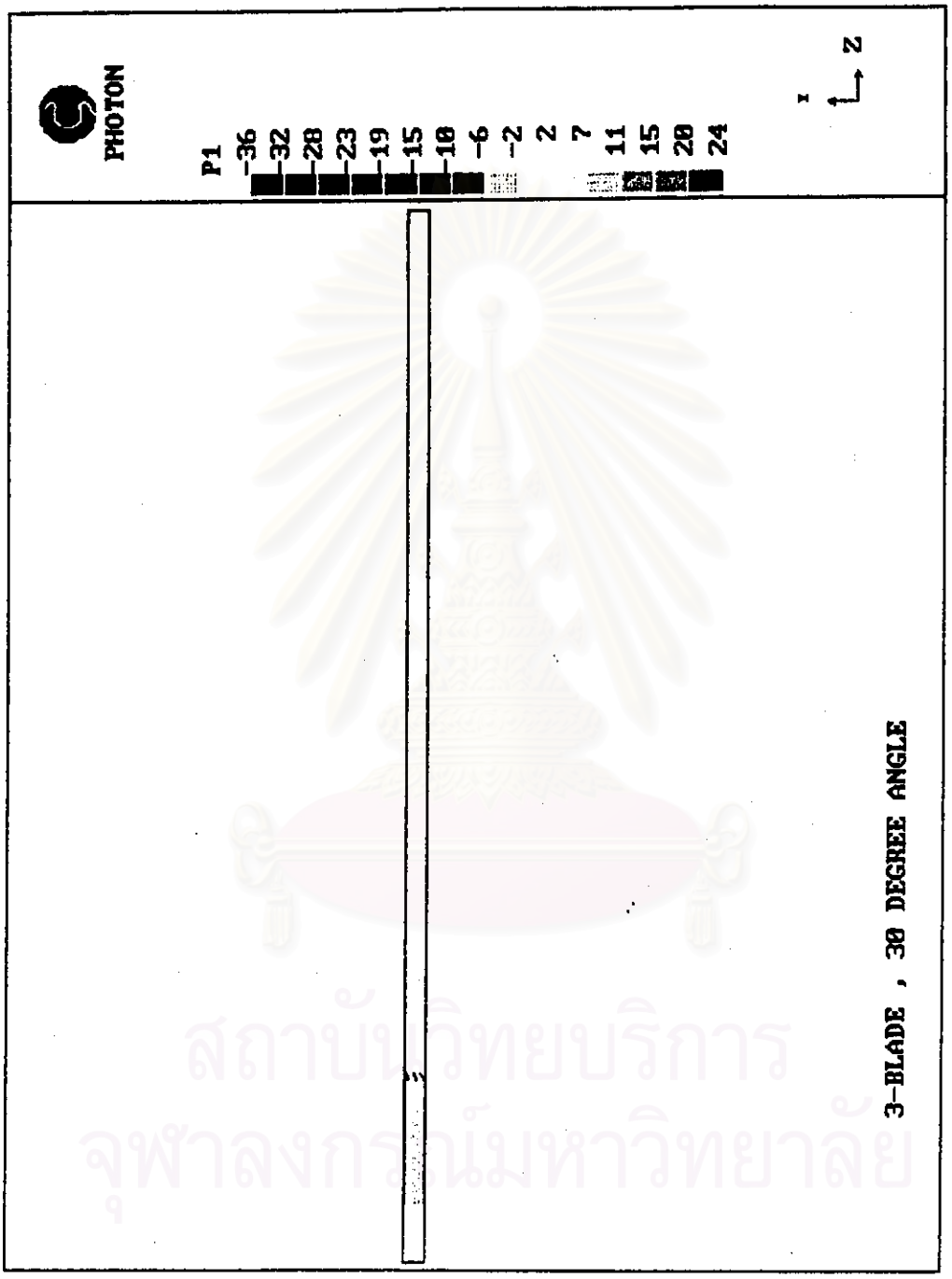

Figure 7.53 Pressure distribution of 3-blade damper with 30 degree angle.